

**LARGE DEFLECTIONS OF CANTILEVER BEAM OBEYING
GENERALIZED LUDWICK'S MATERIAL MODEL SUBJECTED TO
FOLLOWER DISTRIBUTED LOAD**



SOKHENG TOUCH

**A THESIS SUBMITTED IN PARTIAL FULFILLMENT OF THE
REQUIREMENTS FOR THE DEGREE OF MASTER OF ENGINEERING
PROGRAM IN CIVIL ENGINEERING**

FACULTY OF ENGINEERING

RAJAMANGALA UNIVERSITY OF TECHNOLOGY THANYABURI

ACADEMIC YEAR 2014

**COPYRIGHT OF RAJAMANGALA UNIVERSITY
OF TECHNOLOGY THANYABURI**

**LARGE DEFLECTIONS OF CANTILEVER BEAM OBEYING
GENERALIZED LUDWICK'S MATERIAL MODEL SUBJECTED TO
FOLLOWER DISTRIBUTED LOAD**

SOKHENG TOUCH

**A THESIS SUBMITTED IN PARTIAL FULFILLMENT OF THE
REQUIREMENTS FOR THE DEGREE OF MASTER OF ENGINEERING
PROGRAM IN CIVIL ENGINEERING**

FACULTY OF ENGINEERING

RAJAMANGALA UNIVERSITY OF TECHNOLOGY THANYABURI

ACADEMIC YEAR 2014

**COPYRIGHT OF RAJAMANGALA UNIVERSITY
OF TECHNOLOGY THANYABURI**

Thesis Title Large Deflections of Cantilever Beam Obeying Generalized Ludwick's
Material Model Subjected to Follower Distributed Load


Name-Surname Mr. Sokheng Touch

Program Civil Engineering

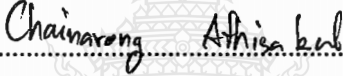
Thesis Advisor Mr. Boonchai Phungpaingam, Ph.D.

Academic Year 2014

THESIS COMMITTEE


.....
(Mr. Jatuphon Tangpagasit, Ph.D.)

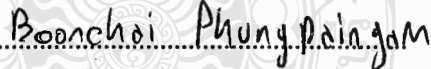
Chairman


.....
(Assistant Professor Chainarong Athisakul, Ph.D.)

Committee


.....
(Ms. Meng Jing, D.Eng.)

Committee


.....
(Mr. Boonchai Phungpaingam, Ph.D.)

Committee

Approved by the Faculty of Engineering, Rajamangala University of Technology
Thanyaburi in Partial Fulfillment of the Requirements for the Master's Degree

.....Dean of Faculty of Engineering
(Assistant Professor Sivakorn Anghong, Ph.D.)

Date 17 Month August Year 2015

Thesis Title	Large Deflections of Cantilever Beam Obeying Generalized Ludwick's Material Model Subjected to Follower Distributed Load
Name – Surname	Mr. Sokheng Touch
Program	Civil Engineering
Thesis Advisor	Mr. Boonchai Phungpaingam, Ph.D.
Academic Year	2014

ABSTRACT

This thesis presents the large deflection behavior of a cantilever beam subjected to follower distributed load where material of the cantilever beam obeys the generalized Ludwick's constitutive law. The cross-section of the beam is prismatic and rectangular. The follower distributed load is applied in transverse direction and it always keeps the right angle to the beam axis.

The stress-strain relationship of such materials is presented by generalized Ludwick's constitutive law. To derive the set of governing differential equations, equilibrium equations, moment-curvature relation obeying the generalized Ludwick's material model and nonlinear geometric relations have been considered. A set of highly nonlinear simultaneous first-order differential equations with boundary conditions is established. The shooting method is employed to solve the problem. Furthermore, two cases of parametric studies are considered. One is n and ϵ_0 are independent and the other is n and ϵ_0 can be related to each other.

From the results, there are many interesting features associated with the nonlinearly material properties of large deflections of cantilever beam subjected to follower distributed load. It is worth noting that follower distributed load \bar{w} increases as the rotational angle θ_0 increases and the stable equilibrium paths can be observed. Last but not least, the numerical results are compared with previous studies (linear material) in order to test the validity and accuracy of the present method, and they are in good agreement.

Keywords: large deflection, cantilever beam, follower force, generalized Ludwick constitutive law, shooting method.

Acknowledgements

For this thesis, first of all, I would like to express my sincere gratitude to my thesis advisor Dr. Boonchai Phungpaingam for the valuable of guidance and encouragement which helped me in all the time of my research. His encouragement, thoughtfulness, and patience are greatly admired. It has been my pleasure to him as a professor as a mentor.

Furthermore, I would like to thank to the thesis committees, Dr. Jatuphon Tangpagasit, Dr. Meng Jing, and Assistant Professor Dr. Chainarong Athisakul from department of civil engineering at King Mongkut's University of Technology Thonburi (KMUTT) for their valuable comments and helpful suggestions.

Otherwise, I would like to thank to all of the professors for their valuable lectures and experiences while I was studying. What is more, I would like to thank to Dr. Boonchai Phungpaingam for helpfulness in coordination for documentations.

Finally, most importantly, I would like to thank my family for all love and encouragement. Without their support, I would have never reached this point.

Sokheng Touch

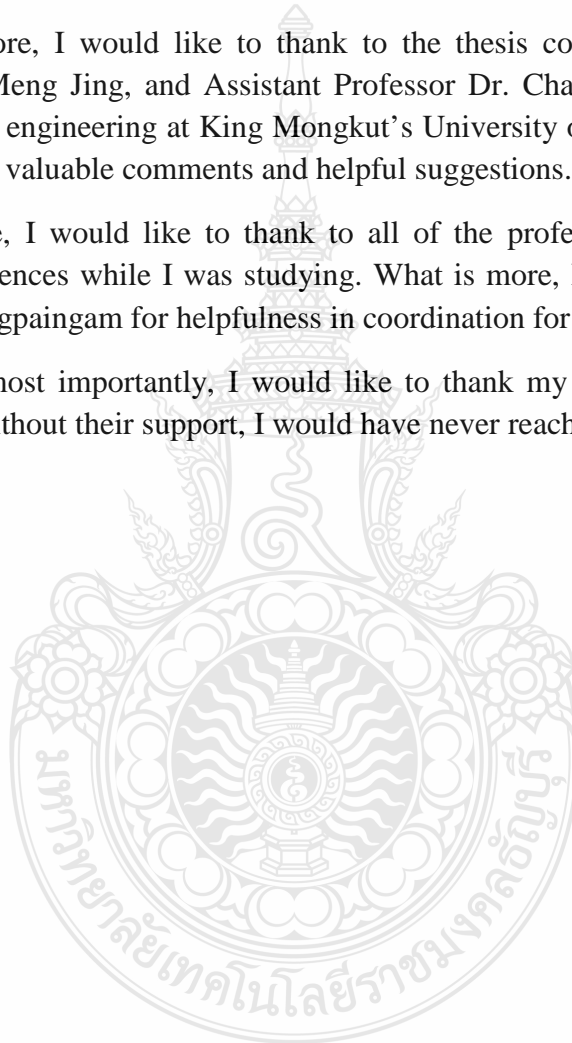


Table of Contents

	Page
Abstract.....	(3)
Acknowledgements.....	(4)
Table of Contents.....	(5)
List of Tables	(7)
List of Figures.....	(10)
List of Abbreviations	(16)
CHAPTER 1 INTRODUCTION	17
1.1 Background and Statement of the Problems.....	17
1.2 Objectives	22
1.3 Hypothesis	22
1.4 Scope of Study.....	22
1.5 Conceptual Framework.....	22
1.6 Contribution to Knowledge	23
CHAPTER 2 REVIEW OF THE LITERATURE	24
2.1 General.....	24
2.2 Related Research	26
2.2.1 Linear Material	26
2.2.2 Non-linear Elastic Ludwick Material	27
2.2.3 Non-linear Elastic generalized Ludwick Material.....	28
CHAPTER 3 MATHEMATICAL MODEL.....	30
3.1 Assumption of the Analysis.....	30
3.2 Model Description	30
3.3 Stress-strain Relationships.....	31
3.3.1 Constitutive Relationships.....	31
3.4 Governing Equations	36
3.5 Boundary Conditions	38

Table of Contents (Continued)

	Page
CHAPTER 4 RESEARCH METHODOLOGY	39
4.1 General	39
4.2 Method of Solution	39
CHAPTER 5 RESULTS AND DISCUSSIONS	43
5.1 Numerical Solutions	44
5.1.1 Case 1: n and ε_0 are varied independently	44
5.1.2 Case 2: n and ε_0 are related to each other	101
5.1.3 Effects of the dimension of the cross-section	110
CHAPTER 6 CONCLUSIONS	113
6.1 Conclusions	113
6.2 Suggestions	114
Bibliography	115
Appendices.....	119
Appendix A Runge-Kutta Method	120
Appendix B Newton-Raphson Method	122
Appendix C Shooting Method	125
Appendix D Computational Program	128
Appendix E Equilibrium Equations of Beam Segment	139
Appendix F The Inner Bending Moment-cuvature Relationship	142
Appendix G Moment Differentiation of Generalized Ludwick Material....	144
Appendix H Numerical Results	146
Appendix I Publication	153
Biography.....	172

List of Tables

	Page
Table 5.1 Comparison results between Rao and Rao [1] and presented study	43
Table 5.2 Numerical results for cantilever beam made of the generalized Ludwick nonlinear elastic material: $\varepsilon_0 = 0.001$	45
Table 5.3 Numerical results for cantilever beam made of the generalized Ludwick material for $n = 0.50$	49
Table 5.4 Numerical results for cantilever beam made of the generalized Ludwick material for $n = 1.00$	49
Table 5.5 Numerical results for cantilever beam made of the generalized Ludwick material for $n = 1.30$	50
Table 5.6 Numerical results for cantilever beam made of the generalized Ludwick nonlinear elastic material: $\varepsilon_0 = 0.002$	51
Table 5.7 Numerical results for cantilever beam made of the generalized Ludwick material for $n = 0.50$	55
Table 5.8 Numerical results for cantilever beam made of the generalized Ludwick material for $n = 1.00$	55
Table 5.9 Numerical results for cantilever beam made of the generalized Ludwick material for $n = 1.30$	56
Table 5.10 Numerical results for cantilever beam made of the generalized Ludwick nonlinear elastic material: $\varepsilon_0 = 0.003$	57
Table 5.11 Numerical results for cantilever beam made of the generalized Ludwick material for $n = 0.50$	61
Table 5.12 Numerical results for cantilever beam made of the generalized Ludwick material for $n = 1.00$	61
Table 5.13 Numerical results for cantilever beam made of the generalized Ludwick material for $n = 1.30$	62
Table 5.14 Numerical results for cantilever beam made of the generalized Ludwick nonlinear elastic material: $\varepsilon_0 = 0.004$	63
Table 5.15 Numerical results for cantilever beam made of the generalized Ludwick material for $n = 0.50$	66

List of Tables (Continued)

	Page
Table 5.16 Numerical results for cantilever beam made of the generalized Ludwick material for $n = 1.00$	67
Table 5.17 Numerical results for cantilever beam made of the generalized Ludwick material for $n = 1.30$	67
Table 5.18 Numerical results for cantilever beam made of the generalized Ludwick nonlinear elastic material: $\varepsilon_0 = 0.005$	68
Table 5.19 Numerical results for cantilever beam made of the generalized Ludwick material for $n = 0.50$	72
Table 5.20 Numerical results for cantilever beam made of the generalized Ludwick material for $n = 1.00$	72
Table 5.21 Numerical results for cantilever beam made of the generalized Ludwick material for $n = 1.30$	73
Table 5.22 Numerical results for cantilever beam made of the generalized Ludwick nonlinear elastic material: $\varepsilon_0 = 0.006$	74
Table 5.23 Numerical results for cantilever beam made of the generalized Ludwick material for $n = 0.50$	77
Table 5.24 Numerical results for cantilever beam made of the generalized Ludwick material for $n = 1.00$	78
Table 5.25 Numerical results for cantilever beam made of the generalized Ludwick material for $n = 1.30$	78
Table 5.26 Numerical results for cantilever beam made of the generalized Ludwick nonlinear elastic material: $\varepsilon_0 = 0.007$	79
Table 5.27 Numerical results for cantilever beam made of the generalized Ludwick material for $n = 0.50$	82
Table 5.28 Numerical results for cantilever beam made of the generalized Ludwick material for $n = 1.00$	83
Table 5.29 Numerical results for cantilever beam made of the generalized Ludwick material for $n = 1.30$	83

List of Tables (Continued)

	Page
Table 5.30 Numerical results for cantilever beam made of the generalized Ludwick nonlinear elastic material: $\varepsilon_0 = 0.008$	84
Table 5.31 Numerical results for cantilever beam made of the generalized Ludwick material for $n = 0.50$	87
Table 5.32 Numerical results for cantilever beam made of the generalized Ludwick material for $n = 1.00$	88
Table 5.33 Numerical results for cantilever beam made of the generalized Ludwick material for $n = 1.30$	88
Table 5.34 Numerical results for cantilever beam made of the generalized Ludwick nonlinear elastic material: $\varepsilon_0 = 0.009$	89
Table 5.35 Numerical results for cantilever beam made of the generalized Ludwick material for $n = 0.50$	92
Table 5.36 Numerical results for cantilever beam made of the generalized Ludwick material for $n = 1.00$	93
Table 5.37 Numerical results for cantilever beam made of the generalized Ludwick material for $n = 1.30$	93
Table 5.38 Numerical results for cantilever beam made of the generalized Ludwick nonlinear elastic material: $\varepsilon_0 = 0.01$	94
Table 5.39 Numerical results for cantilever beam made of the generalized Ludwick material for $n = 0.50$	97
Table 5.40 Numerical results for cantilever beam made of the generalized Ludwick material for $n = 1.00$	98
Table 5.41 Numerical results for cantilever beam made of the generalized Ludwick material for $n = 1.30$	98
Table 5.42 Numerical results for cantilever beam made of the generalized Ludwick material $n > 1$, $\bar{b} = 0.2\text{m}$ and $\bar{h} = 0.2\text{m}$	103
Table 5.43 Numerical results for cantilever beam made of the generalized Ludwick material $n < 1$, $\bar{b} = 0.2\text{m}$ and $\bar{h} = 0.2\text{m}$	104
Table 5.44 Numerical results for cantilever beam made of the generalized Ludwick material for $n = 0.55$	108
Table 5.45 Numerical results for cantilever beam made of the generalized Ludwick material for $n = 1.30$	108

List of Figures

	Page
Figure 1.1 Basic box wing configuration	18
Figure 1.2 Diamond box wing configuration	18
Figure 1.3 Joined wing configuration	19
Figure 1.4 Crane Configuration	19
Figure 1.5 Cantilever Bridge Configuration	20
Figure 1.6 Corbel Configuration.....	20
Figure 1.7 MEMS cantilever switch.....	21
Figure 2.1 Relationships between γ^2 and $(\tan \gamma)^2$	25
Figure 3.1 A cantilever beam subjected to the follower distributed load with undeformed configuration	30
Figure 3.2 A cantilever beam subjected to the follower distributed load with deformed configuration	31
Figure 3.3 Stress–strain relationships in tensile domain	32
Figure 3.4 Free-body diagram of an infinitesimal element of the beam	33
Figure 3.5 Geometric relationship of beam element	33
Figure 3.6 Stress distribution of generalized Ludwick’s type of the beam	33
Figure 3.7 Positive and negative of bending moment and curvature relations.....	34
Figure 3.8 Boundary condition of cantilever beam	38
Figure 4.1 Flow chart of computational procedures by using Matlab program 1 ...	41
Figure 4.2 Flow chart of computational procedures by using Matlab program 2 ...	42
Figure 5.1 Load-displacement curve for the nonlinearly cantilever beam subjected to follower distributed load $\varepsilon_0 = 0.001$	46
Figure 5.2 Equilibrium configurations for $\theta_0 = 1.2$ and $\theta_0 = 2.0$	47
Figure 5.3 Deflection configurations of the nonlinearly cantilever beam subjected to follower distributed load $n = 0.50$	47

List of Figures (Continued)

	Page
Figure 5.4 Deflection configurations of the nonlinearly cantilever beam subjected to follower distributed load $n = 1.00$	48
Figure 5.5 Deflection configurations of the nonlinearly cantilever beam subjected to follower distributed load $n = 1.30$	48
Figure 5.6 Load-displacement curve for the nonlinearly cantilever beam subjected to follower distributed load $\varepsilon_0 = 0.002$	52
Figure 5.7 Equilibrium configurations for $\theta_0 = 1.2$ and $\theta_0 = 2.0$	53
Figure 5.8 Deflection configurations of the nonlinearly cantilever beam subjected to follower distributed load $n = 0.50$	53
Figure 5.9 Deflection configurations of the nonlinearly cantilever beam subjected to follower distributed load $n = 1.00$	54
Figure 5.10 Deflection configurations of the nonlinearly cantilever beam subjected to follower distributed load $n = 1.30$	54
Figure 5.11 Load-displacement curve for the nonlinearly cantilever beam subjected to follower distributed load $\varepsilon_0 = 0.003$	58
Figure 5.12 Equilibrium configurations for $\theta_0 = 1.2$ and $\theta_0 = 2.0$	58
Figure 5.13 Deflection configurations of the nonlinearly cantilever beam subjected to follower distributed load $n = 0.50$	59
Figure 5.14 Deflection configurations of the nonlinearly cantilever beam subjected to follower distributed load $n = 1.00$	59
Figure 5.15 Deflection configurations of the nonlinearly cantilever beam subjected to follower distributed load $n = 1.30$	60
Figure 5.16 Load-displacement curve for the nonlinearly cantilever beam subjected to follower distributed load $\varepsilon_0 = 0.004$	64

List of Figures (Continued)

	Page
Figure 5.17 Equilibrium configurations for $\theta_0 = 1.2$ and $\theta_0 = 2.0$	64
Figure 5.18 Deflection configurations of the nonlinearly cantilever beam subjected to follower distributed load $n = 0.50$	65
Figure 5.19 Deflection configurations of the nonlinearly cantilever beam subjected to follower distributed load $n = 1.00$	65
Figure 5.20 Deflection configurations of the nonlinearly cantilever beam subjected to follower distributed load $n = 1.30$	66
Figure 5.21 Load-displacement curve for the nonlinearly cantilever beam subjected to follower distributed load $\varepsilon_0 = 0.005$	69
Figure 5.22 Equilibrium configurations for $\theta_0 = 1.2$ and $\theta_0 = 2.0$	70
Figure 5.23 Deflection configurations of the nonlinearly cantilever beam subjected to follower distributed load $n = 0.50$	70
Figure 5.24 Deflection configurations of the nonlinearly cantilever beam subjected to follower distributed load $n = 1.00$	71
Figure 5.25 Deflection configurations of the nonlinearly cantilever beam subjected to follower distributed load $n = 1.30$	71
Figure 5.26 Load-displacement curve for the nonlinearly cantilever beam subjected to follower distributed load $\varepsilon_0 = 0.006$	75
Figure 5.27 Equilibrium configurations for $\theta_0 = 1.2$ and $\theta_0 = 2.0$	75
Figure 5.28 Deflection configurations of the nonlinearly cantilever beam subjected to follower distributed load $n = 0.50$	76
Figure 5.29 Deflection configurations of the nonlinearly cantilever beam subjected to follower distributed load $n = 1.00$	76

List of Figures (Continued)

	Page
Figure 5.30 Deflection configurations of the nonlinearly cantilever beam subjected to follower distributed load $n = 1.30$	77
Figure 5.31 Load-displacement curve for the nonlinearly cantilever beam subjected to follower distributed load $\varepsilon_0 = 0.007$	80
Figure 5.32 Equilibrium configurations for $\theta_0 = 1.2$ and $\theta_0 = 2.0$	80
Figure 5.33 Deflection configurations of the nonlinearly cantilever beam subjected to follower distributed load $n = 0.50$	81
Figure 5.34 Deflection configurations of the nonlinearly cantilever beam subjected to follower distributed load $n = 1.00$	81
Figure 5.35 Deflection configurations of the nonlinearly cantilever beam subjected to follower distributed load $n = 1.30$	82
Figure 5.36 Load-displacement curve for the nonlinearly cantilever beam subjected to follower distributed load $\varepsilon_0 = 0.008$	85
Figure 5.37 Equilibrium configurations for $\theta_0 = 1.2$ and $\theta_0 = 2.0$	85
Figure 5.38 Deflection configurations of the nonlinearly cantilever beam subjected to follower distributed load $n = 0.50$	86
Figure 5.39 Deflection configurations of the nonlinearly cantilever beam subjected to follower distributed load $n = 1.00$	86
Figure 5.40 Deflection configurations of the nonlinearly cantilever beam subjected to follower distributed load $n = 1.30$	87
Figure 5.41 Load-displacement curve for the nonlinearly cantilever beam subjected to follower distributed load $\varepsilon_0 = 0.009$	90
Figure 5.42 Equilibrium configurations for $\theta_0 = 1.2$ and $\theta_0 = 2.0$	90

List of Figures (Continued)

	Page
Figure 5.43 Deflection configurations of the nonlinearly cantilever beam subjected to follower distributed load $n = 0.50$	91
Figure 5.44 Deflection configurations of the nonlinearly cantilever beam subjected to follower distributed load $n = 1.00$	91
Figure 5.45 Deflection configurations of the nonlinearly cantilever beam subjected to follower distributed load $n = 1.30$	92
Figure 5.46 Load-displacement curve for the nonlinearly cantilever beam subjected to follower distributed load $\varepsilon_0 = 0.01$	95
Figure 5.47 Equilibrium configurations for $\theta_0 = 1.2$ and $\theta_0 = 2.0$	95
Figure 5.48 Deflection configurations of the nonlinearly cantilever beam subjected to follower distributed load $n = 0.50$	96
Figure 5.49 Deflection configurations of the nonlinearly cantilever beam subjected to follower distributed load $n = 1.00$	96
Figure 5.50 Deflection configurations of the nonlinearly cantilever beam subjected to follower distributed load $n = 1.30$	97
Figure 5.51 Load-displacement curve for the nonlinearly cantilever beam subjected to follower distributed load $n = 0.50$	99
Figure 5.52 Load-displacement curve for the nonlinearly cantilever beam subjected to follower distributed load $n = 1.30$	100
Figure 5.53 Comparison of stress–strain curve between linear and nonlinear generalized Ludwick’s material.....	102
Figure 5.54 Load-displacement curve for the nonlinearly cantilever beam subjected to follower distributed load $n = 0.55, 1.00, \text{ and } 1.30$	105
Figure 5.55 Equilibrium configurations for $\theta_0 = 1.2$ and $\theta_0 = 2.0$	106

List of Figures (Continued)

	Page
Figure 5.56 Deflection configurations of the nonlinearly cantilever beam subjected to follower distributed load $n = 0.55$	106
Figure 5.57 Deflection configurations of the nonlinearly cantilever beam subjected to follower distributed load $n = 1.30$	107
Figure 5.58 Stress–strain relationships in tensile domain for generalized Ludwick	109
Figure 5.59 Stress–strain relationships (adjusted scale) in tensile domain for generalized Ludwick	109
Figure 5.60 Load-displacement for the nonlinearly cantilever beam subjected to follower distributed load $\varepsilon_0 = 0.001$ and $n = 0.50$	110
Figure 5.61 Load-displacement for the nonlinearly cantilever beam subjected to follower distributed load $\varepsilon_0 = 0.002$ and $n = 0.50$	110
Figure 5.62 Load-displacement for the nonlinearly cantilever beam subjected to follower distributed load $\varepsilon_0 = 0.001$ and $n = 1.30$	111
Figure 5.63 Load-displacement for the nonlinearly cantilever beam subjected to follower distributed load $\varepsilon_0 = 0.002$ and $n = 1.30$	111

List of Abbreviations

MEMS	Micro-electro-mechanical System
DTM	Differential Transformation Method
VIM	Variational Iteration Method
INC	Increment
LIM	Limitation



CHAPTER 1

INTRODUCTION

1.1 Background and Statement of the Problems

Nowadays, the analysis of large deflection of material nonlinearity for slender structures is of importance in developments in mechanical engineering, aerospace engineering, electronic engineering, robotics and manufacturing, etc. To deal with these structures, the large deflection beam theory plays a vital role to carry out the problem. In general, most of the structures show some degrees of nonlinearities such as geometric and material nonlinearities. According to this practice, structural failures may occur when these nonlinearities are neglected. Currently, these often happen as designers continue to carry out the innovation of aircraft concepts that encourage to work hard on the existing design components and industrial standards. Moreover, parametric studies [1], [2], [3], and [4] present the influence of nonlinear geometric parameters and boundary conditions in order to distinguish features that make it crucial.

Cantilevers are mostly found in construction that used for overhanging structural elements, particularly in cantilever bridges, tower crane, cantilever retaining walls, and balconies, etc. It is also chosen to design the joined wing of aircrafts.

Furthermore, cantilever beam can be applied to a variety of applications, such as aircraft wings, helicopter blades, Microelectromechanical systems (MEMS), and high-rise building. There are two types of loading that may encounter to any system. One is the conservative load (e.g., load due to gravity) where the direction of the load is independent to the path of loading. The other one is the non-conservative load (e.g., friction force, follower force) where the direction of the load depends on the path of the loading. The definition of the follower loads are load paths which rotated with the deformation curve in the analysis of geometric nonlinearity. Some special structures may be loaded by follower force (e.g., air pressure under the aircraft wings, friction force) where its direction depends on path of deflection. Therefore, to fully anticipate the behaviors of a slender structure made of special material (generalized Ludwick's material) under the follower force, one needs to regard the influence of geometric and material nonlinearities inherent in the system.

Moreover, the follower load acting on the cantilever beam can be applied to Micro-electro-mechanical systems (MEMS). For example, MEMS cantilever switch consisting of overhanging beams over a ground electrode [5]. When applying a control voltage between the top pole and the ground plane, cantilever beam is distorted made by electrostatic force. As the beam deforms, the charge redistributes along the conductor's

surface (Fig. 1.7). To further illustrate this point, some joint wings of the aircraft and the MEMS accelerometer related to this research are presented.

As a consequence of this issue, researching on large deflection of the cantilever beam with nonlinearities materials becomes of importance. Otherwise, in this research topic is to apply the shooting method incorporated with the seventh-order Runge–Kutta method to solve the governing equations of the nonlinear problems. To investigate the large deflection behavior of the presented problem, the set of governing differential equations can be obtained from the equilibrium equations, moment–curvature relation obeying the generalized Ludwick’s constitutive law and nonlinear geometric relations. The following figures are explained some applications of cantilever beam.

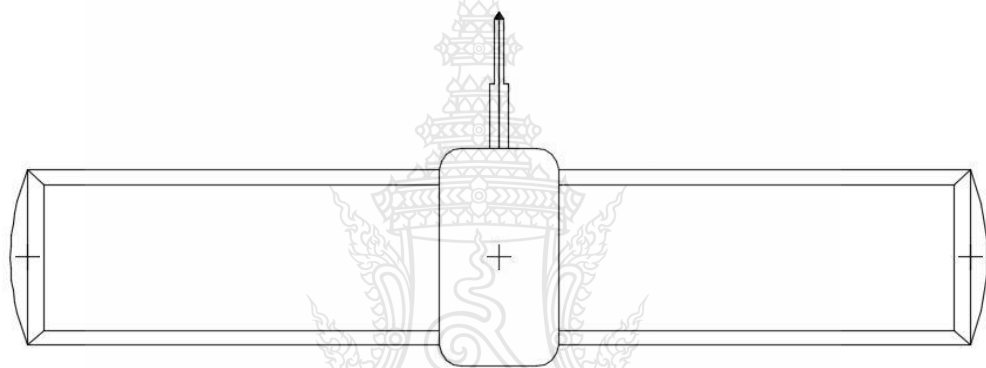


Figure 1.1 Basic box wing configuration

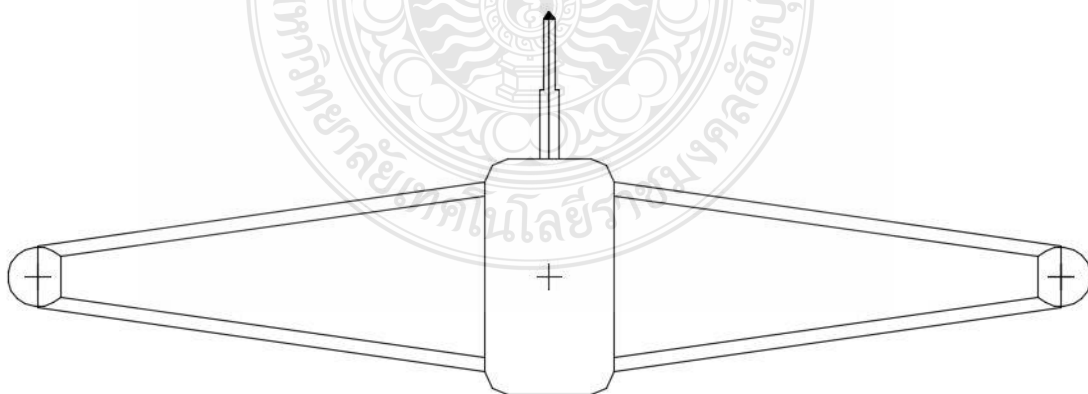


Figure 1.2 Diamond box wing configuration

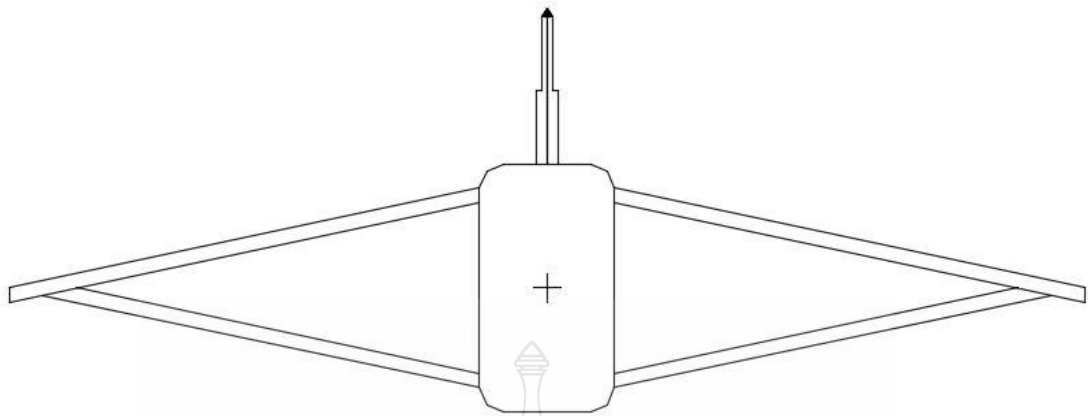


Figure 1.3 Joined wing configuration

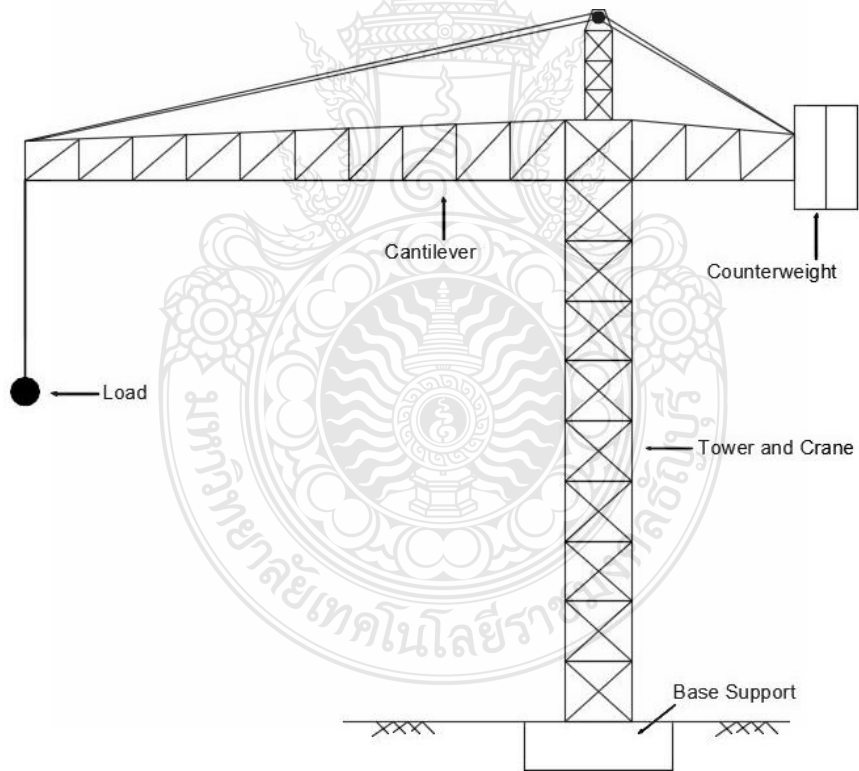


Figure 1.4 Crane configuration

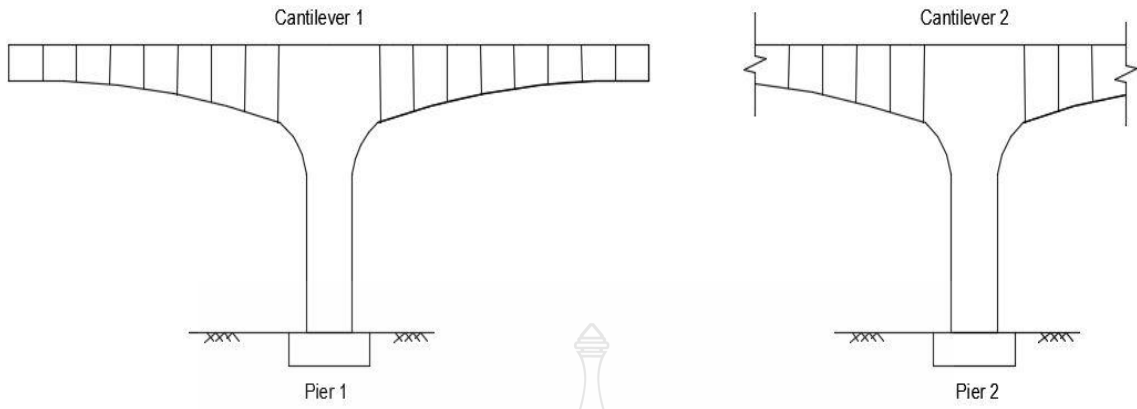


Figure 1.5 Cantilever Bridge configuration

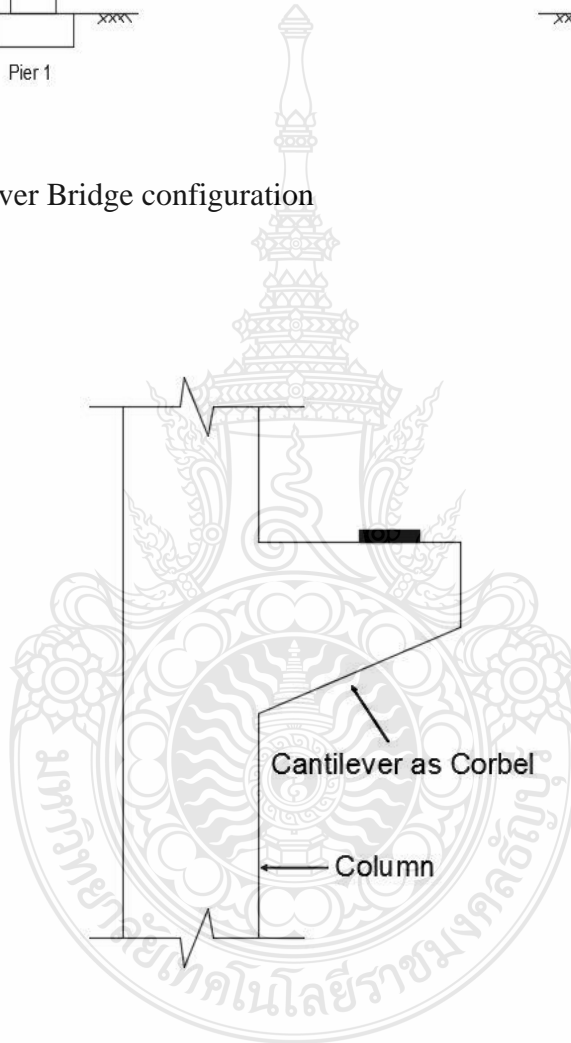
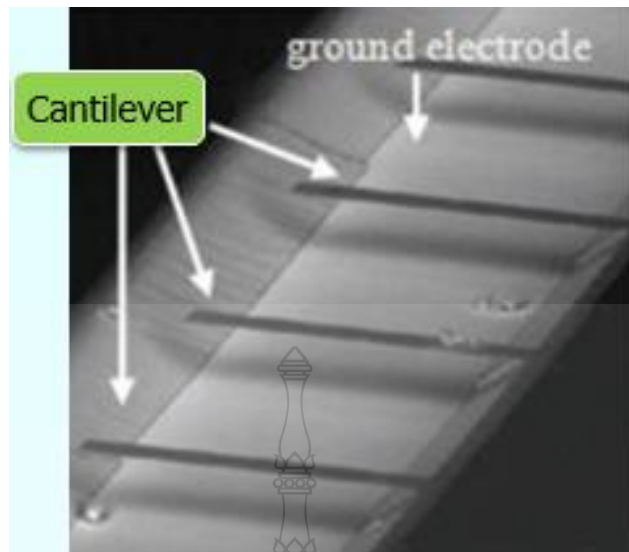
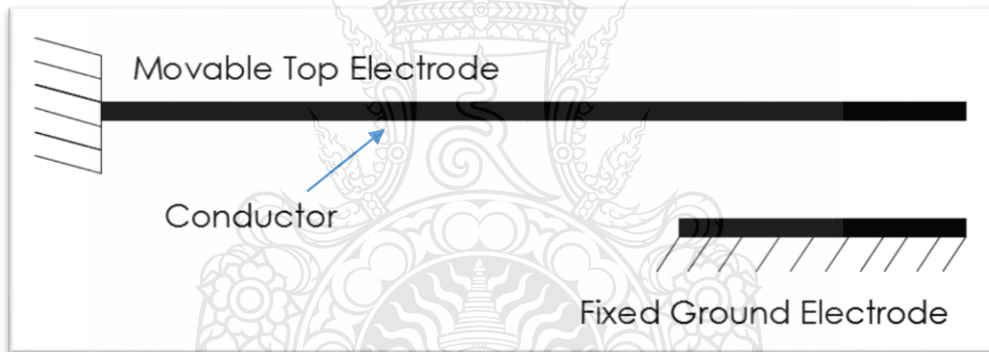


Figure 1.6 Corbel configuration



(a)



(b)

Figure 1.7 MEMS cantilever switch, (a) Image courtesy Advanced Diamond Technologies (b) Modeled geometry (www.thindiamond.com)

1.2 Objectives

1.2.1 Investigate large deflection behavior of a cantilever beam subjected to follower distributed load made from nonlinearly materials obeying generalized Ludwick's constitutive law.

1.2.2 Study the effect of nonlinearity materials on large deflection behavior of the beam obeying generalized Ludwick's constitutive law.

1.3 Hypothesis

The basic assumptions made in the formulation of the present problem studied are as follows:

1.3.1 Material of the beam is made of incompressible, homogeneous, isotropic obeying the generalized Ludwick's constitutive law.

1.3.2 Bernoulli hypothesis is adapted to this study.

1.3.3 Shear deformation is negligible because the beam is considered as a slender member.

1.4 Scope of Study

1.4.1 Cross-section of the beam is rectangular cross-section.

1.4.2 Material properties obey generalized Ludwick's constitutive law.

1.4.3 Two cases of parametric study are considered. One is n and ε_0 are independent and the other is n and ε_0 can be related to each other.

1.4.4 Only static behavior will be considered.

1.5 Conceptual Framework

This research is to analyze the large deflection behavior of a cantilever beam obeying generalized Ludwick's material model subjected to follower distributed load. The governing equations are derived by considering the geometrical and material nonlinearities. A set of highly nonlinear simultaneous first-order differential equations with boundary conditions is set up and numerically solved by using the shooting method incorporated with integration technique employing the seventh-order Runge–Kutta with adaptive step size scheme.

According to the previous mention, the framework of this study can be raised as the followings:

1.5.1 Literatures review.

1.5.2. Mathematical model.

1.5.3 Program codes.

1.5.4 Analyze the results.

1.5.5 Conclusions.

1.6 Contribution to Knowledge

The large deflection behavior of a cantilever beam obeying generalized Ludwick's constitutive law subjected to follower distributed load can be applied to a variety of applications. For example, aerospace structures, especially, joined-wing aircraft is an interesting topic to many researchers. According to related works, several of them [6], [7], [8], [9], and [10] described the large deflection of a cantilever beam of linear and nonlinear materials subjected to conservative load. While, there is a limited amount of research conducting the cantilever beam subjected to follower distributed load where the material property can be described by the generalized Ludwick's constitutive law. Depending on the lack of research on the problem of generalized Ludwick material under the follower distributed load. Therefore, this research could be a benchmark for the other investigations.

The large deflection of the cantilever beam made from the generalized Ludwick's material under the follower distributed load is studied. Moreover, the mathematical model illustrated the method for carrying out the problem concerning the material and geometric nonlinearities. The stress-strain relationship played an important role to solve the problem of nonlinearly materials such as Polymer, Alloy, Acetal plastic, and Glass fiber [11]. Hence in this research, the study in effects of material nonlinearity becomes more important and interesting research topic. Some contributions are listed as the following.

1.6.1 Realize the behavior of a cantilever beam subjected to follower distributed load made from nonlinearly materials obeying generalized Ludwick's constitutive law.

1.6.2 Know about the effects of the material nonlinearity (n and ε_0) which influence on the behavior of the cantilever beam.

1.6.3 Benchmark for the other investigators.

CHAPTER 2

REVIEW OF THE LITERATURE

2.1 General

Slender structural elements, such as beams and columns, usually found in the parts of the structures. These elements may have a deformation with large deflections but small strains. That is why the analysis of geometrical nonlinearities must be established to carry out the problem in this research study. The analysis of geometrical and material nonlinearities thus often goes with some engineering applications such as marine risers/pipes, marine cables, car tires, and aerospace structures, etc.

In order to solve the large deflection problem, the Elastica theory is generally utilized. The Elastica is the equilibrium shape (large displacement) based on Euler's theory. Thus in this research the Euler-Bernoulli beam theory is selected to deal with the problem of large deflection of a cantilever beam.

In the Euler-Bernoulli beam theory that is presented here, the exact curvature relation can be expressed by

$$\kappa = \frac{1}{\rho} = \frac{d\theta}{ds} = \frac{\frac{d^2 y}{dx^2}}{\left[1 + \left(\frac{dy}{dx}\right)^2\right]^{\frac{3}{2}}}. \quad (2.1)$$

When the slope $\frac{dy}{dx}$ is considered to be small, the curvature expression becomes

$$\frac{d^2 y}{dx^2} = \frac{1}{\rho} \cong \frac{M}{EI}. \quad (2.2)$$

Hence the equation (2.2) can be applied to analyze the deflection of the beam-column in the case of the small deflection. However, this theory is supposed to give good results for small deflections of a beam.

In some cases, large deflections can be occurred when the material properties are in elastic material. In this case, the equation (2.2) cannot be employed to solve the large deflection problem. To analyze large deflection, the exact curvature relation appeared in equation (2.1) is chosen to handle the problem. Moreover, to deal with the nonlinear differential equations, some methods are introduced to solve the problem such

as the elliptic integrals method, and the shooting method incorporated with Runge-Kutta, etc.

As revealed in equation (2.1), it can be seen that $\frac{dy}{dx} = \tan \gamma$. In case of $\gamma \ll 1$ (small deflection), then we can get $\tan \gamma \approx \gamma$. After making a comparison between large and small deflection with the relationship between γ^2 and $(\tan \gamma)^2$, the following graph (Fig. 2.1) is chosen to describe in order to give the information when the large deflection equation should be utilized. Furthermore, it can be concluded that when the differences between γ^2 and $(\tan \gamma)^2$ is larger than 1%, the large deflection behavior is initially presented.

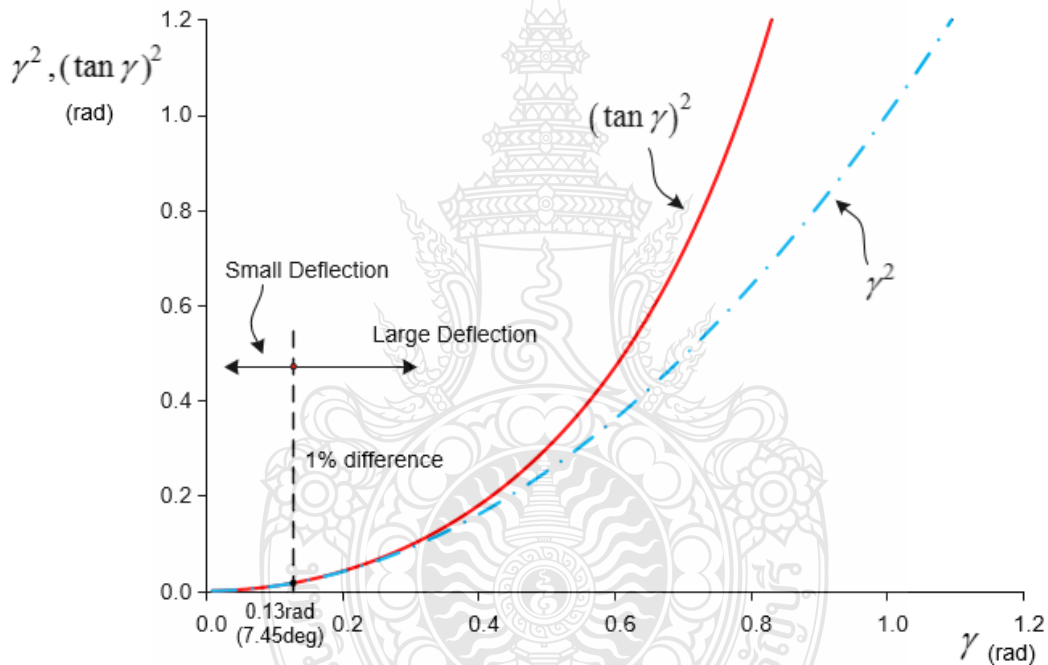


Figure 2.1 Relationships between γ^2 and $(\tan \gamma)^2$

Nowadays nonlinear elastic materials are applied to many nonlinear analysis of structural elements such as Ludwick's material, generalized Ludwick's material, etc. Furthermore, the purpose of this research is to study the effects of the degree of material nonlinearity parameters ε_0 and n on the large deflection behavior of a cantilever beam obeying generalized Ludwick's material model subjected to a follower distributed load. The Euler-Bernoulli beam theory and the inner bending moment–curvature relationship are employed to acquire the governing equations. The shooting method and seventh order

Runge–Kutta method are employed to get the numerical solution of the large deflection problem of a cantilever beam.

Generally, most of the structures in civil engineering are behaved in linear elastic behavior due to the serviceability purpose. Aside from these, nonlinear elastic behavior always occurs in slender structures, especially found in aerospace applications (e.g., joint-wing of the aircraft affected by wind propulsion like cantilever beams). The modeling and the computational process are complicated. Thus the analysis of geometrical nonlinearities must be utilized to deal with the problem. The shooting method incorporated with Runge-Kutta are also proposed to solve nonlinear elastic behavior.

2.2 Related Research

There are many contributions related to the analysis of material nonlinearities of structural elements. Furthermore, the main purposes in the previous research studies perceive only the geometrical nonlinearities. In the last few decades, the problem of large deflection of a cantilever beam obeying generalized Ludwick's material model subjected to a follower distributed load has not been investigated by many researchers. Most contributions related to the problem are revealed as below.

2.2.1 Linear Material

Rao and Roa [12] studied large-deflection of a cantilever beam subjected to a rotational distributed loading. The model formulation is formulated by nonlinear differential equation of the second order. Meanwhile, the large deflection problem of cantilever beam subjected to a follower force and direct method for analysis of the flexible cantilever beams subjected to a follower forces, respectively, were considered by Shvartsman [13] and [14]. However, Kocaturk et al. [6] investigated the large deflection static analysis of a cantilever beam subjected to a point load. The method of nonlinear finite element is introduced. Phungpaingam et al. [15] investigated the post-buckling of beam subjected to follower. The elastica theory and the shooting method are applied to carry out the numerical results. Furthermore, the shooting method is set up to solve the problem of the large deflection of a cantilever beam with geometric nonlinearity [16]. While, Chen [17] proposed an integral approach for large deflection cantilever beams. The moment integral treatment are formulated to get the numerical solution. Otherwise, large deflections of a cantilever beam under an inclined end load studied by Mutyalarao et al [7]. Nallathambi et al. [18] described large deflection of constant curvature cantilever beam under follower load. The fourth order Runge–Kutta method and shooting method are proposed to get the numerical solution. And another is Kang and Li [19] established large and small deformation theories to solve the problem of the bending of functionally graded cantilever beam with power-law nonlinearity subjected to an end force. The

problem of application of the differential transformation method and variational iteration method to large deformation of cantilever beams under point load were considered by Salehi et al. [20]. The differential transformation method (DTM) and the variational iteration method (VIM) are proposed to get the results. However, Lu Li and Rong Li [21] focused on studying nonlinear bending of a cantilever beam subjected to a tip concentrated follower force. The theory of geometric material nonlinearities is applied to formulate the governing equations accompanies the shooting method to get the numerical results. One more thing is the model study and active control of a rotating flexible cantilever beam was dealt by Cai, G.P. et al. [22]. The finite element discretization method and Hamilton theory are proposed to carry out the numerical results. Moreover, Xiang et al. [23] researched on nonlinear analysis of a cantilever elastic beam under non-conservative distributed load. The numerical results are solved by using the shooting method. Taking a look at this problem, Kim, J.O. et al. [24] employed finite element method to deal with beam stability on an elastic foundation subjected to distributed follower force.

Vazquez-Leal, et al. [25] examined the approximations for large deflection of a cantilever beam under a terminal follower force and nonlinear pendulum. The homotopy perturbation method and Laplace-Padé post treatment are established to solve the problems. Otherwise, the effect of subtangential parameter on the stability and dynamic of a cantilever tapered beams subjected to follower forces was researched by Auciello [26]. The variational approach with orthogonal polynomials is established to deal with the problem of the stability and dynamic of a cantilever tapered beams.

Another application of the cantilever beam problem can be proposed to Micro-electro-mechanical systems (MEMS). Presently, cantilever beam MEMS are very popular to many researchers to analyze and design new materials or structures to meet the requirement of the micro devices [27]. Otherwise, cantilever beam MEMS can be found in MEMS switch [28], atomic force microscopes [29], electronic filters [30], MEMS resonator [31], and data storage devices [32].

Last but not least, the following related researches are illustrated the nonlinear elastic Ludwick material.

2.2.2 Non-linear Elastic Ludwick Material

Determining large deflections for combined load cases made of Ludwick material by means of different arc length assumptions was investigated by Eren [33]. For mathematical formulation, materials of geometric nonlinearities are mentioned. The theory of Euler–Bernoulli is established to compute the horizontal and vertical deflections. Furthermore, Brojan et al. [8] analyzed non-prismatic nonlinearly elastic cantilever beams subjected to an end moment. The material is made of the Ludwick constitutive law. Moreover, Athisakul et al. [34] applied the shooting method to carry out

the numerical results with the problem of the effect of material nonlinearity on large deflection of variable-arc-length beams subjected to uniform self-weight.

One more interesting work is that Lee [9] investigated large deflection of cantilever beams of nonlinear elastic material under a combined loading. The shearing force formulation is set up to formulate the governing equation to solve the problem. Butcher's fifth order Runge–Kutta method is employed to compute the numerical results. Narmluk et al. [35] also observed the large deflections of cantilever beams made of non-linear elastic material under a follower tip loading obeying Ludwick's constitutive law. The shooting method and Runge-Kutta-Fehlberg integration technique are proposed to carry out the problem. Last but not least, the problem of Semi-exact solutions for large deflections of cantilever beams of non-linear elastic behavior was investigated by Solano-Carrillo [11].

Borboni and Santis [10] dealt with the problem of large deflection of a non-linear, elastic, asymmetric Ludwick cantilever beam subjected to horizontal force, vertical force and bending torque at the free end. The Euler–Bernoulli beam theory was created to solve the problem. Otherwise, large deflections of cantilever column made from Ludwick's material model under tension from guyed cable was proposed by Phonok [36]. The moment-curvature expression is formulated to establish the governing equations to deal with the problem. The shooting method and Runge-Kutta integration technique are applied to get the numerical results. And, the non-linear material used in this research study $n=0.5, 1.0, 2.0$ and 3.0 .

2.2.3 Non-linear Elastic Generalized Ludwick Material

Brojan et al. [1] dealt with the large deflections of non-linearly elastic non-prismatic cantilever beams made from materials obeying the generalized Ludwick constitutive law. In the model formulation, the moment-curvature formula was set up to get the the governing equations and the boundary conditions in order to solve the problem. The similar problems of generalized Ludwick constitutive law are post-buckling of linearly tapered column and simply supported column made of nonlinear elastic materials obeying the generalized Ludwick constitutive law were studied by Saetiew and Chucheepsakul [2] and [3], respectively. The geometrical material nonlinearities are employed to formulate the governing equations. The shooting method is selected to carry out the numerical results. Last but not least, Brojan et al. [37] illustrated on static stability of nonlinearly elastic Euler's columns obeying the modified Ludwick's law. Four system states in static equilibrium are perceived as neutral, unstable, locally stable, and globally stable state.

As described literatures above, it was remarkable that research studies on the behavior of the large deflection problems that are made of material nonlinearities have carry out mostly the cantilever beams and columns. Only the small amount of research

studies handled the problem with a slender, follower distributed load cantilever beam. Brojan et al. [4] considered the large deflections of non-prismatic nonlinearly elastic cantilever beams subjected to non-uniform continuous load and a concentrated load at the free end obeying generalized Ludwick's constitutive law.

Nonetheless, up to this time the large-deflection of a cantilever beam obeying generalized Ludwick's material model subjected to a follower distributed load has not been yet clarified elsewhere.

By perceiving the effects of geometrical and material nonlinearities, the governing equations obtained for the large deflection behavior are highly nonlinear. Generally, the closed-form solutions cannot be employed in this situation. The shooting method is then required and played a vital role to obtain numerical solutions.



CHAPTER 3

MATHEMATICAL MODEL

3.1 Assumption of the Analysis

This research is to analyze the large deflection behavior of a cantilever beam obeying generalized Ludwick's material model subjected to follower distributed load. The geometrical and material nonlinearities are employed to get the governing equations. Moreover, a set of highly nonlinear first-order differential equations with boundary conditions is set up and carried out numerically by using the shooting method incorporated with integration technique employing the seventh-order Runge–Kutta with adaptive step size control, as already mentioned in conceptual framework in chapter 1.

3.2 Model Description

Displayed in Fig. 3.1, OB is the length of cantilever beam subjected to a follower distributed load (w) with the undeformed configuration. Under loading, the beam undergoes large deflection and the deformed shape of the cantilever beam is presented by OA (Fig. 3.2). After deflection, the direction of the distributed load remains perpendicular to the axis of the beam. Moreover, in the research study, the intrinsic coordinate systems are s and θ . It is also required to carry out the tip angle α , the deflections at the tip of the cantilever beam X_o, Y_o , and the deformed configuration for follower distributed load.

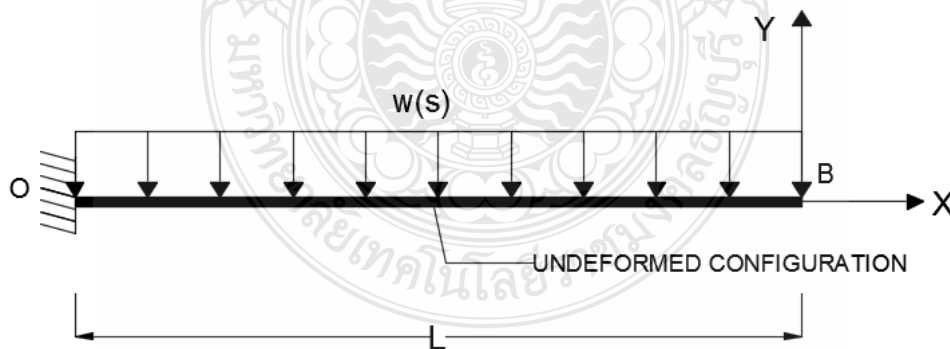


Figure 3.1 A cantilever beam subjected to the follower distributed load with undeformed configuration

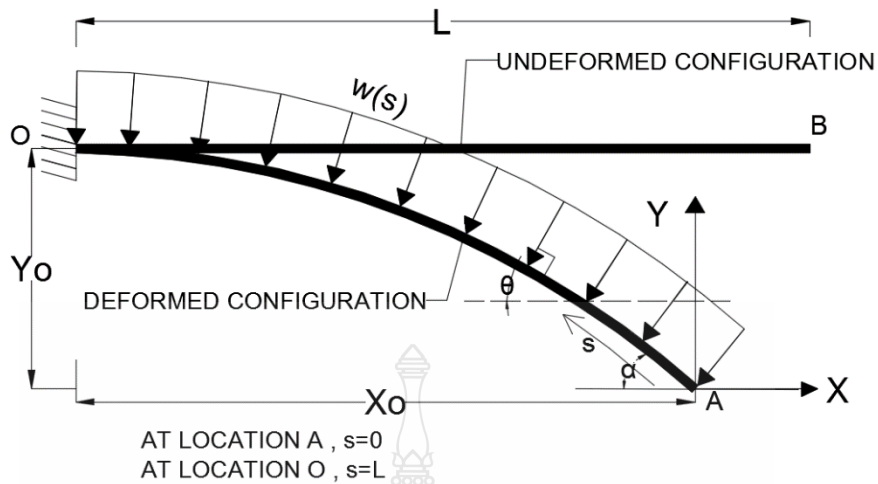


Figure 3.2 A cantilever beam subjected to the follower distributed load with deformed configuration

3.3 Stress-strain Relationships

The equilibrium of moment, geometric relationships, and constitutive relationships are employed to get the mathematical formulation. A set of strongly nonlinear differential equations is acquired to illustrate the deformed shape of the cantilever beam subjected to a follower distributed load, as shown in Fig. 3.2. The solution procedures are also behaved in this section.

3.3.1 Constitutive relationships

The generalizations of the Hooke's law named Ludwick-type nonlinear elastic constitutive formula is chosen to describe the nonlinear elastic behavior. Its nonlinear stress-strain relationship can be written as shown below.

$$\sigma = \begin{cases} E|\varepsilon|^{1/n} & ; \varepsilon \geq 0, \\ -E|\varepsilon|^{1/n} & ; \varepsilon < 0. \end{cases} \quad (3.1)$$

where σ normal stress

ε normal strain (for tensile $\varepsilon \geq 0$ and compressive $\varepsilon < 0$ domain)

E material constant

n dimensionless parameter indicating the degree of material nonlinearity

The nonlinear elastic material is “soft” for $n < 1$, i.e., decreasing modulus of the material $d\sigma/d\varepsilon$. Otherwise, nonlinear elastic material is “hard” for $n > 1$, i.e., increasing modulus of the material $d\sigma/d\varepsilon$. Obviously, the case of linear elastic (Hookean) material corresponds to $n = 1$.

However, Ludwick’s model (nonlinear) which is a generalization of the Hooke’s model embraces a description of elastic behavior of a wider range of materials but is not so mathematically compliant. Besides that, it has a major deficiency. Namely, the stress gradient is infinite (or zero) for sufficiently small strains, Fig. 3.3. Since it is impossible to demonstrate the actual material behaviors, Jung and Kang [38] suggested a generalized form of the Ludwick constitutive law, mathematically described by the following expression,

$$\sigma = \begin{cases} E \left\{ (|\varepsilon| + \varepsilon_0)^{1/n} - \varepsilon_0^{1/n} \right\} & ; \varepsilon \geq 0, \\ -E \left\{ (|\varepsilon| + \varepsilon_0)^{1/n} - \varepsilon_0^{1/n} \right\} & ; \varepsilon < 0. \end{cases} \quad (3.2)$$

in which an additional parameter ε_0 is supplemented to prevent those shortcomings.

Three parameters E, n and ε_0 are employed to develop the generalized Ludwick’s constitutive law and applied to carry out the stress-strain curves acquired by the previous experiments. As a result of Eq. (3.2), setting $\varepsilon_0 = 0$ leads to Ludwick-type material; therefore, the Hooke’s law is acquired by setting $n = 1$.

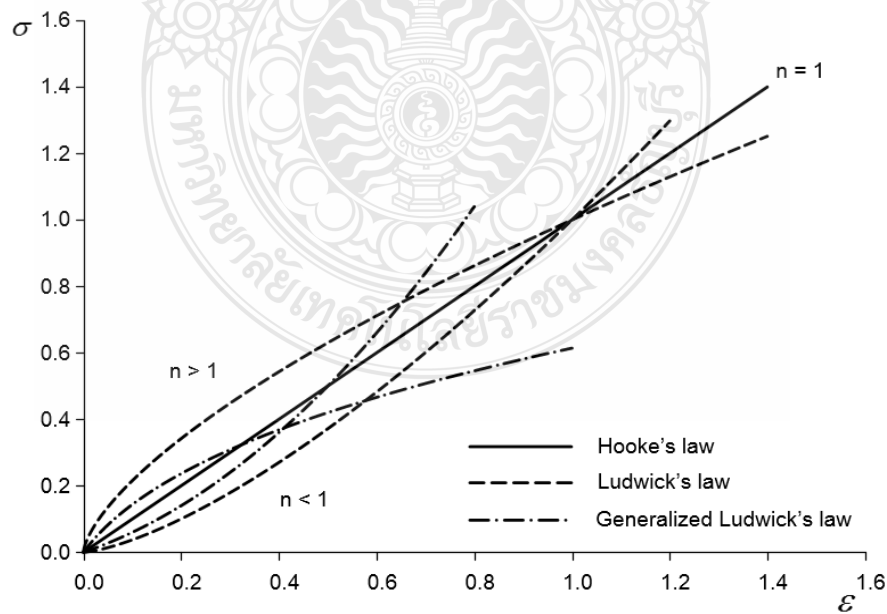


Figure 3.3 Stress–strain relationships in tensile domain

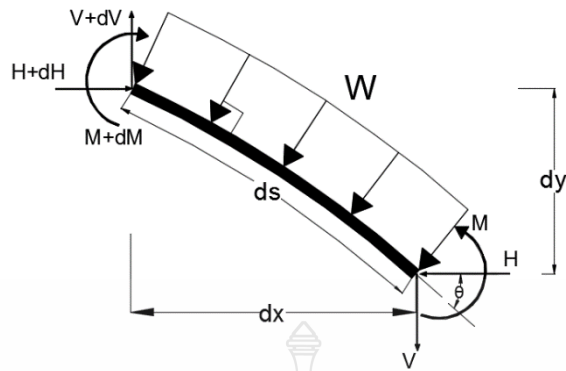


Figure 3.4 Free-body diagram of an infinitesimal element of the beam

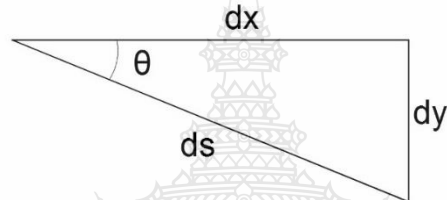


Figure 3.5 Geometric relationship of beam element

The inner bending moment of a beam can be revealed with normal stress σ at any cross-section as shown in Fig. 3.6.

$$M = - \int_A \sigma y dA. \quad (3.3)$$

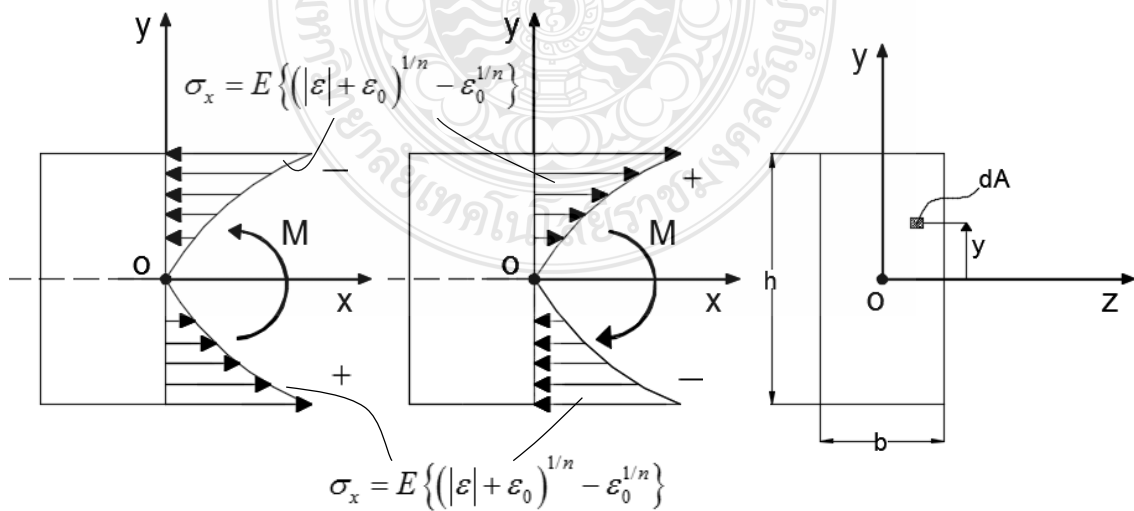


Figure 3.6 Stress distribution of generalized Ludwick's type of the beam

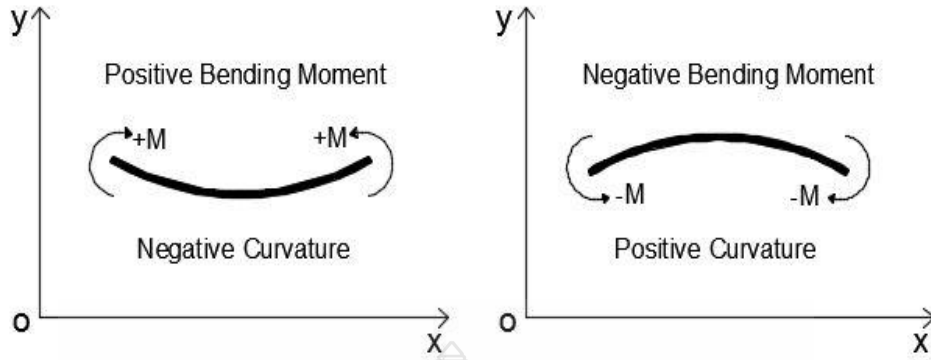


Figure 3.7 Positive and negative of bending moment and curvature relations

Where σ is related to the corresponding strain in compression and tension, see Eq. (3.2). Let $dA = bdy$ be the infinitesimal cross-sectional area of the beam. Furthermore, employing the expression of normal strain-curvature $\varepsilon = -\kappa y$; hence

$$M = \int_A E \left[(|\varepsilon| + \varepsilon_0)^{1/n} - \varepsilon_0^{1/n} \right] y dA. \quad (3.4)$$

After some work, the inner bending moment-curvature utilizing material nonlinearities of cantilever beam obeying the generalized Ludwick's constitutive law can be obtained as follows:

$$M = Eb \left[\left(\kappa \frac{h}{2} + \varepsilon_0 \right)^{\frac{n+1}{n}} \left[\frac{\kappa h n (n+1) - 2n^2 \varepsilon_0}{\kappa^2 (2n+1)(n+1)} \right] + \frac{2n^2 \varepsilon_0^{\frac{2n+1}{n}}}{\kappa^2 (2n+1)(n+1)} - \varepsilon_0^n \frac{h^2}{4} \right]. \quad (3.5)$$

Having done this, by setting $\varepsilon_0 = 0$ into Eq. (3.5), the inner bending moment-curvature relationship of Ludwick-type is acquired.

$$M = EI_n (\kappa)^{\frac{1}{n}}, \quad (3.6a)$$

$$\text{where } I_n = \left(\frac{1}{2} \right)^{\frac{n+1}{n}} \left(\frac{n}{2n+1} \right) b h^{(2n+1)}. \quad (3.6b)$$

Otherwise, by specifying the value $n = 1$ into Eq. (3.6), the inner bending moment–curvature relationship of Hooke’s law is achieved.

$$M = EI_0\kappa, \quad (3.7)$$

in which $I_0 = \frac{bh^3}{12}$ is the moment of inertia of the rectangular cross-sectional area.

The result by differentiating Eq. (3.5) once with respect to the arc length s reveals:

$$\frac{dM}{ds} = E \left[\frac{b \left(\frac{\kappa h}{2} \right) (n+1) \left(\kappa \frac{h}{2} + \varepsilon_0 \right)^{\frac{1}{n}} h}{\kappa^2 (2n+1)} - \frac{bn\varepsilon_0 \left(\kappa \frac{h}{2} + \varepsilon_0 \right)^{\frac{1}{n}} h}{\kappa^2 (2n+1)} - \frac{bn \left(\kappa \frac{h}{2} + \varepsilon_0 \right)^{\frac{n+1}{n}} h}{\kappa^2 (2n+1)} \right. \\ \left. + \frac{b4n^2\varepsilon_0 \left(\kappa \frac{h}{2} + \varepsilon_0 \right)^{\frac{n+1}{n}}}{\kappa^3 (2n+1)(n+1)} - \frac{b4n^2\varepsilon_0^{\frac{2n+1}{n}}}{\kappa^3 (2n+1)(n+1)} \right] \frac{d\kappa}{ds}, \quad (3.8)$$

$$\frac{dM}{ds} = EI_{n\kappa} \frac{d\kappa}{ds}, \quad (3.9a)$$

where

$$I_{n\kappa} = b \left[\frac{\left(\frac{\kappa h}{2} \right) (n+1) \left(\kappa \frac{h}{2} + \varepsilon_0 \right)^{\frac{1}{n}} h}{\kappa^2 (2n+1)} - \frac{n\varepsilon_0 \left(\kappa \frac{h}{2} + \varepsilon_0 \right)^{\frac{1}{n}} h}{\kappa^2 (2n+1)} - \frac{n \left(\kappa \frac{h}{2} + \varepsilon_0 \right)^{\frac{n+1}{n}} h}{\kappa^2 (2n+1)} \right. \\ \left. + \frac{4n^2\varepsilon_0 \left(\kappa \frac{h}{2} + \varepsilon_0 \right)^{\frac{n+1}{n}}}{\kappa^3 (2n+1)(n+1)} - \frac{4n^2\varepsilon_0^{\frac{2n+1}{n}}}{\kappa^3 (2n+1)(n+1)} \right]. \quad (3.9b)$$

3.4 Governing Equations

The theory of elastica is applied to get a set of governing equations. Applying the equilibrium equations, bending moment-curvature, and the geometric relations to the infinitesimal element ds of the deformed beam Fig. 3.4 and 3.5, the set of differential equations this can be obtained as:

$$\frac{dx}{ds} = \cos \theta, \quad (3.10)$$

$$\frac{dy}{ds} = \sin \theta, \quad (3.11)$$

$$\frac{dV}{ds} = w \cos \theta, \quad (3.12)$$

$$\frac{dH}{ds} = w \sin \theta, \quad (3.13)$$

$$\frac{dM}{ds} = -(V \cos \theta + H \sin \theta). \quad (3.14)$$

By substituting Eq. (3.14) into Eq. (3.9), this can be achieved.

$$\frac{d\kappa}{ds} = \frac{-(V \cos \theta + H \sin \theta)}{EI_{nk}}, \quad (3.15)$$

$$\frac{d\theta}{ds} = \kappa. \quad (3.16)$$

The following non-dimensional terms are demonstrated to improve the generality in the computational process.

$$\left. \begin{aligned} \bar{x} &= \frac{x}{L}, & \bar{y} &= \frac{y}{L}, & \bar{s} &= \frac{s}{L}, & \bar{\kappa} &= \kappa L, \\ \bar{w} &= \frac{wL^3}{EI_0}, & \bar{V} &= \frac{VL^2}{EI_0}, & \bar{b} &= \frac{b}{L}, & \bar{h} &= \frac{h}{L}, \\ \bar{I}_0 &= \frac{I_0}{L^4}, & \bar{I}_{nk} &= \frac{I_{nk}}{L^4}, & \bar{M} &= \frac{ML}{EI_0}, & \bar{H} &= \frac{HL^2}{EI_0}. \end{aligned} \right\} \quad (3.17)$$

As mentioned earlier, by employing the non-dimensional terms above, Eq. (3.9) can be derived in non-dimensional expression as:

$$\frac{d\bar{M}}{d\bar{s}} = \frac{\bar{I}_{n\kappa}}{\bar{I}_0} \frac{d\bar{\kappa}}{d\bar{s}}, \quad (3.18)$$

where

$$\bar{I}_{n\kappa} = \bar{b} \left[\frac{\left(\frac{\bar{\kappa}\bar{h}}{2}\right)(n+1)\left(\bar{\kappa}\frac{\bar{h}}{2} + \varepsilon_0\right)^{\frac{1}{n}}\bar{h}}{\bar{\kappa}^2(2n+1)} - \frac{n\varepsilon_0\left(\bar{\kappa}\frac{\bar{h}}{2} + \varepsilon_0\right)^{\frac{1}{n}}\bar{h}}{\bar{\kappa}^2(2n+1)} - \frac{n\left(\bar{\kappa}\frac{\bar{h}}{2} + \varepsilon_0\right)^{\frac{n+1}{n}}\bar{h}}{\bar{\kappa}^2(2n+1)} \right. \\ \left. + \frac{4n^2\varepsilon_0\left(\bar{\kappa}\frac{\bar{h}}{2} + \varepsilon_0\right)^{\frac{n+1}{n}}}{\bar{\kappa}^3(2n+1)(n+1)} - \frac{4n^2\varepsilon_0^{\frac{2n+1}{n}}}{\bar{\kappa}^3(2n+1)(n+1)} \right], \quad (3.19a)$$

$$\bar{I}_0 = \frac{\bar{b} \cdot \bar{h}^3}{12}. \quad (3.19b)$$

Furthermore, the Eqs. (3.10) – (3.14) can be expressed in the non-dimensional forms as

$$\frac{d\bar{x}}{d\bar{s}} = \cos \theta, \quad (3.20)$$

$$\frac{d\bar{y}}{d\bar{s}} = \sin \theta, \quad (3.21)$$

$$\frac{d\bar{V}}{d\bar{s}} = \bar{w} \cos \theta, \quad (3.22)$$

$$\frac{d\bar{H}}{d\bar{s}} = \bar{w} \sin \theta, \quad (3.23)$$

$$\frac{d\bar{M}}{d\bar{s}} = -(\bar{V} \cos \theta + \bar{H} \sin \theta). \quad (3.24)$$

3.5 Boundary Conditions

The boundary conditions are as follows:

At $\bar{s} = 1$

$$\theta = 0, \bar{x} \neq 0, \bar{y} \neq 0, \bar{V} \neq 0, \bar{N} \neq 0. \quad (3.25)$$

At $\bar{s} = 0$

$$\bar{x} = 0, \bar{y} = 0, \bar{V} = 0, \bar{N} = 0, \theta = \theta_0. \quad (3.26)$$

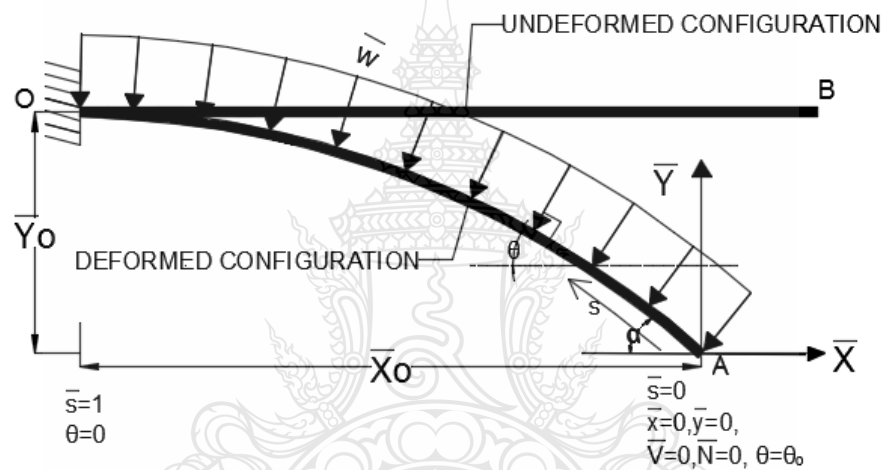


Figure 3.8 Boundary condition of cantilever beam subjected to follower distributed load

CHAPTER 4

RESEARCH METHODOLOGY

4.1 General

In this study, the process is to carry out the effects of the nonlinear materials (n) of the cantilever beam which influence over the large deflections of the beam made from generalized Ludwick's constitutive law under the follower distributed load. According to proposed model, the governing equations with suitable boundary conditions are set up to deal with this problem. Moreover, the solutions of the problem are numerically solved by using the shooting method incorporated with integration technique employing the seventh-order Runge–Kutta with adaptive step size control. After satisfying the boundary condition, the results can be obtained.

4.2 Method of Solution

Since a set of governing equations is a complicated nonlinear differential equation, hence the behavior of the deflected cantilever beam problem is described by numerical solutions.

By substituting Eq. (3.24) into Eq. (3.18) and choosing Eqs. (3.20) – (3.23) of the geometric relationship and free-body diagram of an infinitesimal element of the beam, a set of nonlinear differential equations is achieved:

$$\frac{d\theta}{ds} = \bar{\kappa}, \quad (4.1a)$$

$$\frac{d\bar{\kappa}}{ds} = -(\bar{V} \cos \theta + \bar{H} \sin \theta) \frac{\bar{I}_0}{\bar{I}_{nk}}, \quad (4.1b)$$

$$\frac{d\bar{V}}{ds} = \bar{w} \cos \theta, \quad (4.1c)$$

$$\frac{d\bar{H}}{ds} = \bar{w} \sin \theta, \quad (4.1d)$$

$$\frac{d\bar{x}}{ds} = \cos \theta, \quad (4.1e)$$

$$\frac{d\bar{y}}{ds} = \sin \theta. \quad (4.1f)$$

The boundary conditions of the problem are as follows:

$$\theta(\bar{s} = 0) = \theta_0 \quad \text{and} \quad \theta(\bar{s} = 1) = 0, \quad (4.2a)$$

$$\bar{\kappa}(\bar{s} = 0) = 0 \quad \text{and} \quad \bar{\kappa}(\bar{s} = 1) = 0, \quad (4.2b)$$

$$\bar{x}(\bar{s} = 0) = 0 \quad \text{and} \quad \bar{x}(\bar{s} = 1) = \bar{x}(1), \quad (4.2c)$$

$$\bar{y}(\bar{s} = 0) = 0 \quad \text{and} \quad \bar{y}(\bar{s} = 1) = \bar{y}(1). \quad (4.2d)$$

Two-point boundary value problem of material nonlinearity can be acquired by employing Eq. (4.1) with boundary condition Eq. (4.2), which can be carried out by the shooting method. For a given value of θ_0 , there is an unknown variable (\bar{w}) needs to be computed. The solution steps are listed as follows:

- (1) Assign the dimension of the cross-section in term of non-dimensional parameters (\bar{b} and \bar{h}), and the material constants (n and ε_0) to the problem.
- (2) Given the value of θ_0 and estimate \bar{w} for the first iteration.
- (3) Integrate Eqs. (4.1a) – (4.1f) from $\bar{s} = 0$ to $\bar{s} = 1$ by employing the seventh-order Runge–Kutta method.
- (4) Minimize the objective function Φ as

$$\underset{\bar{w}}{\text{Minimize}} \quad \Phi = |\theta(1)|. \quad (4.3)$$

In the computational process, the value of Φ is required to be less than the tolerance (10^{-7}) for the numerical solutions using the Newton-Raphson iterative scheme.

In the differential equations of material nonlinearity (3.18) and (4.1a)–(4.1b), it is important to realize that singularity can be occurred when setting $\bar{\kappa} = 0$ at the free end. To prevent this shortcoming, we set $\bar{\kappa}(0) = 1 \times 10^{-5}$ instead of zero.

Last but not least, the flow charts for the computational procedures are illustrated in Fig. 4.1 and 4.2 as below.

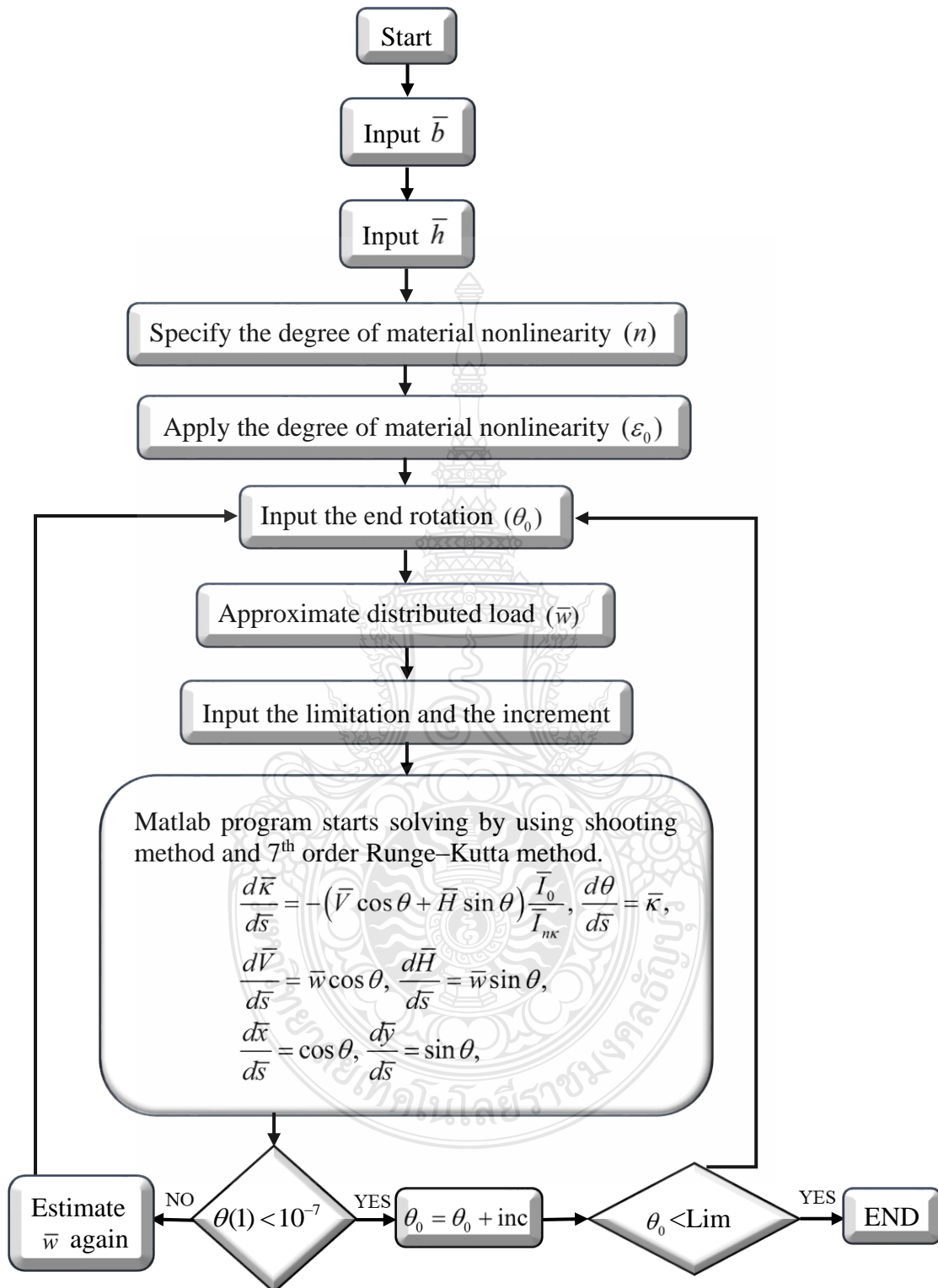


Figure 4.1 Flow chart of computational procedures by using Matlab program 1

The second flow chart is applied $\varepsilon_0 = (2n)^{\frac{n}{1-n}}$ and $\varepsilon_0 = \left(\frac{n}{2}\right)^{\frac{n}{1-n}}$ for $n > 1$ and $n < 1$, respectively (Chapter 5, Case 2).

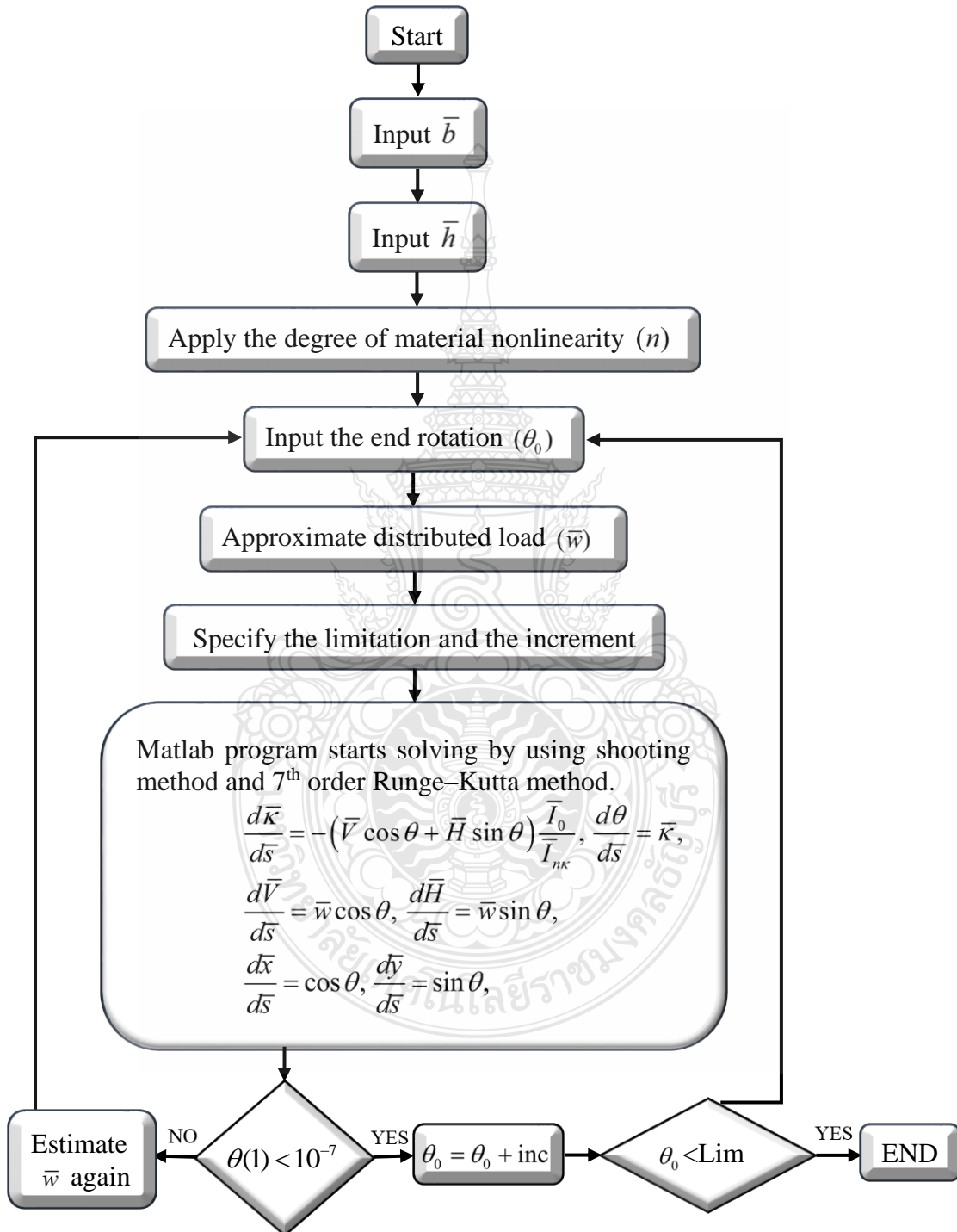


Figure 4.2 Flow chart of computational procedures by using Matlab program 2

CHAPTER 5
RESULTS AND DISCUSSION

This research was analyzed the large deflection behavior of a cantilever beam obeying generalized Ludwick's material model subjected to follower distributed load. In order to deal with the solutions of the problem, the shooting method incorporated with integration technique employing the seventh-order Runge–Kutta is established to get the numerical results comparing with the previous research study [1] investigated the large-deflection behavior of a cantilever beam subjected to a rotational distributed loading which is formulated by means of a second order nonlinear-differential equation.

Having compared the results with Rao and Rao [1], in this research was founded that the values of the rotation angle θ_0 and the follower distributed load \bar{w} are very close to those of Rao and Rao [1] while using $n = 1$. It is also shown in Table 5.1.

Table 5.1 Comparison results between Rao and Rao [1] and the presented study

θ_0		\bar{w}	
deg	rad	Rao and Rao [1]	This research ($n = 1, \varepsilon_0 = 0$)
9.54	0.1665	1.0	0.99980
19.04	0.3323	2.0	1.99978
37.75	0.6589	4.0	4.00016
55.83	0.9744	6.0	6.00041
73.02	1.2744	8.0	7.99981
89.15	1.5560	10.0	9.99972
104.12	1.8172	12.0	11.99933
130.43	2.2764	16.0	16.00006
152.09	2.6545	20.0	19.99959
169.68	2.9615	24.0	24.00033
183.86	3.2090	28.0	28.00096
195.27	3.4081	32.0	32.00189

5.1 Numerical Solutions

In order to study the important parameters, the set of parameters ε_0 and n is divided into two cases. The first case is n and ε_0 are varied independently. Second one is n and ε_0 are related to each other.

To analyze the numerical computations of the large deflections of cantilever beam obeying generalized Ludwick's material model subjected to follower distributed load, the cross-sectional dimensions and length of the cantilever beam are given by the non-dimensional geometric parameters as follows: $\bar{b} = 0.2\text{m}$ and $\bar{h} = 0.2\text{m}$.

5.1.1 Case 1: n and ε_0 are varied independently

To point out the nonlinear constitutive relationships clearly and simply we have chosen the following numerical examples, the rectangular cross-section of cantilever beam is subjected to several different follower distributed loads with the degree of material nonlinearity (n).

Example 1

The case of the cantilever beam with non-dimensional geometric parameters $\bar{b} = 0.2\text{m}$ and $\bar{h} = 0.2\text{m}$ was analyzed first. The nonlinear material parameters that determine are: $\varepsilon_0 = 0.001$ and n varying from 0.50, 0.75..2.00. The results listed in Table 5.2 as shown below.

The result listed in Table 5.2 can be interpreted that when using n varying from 0.50, 0.75..2.00 with nonlinear elastic material $\varepsilon_0 = 0.001$, it is worth noting that the rotation angle θ_0 and the follower distributed load \bar{w} are both increase their values.

Table 5.2 Numerical results for cantilever beam made of the generalized Ludwick nonlinear elastic material: $\varepsilon_0 = 0.001$ and n varying from 0.50, 0.75..2.00

θ_0 (rad)	\bar{w}					
	$\varepsilon_0 = 0.001$					
	$n = 0.50$	$n = 0.75$	$n = 1.00$	$n = 1.50$	$n = 1.75$	$n = 2.00$
0.0	0.000000	0.000000	0.000000	0.000000	0.000000	0.000000
0.2	0.027090	0.351219	1.201348	3.759995	5.044654	6.189575
0.4	0.102706	0.866293	2.410405	5.988260	7.890623	9.176920
0.6	0.243115	1.482040	3.635229	8.003270	10.210257	10.997713
0.8	0.404222	2.181617	4.884284	10.206757	12.268636	13.890772
1.0	0.634518	2.959364	6.166776	12.023368	14.179759	15.832106
1.2	0.922219	3.815147	7.492988	13.791720	16.009048	17.667471
1.4	1.271882	4.752561	8.874687	15.548056	17.802350	19.449509
1.6	1.689311	5.778368	10.251237	17.323316	19.596736	21.219658
1.8	1.181814	6.902510	11.782054	19.147406	21.333519	23.015005
2.0	2.758578	8.138523	13.505596	21.052366	23.309333	24.873164
2.2	3.431161	9.504355	15.280566	23.075574	25.338780	26.836744
2.4	4.214203	11.023700	17.220641	25.263929	27.512862	28.736959
2.6	5.126425	12.728098	19.353487	27.680240	29.824193	31.311607
2.8	6.192100	14.660274	21.790026	30.414219	32.652169	34.001484
3.0	7.443273	16.879618	24.568469	33.429724	35.873586	37.200813
3.14	8.452045	18.648363	26.795681	36.224135	38.556951	39.901154

The relationship of the load-displacement curve for the nonlinearly cantilever beam between the follower distributed load \bar{w} and the rotation angle θ_0 are exhibited with the figure below.

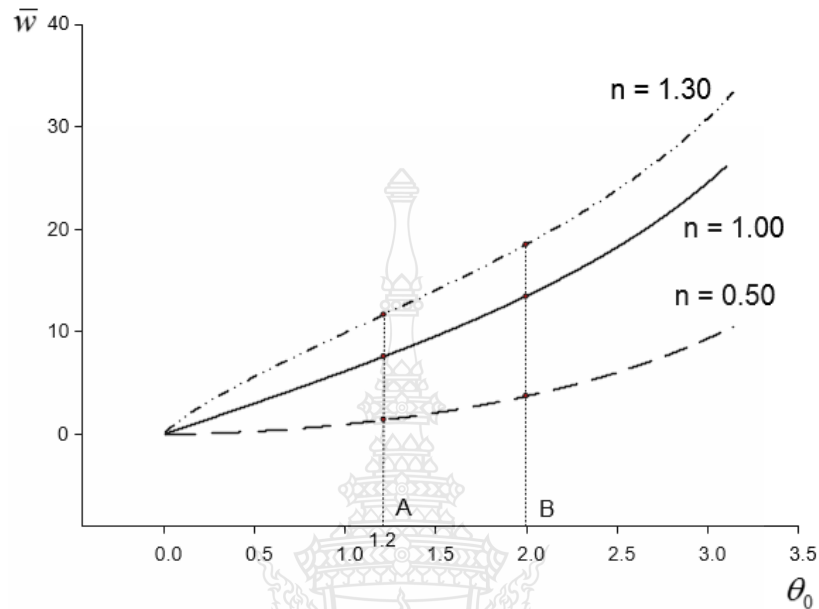


Figure 5.1 Load-displacement curve for the nonlinearly cantilever beam subjected to follower distributed load $\varepsilon_0 = 0.001$

As illustrated in Fig. 5.1, the load–displacement curves of the cantilever beam with various material nonlinearity parameters n are plotted. The behaviors of the cantilever beam for three cases ($n = 1$, $n < 1$, and $n > 1$) with $\varepsilon_0 = 0.001$ are described by using the load–displacement curves (Fig. 5.1).

It should be noted that a linear case $n = 1$ (Fig. 5.1), the well-known load-displacement curve is monotonic and stable. As it can be seen from the Fig. 5.1, the follower distributed load \bar{w} increases as the rotation angle θ_0 increases.

Furthermore, it is remarkable to note that the case of hardening material, where $n > 1$ and $n < 1$ (Fig. 5.1), the follower distributed load \bar{w} and the rotation angle θ_0 both increase in their values.

In addition, the equilibrium configurations for $\theta_0 = 1.2$ and $\theta_0 = 2.0$ are selected to indicate in the Fig. 5.2.

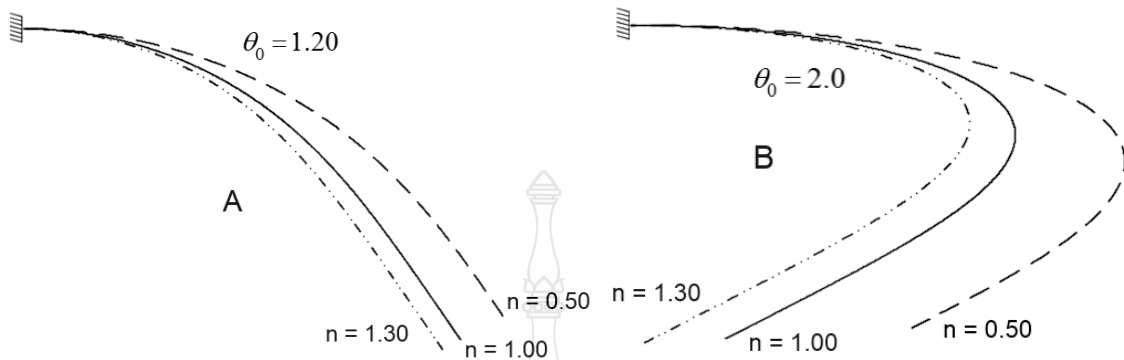


Figure 5.2 Equilibrium configurations for $\theta_0 = 1.2$ and $\theta_0 = 2.0$

Moreover, the nonlinearity material parameters $n = 0.50$, $n = 1$, and $n = 1.30$ are selected to show the deflection configuration in the Fig. 5.3, 5.4, and 5.5, respectively.

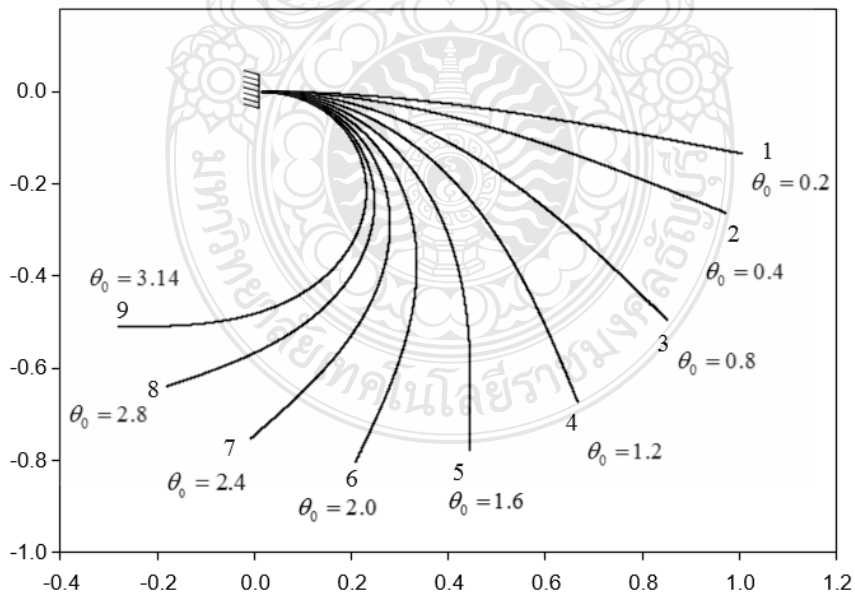


Figure 5.3 Deflection configurations of the nonlinearly cantilever beam subjected to follower distributed load $n = 0.50$

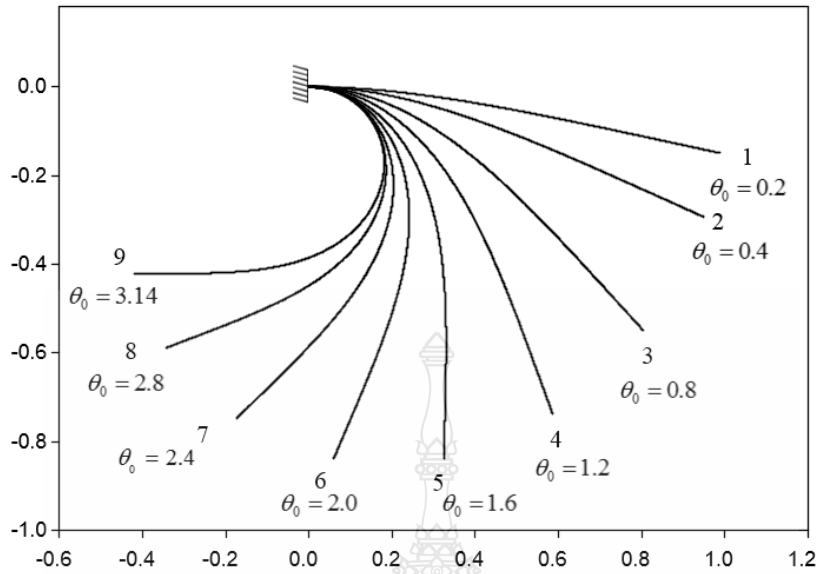


Figure 5.4 Deflection configurations of the nonlinearly cantilever beam subjected to follower distributed load $n = 1$

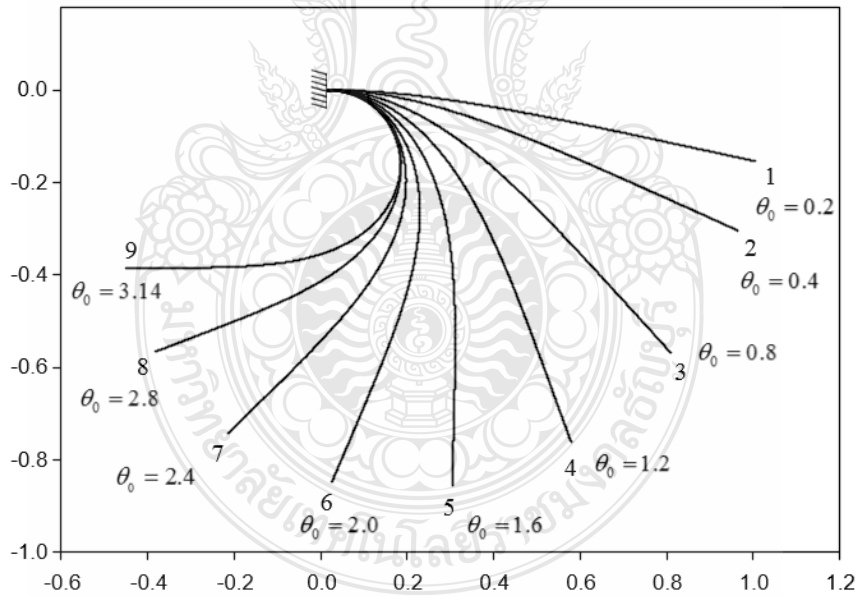


Figure 5.5 Deflection configurations of the nonlinearly cantilever beam subjected to follower distributed load $n = 1.30$

Finally, their deflection configuration results for $n = 0.50$, $n = 1.00$, and $n = 1.30$ are displayed in Table 5.3, 5.4, and 5.5, respectively.

Table 5.3 Numerical results for cantilever beam made of the generalized Ludwick material for $n = 0.50$

Configuration	$n = 0.50$ and $\varepsilon_0 = 0.001$	
	θ_0 (rad)	\bar{w}
1	0.2	2.758578
2	0.4	0.102706
3	0.8	0.404222
4	1.2	0.922219
5	1.6	1.689311
6	2.0	2.758578
7	2.4	4.214203
8	2.8	6.192100
9	3.14	8.452045

Table 5.4 Numerical results for cantilever beam made of the generalized Ludwick material for $n = 1$

Configuration	$n = 1$ and $\varepsilon_0 = 0.001$	
	θ_0 (rad)	\bar{w}
1	0.2	1.201348
2	0.4	2.410405
3	0.8	4.884284
4	1.2	7.492988
5	1.6	10.251237
6	2.0	13.505596
7	2.4	17.220641
8	2.8	21.790026
9	3.14	26.795681

Table 5.5 Numerical results for cantilever beam made of the generalized Ludwick material for $n = 1.30$

Configuration	$n = 1.30$ and $\varepsilon_0 = 0.001$	
	θ_0 (rad)	\bar{w}
1	0.2	2.686490
2	0.4	4.699971
3	0.8	8.234361
4	1.2	11.561950
5	1.6	14.937766
6	2.0	18.566319
7	2.4	22.700362
8	2.8	27.750629
9	3.14	33.369313

As displayed in the figures (5.3, 5.4, and 5.5) and the tables (5.3, 5.4, and 5.5), the deflected shapes with the same slope angle are mostly identical whether the nonlinearity material parameters are selected with different values ($n = 0.50$, $n = 1$, and $n = 1.30$). Otherwise, it is very interesting to take a note that the follower distributed load \bar{w} successively increases while the rotation angle θ_0 increases. But, it is remarkable to note for $n = 0.50$ that the follower distributed load \bar{w} slowly increases near the value of $\theta_0 = 0.8$.

Example 2

As the second example, all the parameters are kept the same as in the first example except $\varepsilon_0 = 0.002$. The results listed in Table 5.6 as shown below.

Table 5.6 Numerical results for cantilever beam made of the generalized Ludwick nonlinear elastic material: $\varepsilon_0 = 0.002$ and n varying from 0.50,0.75..2.00

θ_0 (rad)	\bar{w} $\varepsilon_0 = 0.002$					
	$n = 0.50$	$n = 0.75$	$n = 1.00$	$n = 1.50$	$n = 1.75$	$n = 2.00$
0.0	0.000000	0.000000	0.000000	0.000000	0.000000	0.000000
0.2	0.030000	0.365840	1.390990	3.576958	4.711202	5.533119
0.4	0.108740	0.887916	2.410405	5.986771	7.319147	8.778117
0.6	0.237053	1.509028	3.635229	8.061968	9.661614	11.208064
0.8	0.416733	2.213030	4.884284	9.965219	11.859777	13.319680
1.0	0.650400	2.994707	6.166776	11.773619	13.536827	15.250057
1.2	0.941586	3.854122	7.425458	13.533411	15.584611	17.076075
1.4	1.294879	4.745821	8.874605	15.283949	17.370118	18.849674
1.6	1.716114	5.770527	10.320950	17.018005	19.156962	20.611602
1.8	2.212642	6.951755	11.862522	18.302868	20.978948	22.398432
2.0	2.793697	8.193478	13.505596	20.484577	22.871141	24.247270
2.2	3.470901	9.455371	15.276513	22.388193	24.873694	26.200093
2.4	4.258971	11.084094	17.118820	24.853231	27.027814	28.309105
2.6	5.176734	12.792874	19.370085	27.248978	29.427385	30.644986
2.8	6.248600	14.730014	21.790026	29.172339	32.143407	33.024377
3.0	7.506806	16.955204	24.56884	33.265730	35.338013	36.624828
3.14	8.521145	18.728773	26.79442	35.868720	37.822884	38.729547

The relationship of the load-displacement curve ($\varepsilon_0 = 0.002$) for the nonlinearly cantilever beam between the follower distributed load \bar{w} and the rotation angle θ_0 are demonstrated with the figure below.

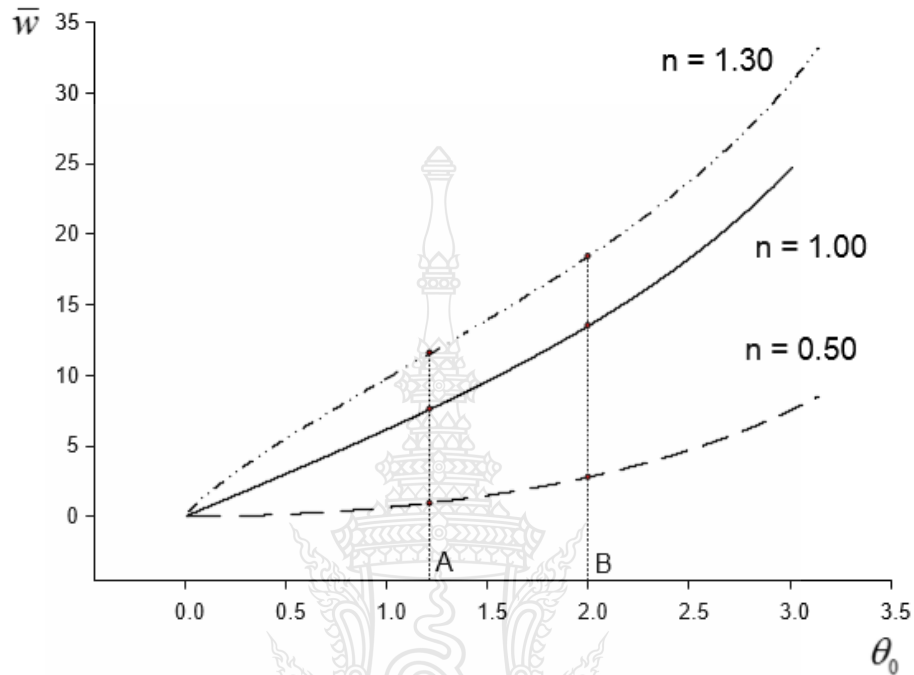


Figure 5.6 Load-displacement curve for the nonlinearly cantilever beam subjected to follower distributed load $\varepsilon_0 = 0.002$

As displayed in Fig. 5.6, the behaviors of the cantilever beam for the nonlinearly parameters $n = 0.50$, $n = 1.00$, and $n = 1.30$ with $\varepsilon_0 = 0.002$ are described by employing the load–displacement curves (Fig. 5.6).

It is worth noting that a linear case $n = 1$ (Fig. 5.6), the well-known load-displacement curve remains monotonic and stable comparing to $\varepsilon_0 = 0.001$. As it can be viewed from the Fig. 5.1, the follower distributed load \bar{w} increases as the rotation angle θ_0 increases.

The equilibrium configurations ($\varepsilon_0 = 0.002$) for $\theta_0 = 1.2$ and $\theta_0 = 2.0$ are selected to indicate in the Fig. 5.7.

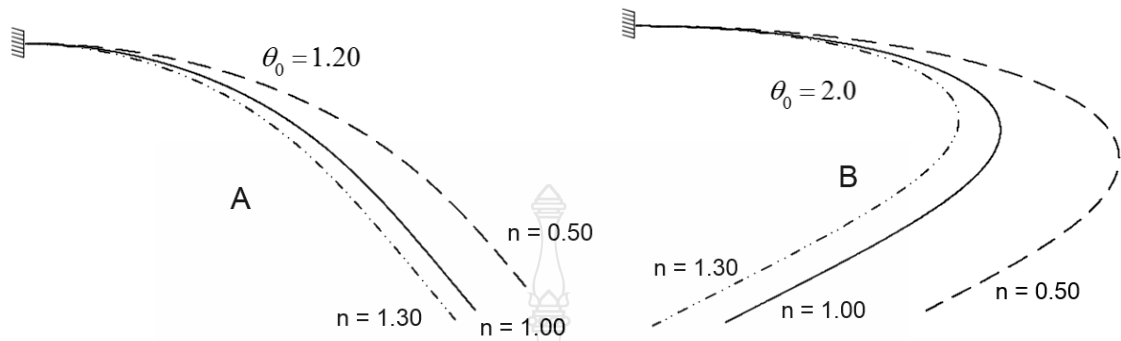


Figure 5.7 Equilibrium configurations for $\theta_0 = 1.2$ and $\theta_0 = 2.0$

Furthermore, the nonlinearity material parameters $n = 0.50$, $n = 1.00$, and $n = 1.30$ are selected to show the deflection configuration in the Fig. 5.8, 5.9, and 5.10, respectively.

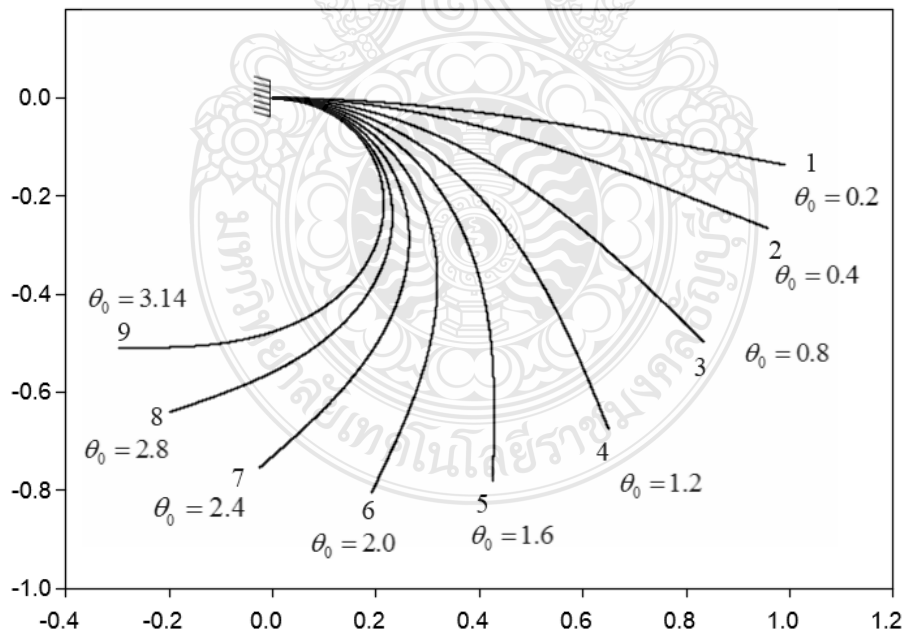


Figure 5.8 Deflection configurations of the nonlinearly cantilever beam subjected to follower distributed load $n = 0.50$

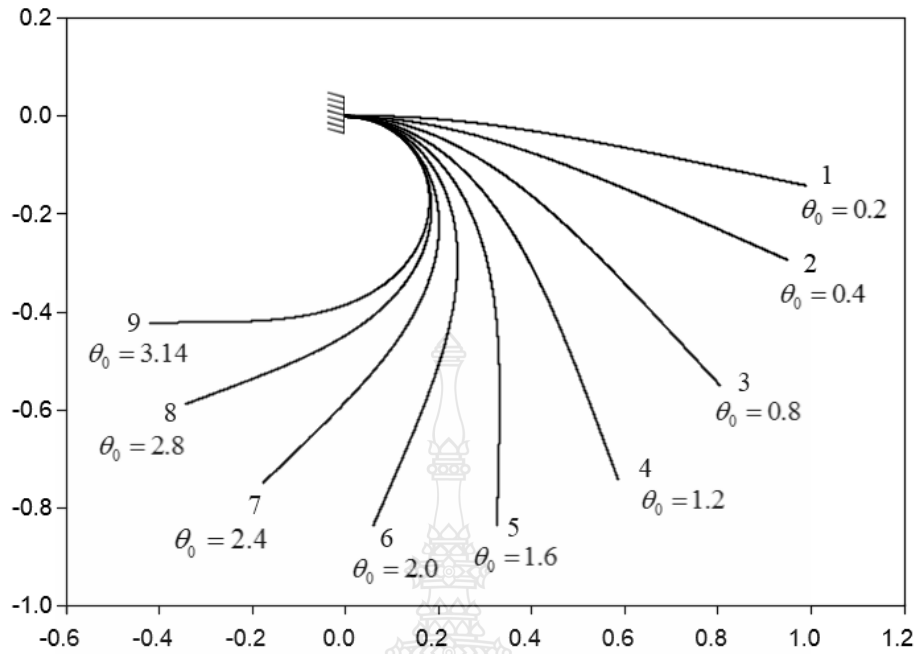


Figure 5.9 Deflection configurations of the nonlinearly cantilever beam subjected to follower distributed load $n = 1.00$

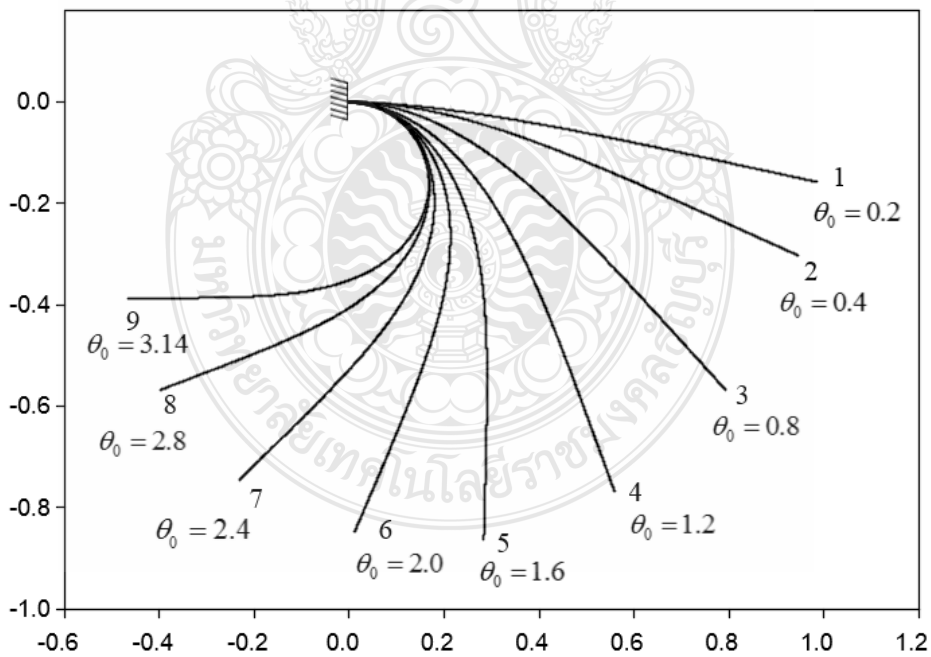


Figure 5.10 Deflection configurations of the nonlinearly cantilever beam subjected to follower distributed load $n = 1.30$

Table 5.7 Numerical results for cantilever beam made of the generalized Ludwick material for $n = 0.50$

Configuration	$n = 0.50$ and $\varepsilon_0 = 0.002$	
	θ_0 (rad)	\bar{w}
1	0.2	0.030000
2	0.4	0.108740
3	0.8	0.416733
4	1.2	0.941586
5	1.6	1.716114
6	2.0	2.793697
7	2.4	4.258971
8	2.8	6.248600
9	3.14	8.521145

Table 5.8 Numerical results for cantilever beam made of the generalized Ludwick material for $n = 1.00$

Configuration	$n = 1.00$ and $\varepsilon_0 = 0.002$	
	θ_0 (rad)	\bar{w}
1	0.2	1.39099
2	0.4	2.410405
3	0.8	4.884284
4	1.2	7.425458
5	1.6	10.32095
6	2.0	13.505596
7	2.4	17.11882
8	2.8	21.790026
9	3.14	26.794424

Table 5.9 Numerical results for cantilever beam made of the generalized Ludwick material for $n = 1.30$

Configuration	$n = 1.30$ and $\varepsilon_0 = 0.002$	
	θ_0 (rad)	\bar{w}
1	0.2	2.389235
2	0.4	4.592765
3	0.8	8.110615
4	1.2	11.118085
5	1.6	14.483269
6	2.0	18.415690
7	2.4	22.421698
8	2.8	27.576021
9	3.14	33.174583

As described in the first example with the nonlinear elastic materials $\varepsilon_0 = 0.001$, the deflected shapes with the same slope angle in the Fig. 5.8, 5.9, and 5.10 are indistinguishable whether the nonlinearity material parameters are chosen with different values ($n = 0.50$, $n = 1$, and $n = 1.30$). It is remarkable for $n = 0.50$ that the follower distributed load \bar{w} slowly increases near the value of $\theta_0 = 1.2$ while others are increasing successively.

Other numerical results for the large deflection of the cantilever beam made of the generalized Ludwick constitutive law are demonstrated as below. The nonlinear elastic materials $\varepsilon_0 = 0.003$ to $\varepsilon_0 = 0.01$ with the degree of material nonlinearity n varying from 0.50, 0.75..2.00 will be chosen to show as the following examples.

Example 3

As the third example, all the parameters are kept the same as in the first example except $\varepsilon_0 = 0.003$. The results listed in Table 5.10 as shown below.

Table 5.10 Numerical results for cantilever beam made of the generalized Ludwick nonlinear elastic material: $\varepsilon_0 = 0.003$ and n varying from 0.50, 0.75..2.00

θ_0 (rad)	\bar{w} $\varepsilon_0 = 0.003$					
	$n = 0.50$	$n = 0.75$	$n = 1.00$	$n = 1.50$	$n = 1.75$	$n = 2.00$
0.0	0.000000	0.000000	0.000000	0.000000	0.000000	0.000000
0.2	0.032822	0.378473	1.201348	3.434369	2.733814	3.810573
0.4	0.114631	0.907267	2.293112	5.822651	7.244021	8.524970
0.6	0.246107	1.533365	3.635229	7.899699	9.525022	10.804016
0.8	0.429035	2.241628	4.884284	9.777679	11.557744	12.634702
1.0	0.666047	3.027102	6.166776	11.578463	13.357236	14.819578
1.2	0.960698	3.890036	7.492988	13.333459	15.456943	16.637830
1.4	1.317599	4.827818	8.874687	15.076714	16.425417	18.403662
1.6	1.742620	5.866771	10.325675	16.848416	18.887403	20.158158
1.8	2.243151	6.997624	11.862520	18.611931	20.571502	21.937452
2.0	2.828475	8.240526	13.505594	20.546486	22.205723	23.778223
2.2	3.510276	9.613594	15.280559	22.557089	24.321443	25.721938
2.4	4.303349	11.140720	17.220642	24.729622	26.492582	27.820101
2.6	5.226624	12.853768	19.370085	27.093822	28.557592	30.142284
2.8	6.304648	14.795595	21.790026	28.627982	31.748275	32.728555
3.0	7.569849	17.026361	24.569119	32.992422	34.921503	35.756704
3.14	8.589725	18.804523	26.795572	35.361549	37.555815	38.208978

Shown in the figure below is the relationship of the load-displacement curve ($\varepsilon_0 = 0.003$) for the nonlinearly cantilever beam between the follower distributed load \bar{w} and the rotation angle θ_0 . As it can be seen from the Fig. 5.11, the follower distributed load \bar{w} increases as the rotation angle θ_0 increases.

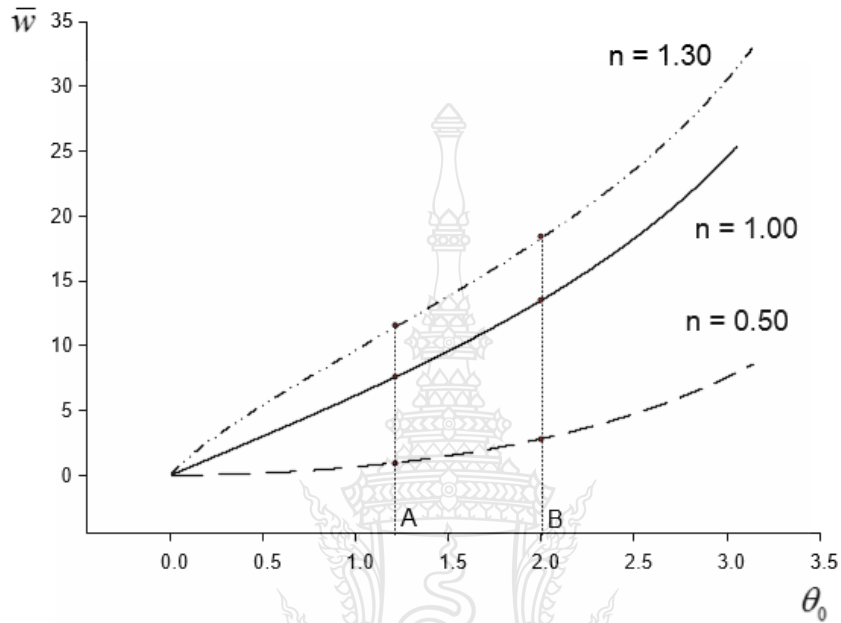


Figure 5.11 Load-displacement curve for the nonlinearly cantilever beam subjected to follower distributed load $\varepsilon_0 = 0.003$

The equilibrium configurations ($\varepsilon_0 = 0.003$) for $\theta_0 = 1.2$ and $\theta_0 = 2.0$ are chosen to demonstrate in the Fig. 5.12.

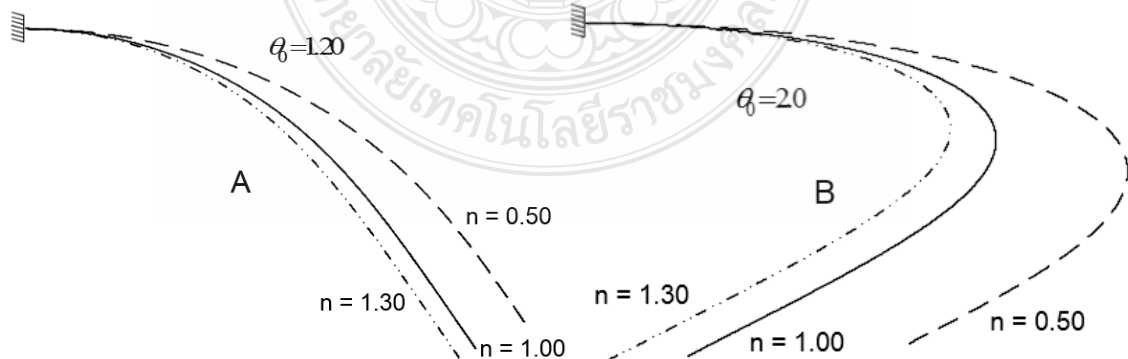


Figure 5.12 Equilibrium configurations for $\theta_0 = 1.2$ and $\theta_0 = 2.0$

The nonlinearity material parameters $n=0.50$, $n=1.00$, and $n=1.30$ are selected to show the deflection configuration in the Fig. 5.13, 5.14 and 5.15, respectively.

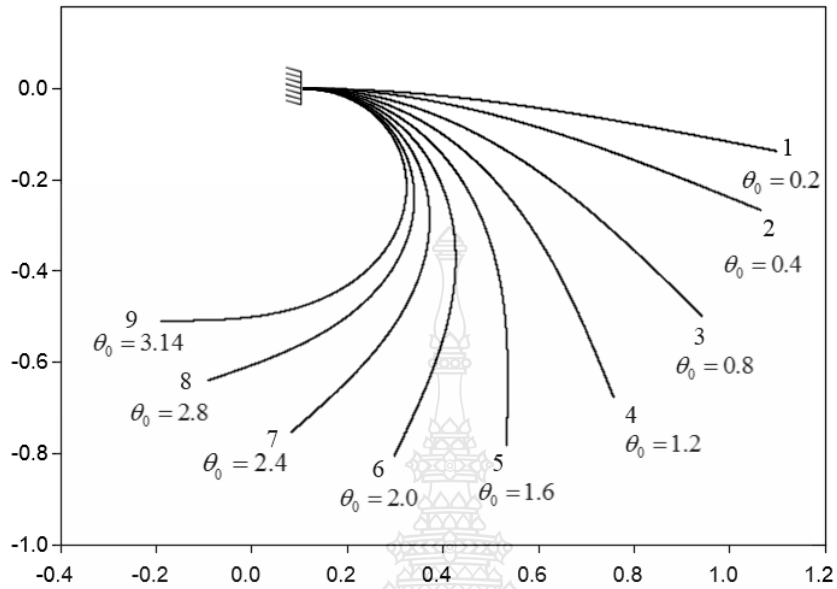


Figure 5.13 Deflection configurations of the nonlinearly cantilever beam subjected to follower distributed load $n = 0.50$

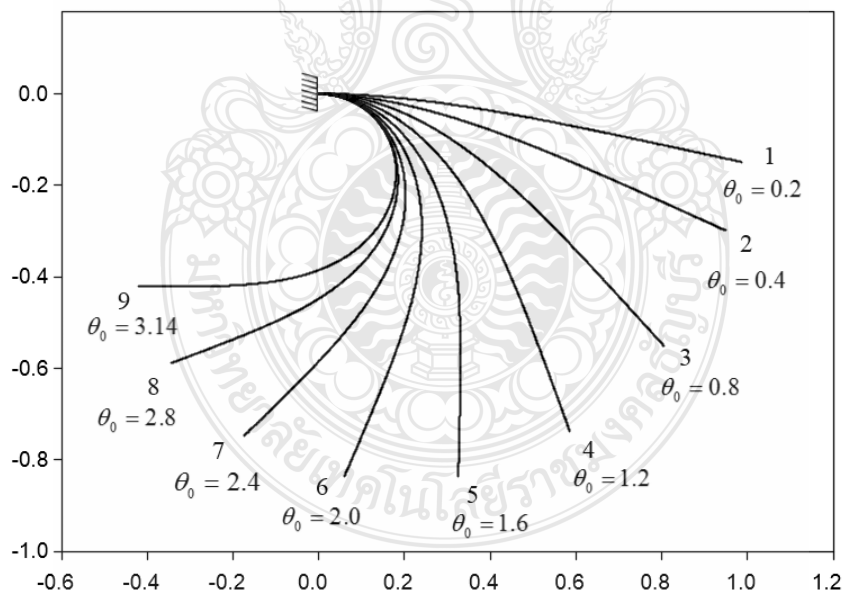


Figure 5.14 Deflection configurations of the nonlinearly cantilever beam subjected to follower distributed load $n = 1.00$

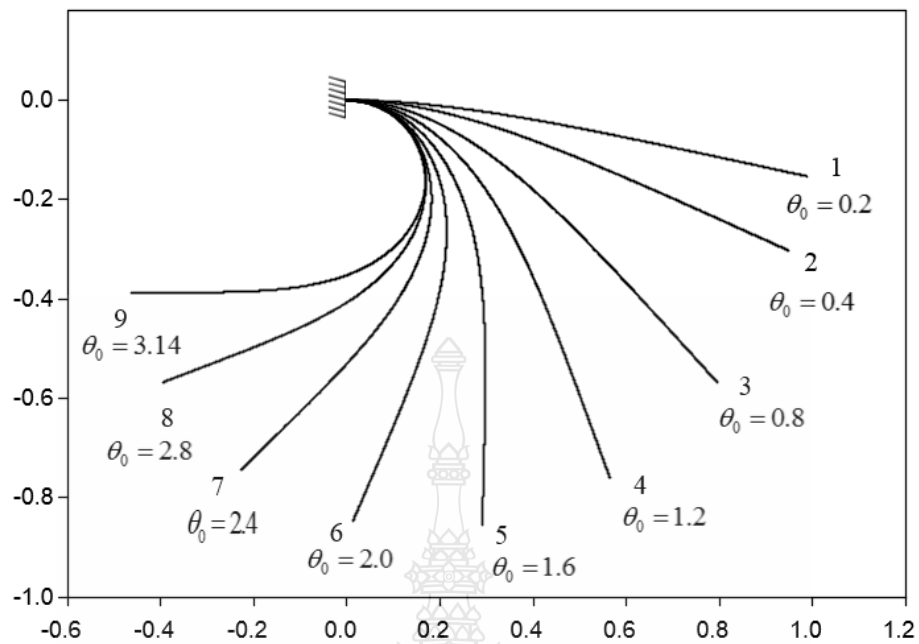


Figure 5.15 Deflection configurations of the nonlinearly cantilever beam subjected to follower distributed load $n = 1.30$

As shown in this example with nonlinear elastic materials $\varepsilon_0 = 0.003$, the deflected shapes with the same slope angle in the Fig. 5.13, 5.14, and 5.15 are identical whether the nonlinearity material parameters are chosen with different values ($n = 0.50$, $n = 1$, and $n = 1.30$).

Their deflection configuration results for $n = 0.50$, $n = 1.00$, and $n = 1.30$ are displayed in Table 5.11, 5.12, and 5.13, respectively.

Table 5.11 Numerical results for cantilever beam made of the generalized Ludwick material for $n = 0.50$

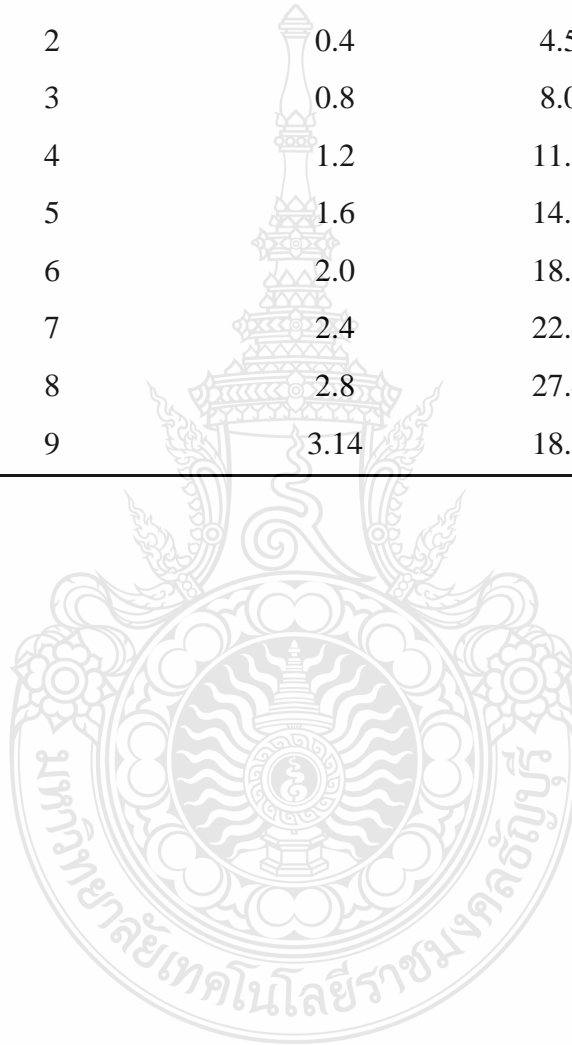
Configuration	$n = 0.50$ and $\varepsilon_0 = 0.003$	
	θ_0 (rad)	\bar{w}
1	0.2	0.032822
2	0.4	0.114631
3	0.8	0.429035
4	1.2	0.960698
5	1.6	1.742620
6	2.0	2.828475
7	2.4	4.303349
8	2.8	6.304648
9	3.14	8.589725

Table 5.12 Numerical results for cantilever beam made of the generalized Ludwick material for $n = 1.00$

Configuration	$n = 1.00$ and $\varepsilon_0 = 0.003$	
	θ_0 (rad)	\bar{w}
1	0.2	1.201348
2	0.4	2.293112
3	0.8	4.884284
4	1.2	7.492988
5	1.6	10.325675
6	2.0	13.505594
7	2.4	17.220642
8	2.8	21.790026
9	3.14	26.795572

Table 5.13 Numerical results for cantilever beam made of the generalized Ludwick material for $n = 1.30$

Configuration	$n = 1.30$ and $\varepsilon_0 = 0.003$	
	θ_0 (rad)	\bar{w}
1	0.2	2.528194
2	0.4	4.509101
3	0.8	8.011507
4	1.2	11.319434
5	1.6	14.679141
6	2.0	18.291713
7	2.4	22.407013
8	2.8	27.431040
9	3.14	18.291713



Example 4

As the fourth example, all the parameters are kept the same as in the first example except $\varepsilon_0 = 0.004$. The results listed in Table 5.14 as shown below.

Table 5.14 Numerical results for cantilever beam made of the generalized Ludwick nonlinear elastic material: $\varepsilon_0 = 0.004$ and n varying from 0.50,0.75..2.00

θ_0 (rad)	\bar{w} $\varepsilon_0 = 0.004$					
	$n = 0.50$	$n = 0.75$	$n = 1.00$	$n = 1.50$	$n = 1.75$	$n = 2.00$
0.0	0.000000	0.000000	0.000000	0.000000	0.000000	0.000000
0.2	0.035582	0.389820	1.201348	3.317766	4.286590	0.062499
0.4	0.120414	0.924927	2.277383	5.687636	7.021656	7.820182
0.6	0.255020	1.555891	3.635229	7.637986	9.178778	10.476525
0.8	0.441169	2.268280	4.884284	9.619852	11.305771	12.400989
1.0	0.681503	3.057446	6.166397	11.413386	13.187961	13.593150
1.2	0.979596	3.877723	7.473941	13.162219	14.539671	16.278647
1.4	1.340087	4.871322	7.783359	14.812065	15.288596	18.035269
1.6	1.768874	5.907026	10.251237	16.644437	17.784550	19.518374
1.8	2.273389	7.041096	11.862454	18.463709	18.823767	21.158680
2.0	2.862963	8.221918	13.505493	20.358031	20.344134	23.346221
2.2	3.549339	9.663816	15.257827	22.048832	24.062405	25.325457
2.4	4.347392	11.194645	17.228803	24.382639	26.311047	27.413831
2.6	5.276152	12.730916	19.365026	26.167583	28.725912	29.083274
2.8	6.360306	14.858255	21.789895	28.031553	30.225745	32.358214
3.0	7.632470	17.094410	24.568438	32.758908	34.568787	35.464044
3.14	8.657857	18.876985	26.660928	35.116941	36.784581	37.923861

Shown in the figure below is the relationship of the load-displacement curve ($\varepsilon_0 = 0.004$) for the nonlinearly cantilever beam between the follower distributed load \bar{w} and the rotation angle θ_0 .

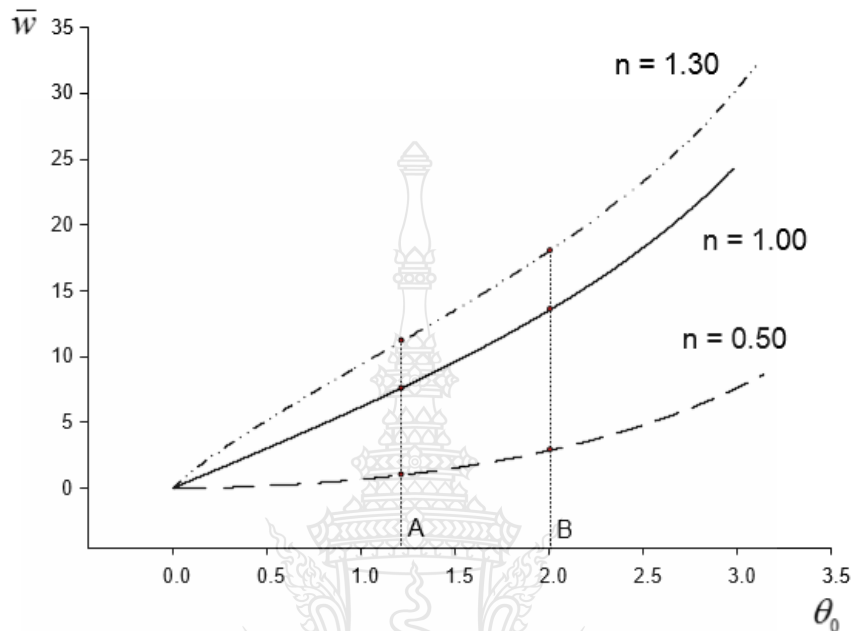


Figure 5.16 Load-displacement curve for the nonlinearly cantilever beam subjected to follower distributed load $\varepsilon_0 = 0.004$

The equilibrium configurations ($\varepsilon_0 = 0.004$) for $\theta_0 = 1.2$ and $\theta_0 = 2.0$ are displayed in the Fig. 5.17.

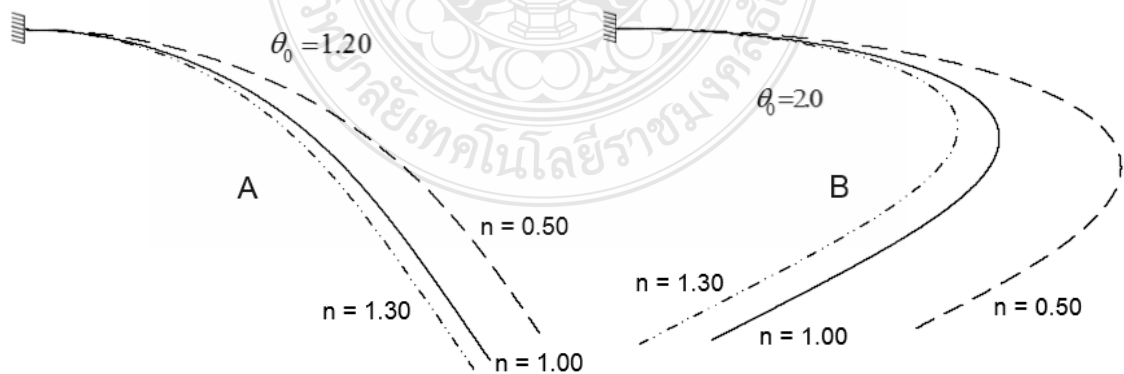


Figure 5.17 Equilibrium configurations for $\theta_0 = 1.2$ and $\theta_0 = 2.0$

The nonlinearity material parameters $n=0.50$, $n=1.00$, and $n=1.30$ are selected to show the deflection configuration in the Fig. 5.18, 5.19 and 5.20, respectively.

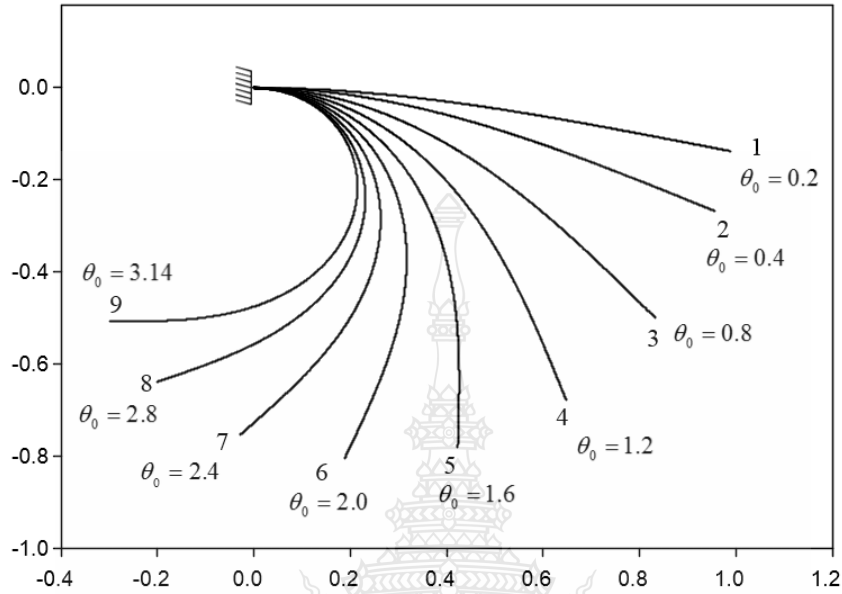


Figure 5.18 Deflection configurations of the nonlinearly cantilever beam subjected to follower distributed load $n=0.50$

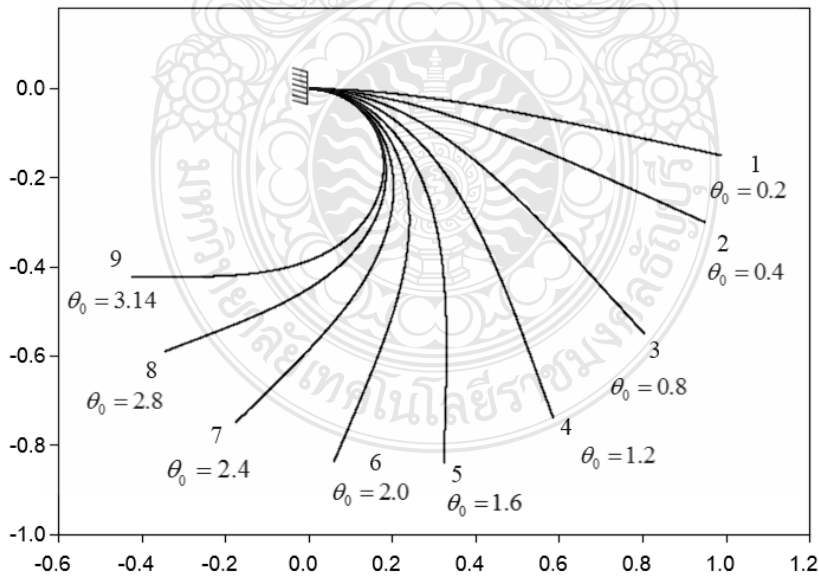


Figure 5.19 Deflection configurations of the nonlinearly cantilever beam subjected to follower distributed load $n=1.00$

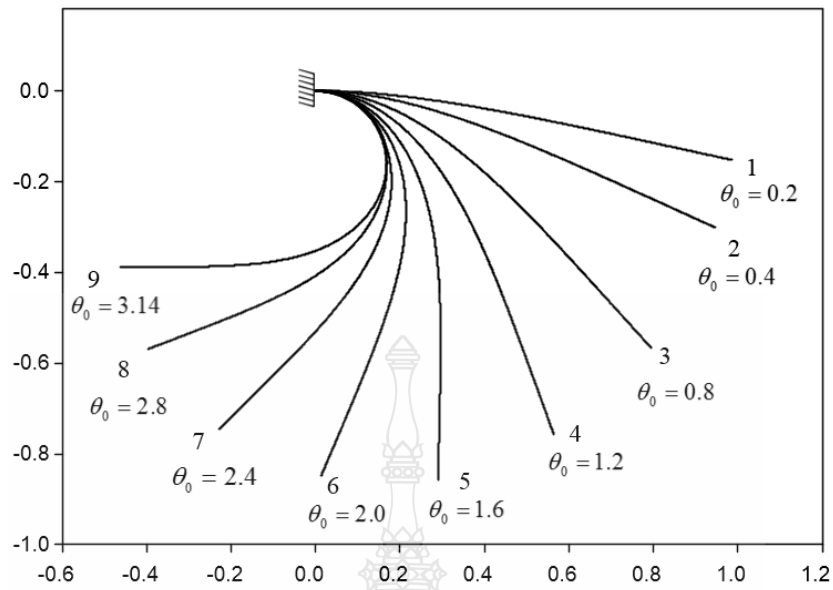


Figure 5.20 Deflection configurations of the nonlinearly cantilever beam subjected to follower distributed load $n = 1.30$

Their deflection configuration results are displayed in tables below.

Table 5.15 Numerical results for cantilever beam made of the generalized Ludwick material for $n = 0.50$

Configuration	$n = 0.50$ and $\varepsilon_0 = 0.004$	
	θ_0 (rad)	\bar{w}
1	0.2	0.035582
2	0.4	0.120414
3	0.8	0.441169
4	1.2	0.979596
5	1.6	1.768874
6	2.0	2.862963
7	2.4	4.347392
8	2.8	6.360306
9	3.14	8.657857

Table 5.16 Numerical results for cantilever beam made of the generalized Ludwick material for $n = 1.00$

Configuration	$n = 1.00$ and $\varepsilon_0 = 0.004$	
	θ_0 (rad)	\bar{w}
1	0.2	1.201348
2	0.4	2.277383
3	0.8	4.884284
4	1.2	7.473941
5	1.6	10.251237
6	2.0	13.505493
7	2.4	17.228803
8	2.8	21.789895
9	3.14	26.660928

Table 5.17 Numerical results for cantilever beam made of the generalized Ludwick material for $n = 1.30$

Configuration	$n = 1.30$ and $\varepsilon_0 = 0.004$	
	θ_0 (rad)	\bar{w}
1	0.2	2.472334
2	0.4	4.438722
3	0.8	7.926483
4	1.2	11.225448
5	1.6	14.491682
6	2.0	18.183139
7	2.4	22.159412
8	2.8	27.303193
9	3.14	32.869493

Example 5

As the fifth example, all the parameters are kept the same as in the first example except $\varepsilon_0 = 0.005$. The results listed in Table 5.18 as shown below.

Table 5.18 Numerical results for cantilever beam made of the generalized Ludwick nonlinear elastic material: $\varepsilon_0 = 0.005$ and n varying from 0.50,0.75..2.00

θ_0 (rad)	\bar{w} $\varepsilon_0 = 0.005$					
	$n = 0.50$	$n = 0.75$	$n = 1.00$	$n = 1.50$	$n = 1.75$	$n = 2.00$
0.0	0.000000	0.000000	0.000000	0.000000	0.000000	0.000000
0.2	0.038297	0.400227	1.201348	3.302631	3.973818	4.705009
0.4	0.126113	0.739948	2.410405	5.571141	6.712540	7.829850
0.6	0.263825	1.567632	3.635229	7.606468	9.015434	9.827292
0.8	0.453184	2.218337	4.884284	9.481738	10.799546	12.170138
1.0	0.696829	3.086207	6.166776	10.996878	12.961780	14.168972
1.2	0.998375	3.955917	7.492988	13.011282	14.759472	15.969968
1.4	1.362396	4.956411	8.874687	14.744769	16.524495	17.721293
1.6	1.794927	5.945479	10.325675	16.498332	18.291967	19.376565
1.8	2.303406	7.057828	11.862520	18.300835	20.094646	21.187090
2.0	2.897210	8.169428	13.505593	20.183303	21.966638	23.054156
2.2	3.588143	9.712033	15.280556	22.182026	23.946989	24.981956
2.4	4.391156	11.16569	17.220624	24.342518	26.084386	27.061539
2.6	5.325375	12.96749	19.370067	26.725423	28.347968	29.405176
2.8	6.415627	14.91857	21.790003	29.417081	31.130740	31.945413
3.0	7.694716	17.15993	24.568442	32.429344	34.095509	35.056072
3.14	8.725589	18.94676	26.627199	35.103484	34.745571	37.263899

The relationship of the load-displacement curve ($\varepsilon_0 = 0.005$) for the nonlinearly cantilever beam between the follower distributed load \bar{w} and the rotation angle θ_0 are demonstrated with the figure below.

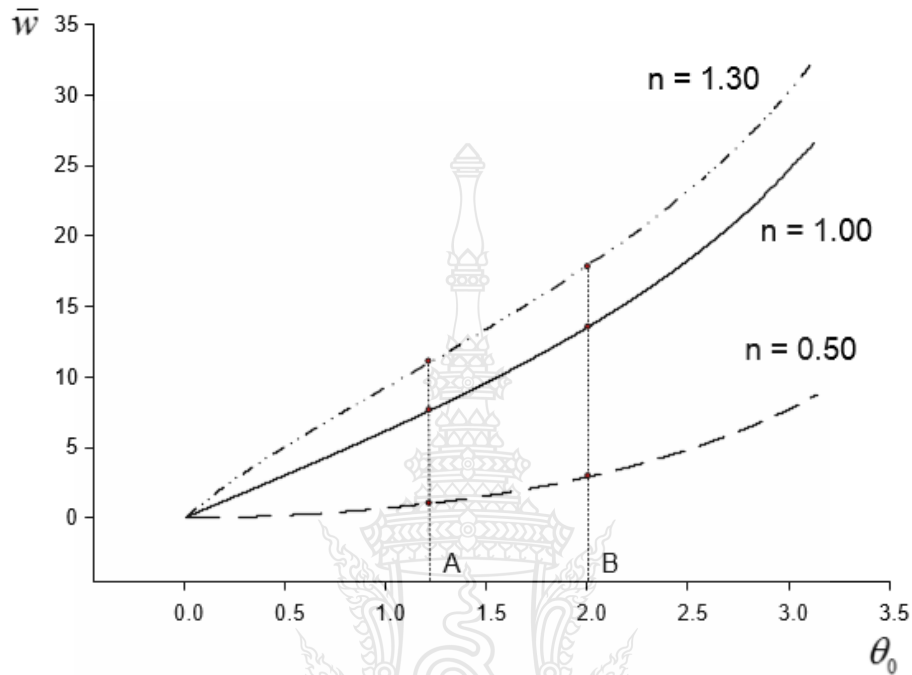


Figure 5.21 Load-displacement curve for the nonlinearly cantilever beam subjected to follower distributed load $\varepsilon_0 = 0.005$

The load-displacement curves of the cantilever beam with various material nonlinearity parameters n are plotted in Fig. 5.21. Demonstrated in this figure is the load-displacement curves to play a key role in explaining the behavior of the cantilever beam for all three possible cases ($n = 1, n < 1$, and $n > 1$) with $\varepsilon_0 = 0.005$.

It is similar to $\varepsilon_0 = 0.001$, a linear case $n = 1$ (Fig. 5.21), the well-known load-displacement curve is monotonic and stable. As it can be seen from the Fig. 5.21, the follower distributed load \bar{w} increases as the rotation angle θ_0 increases.

The equilibrium configurations ($\varepsilon_0 = 0.005$) for $\theta_0 = 1.2$ and $\theta_0 = 2.0$ are selected to indicate in the Fig. 5.22.

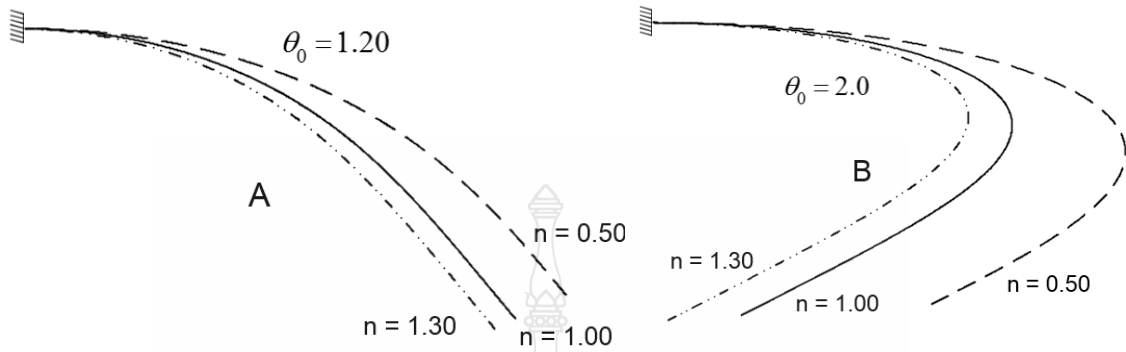


Figure 5.22 Equilibrium configurations for $\theta_0 = 1.2$ and $\theta_0 = 2.0$

Furthermore, the nonlinearity material parameters $n = 0.50, n = 1.00$, and $n = 1.30$ are selected to show the deflection configuration in the Fig. 5.23, 5.24 and 5.25, respectively.

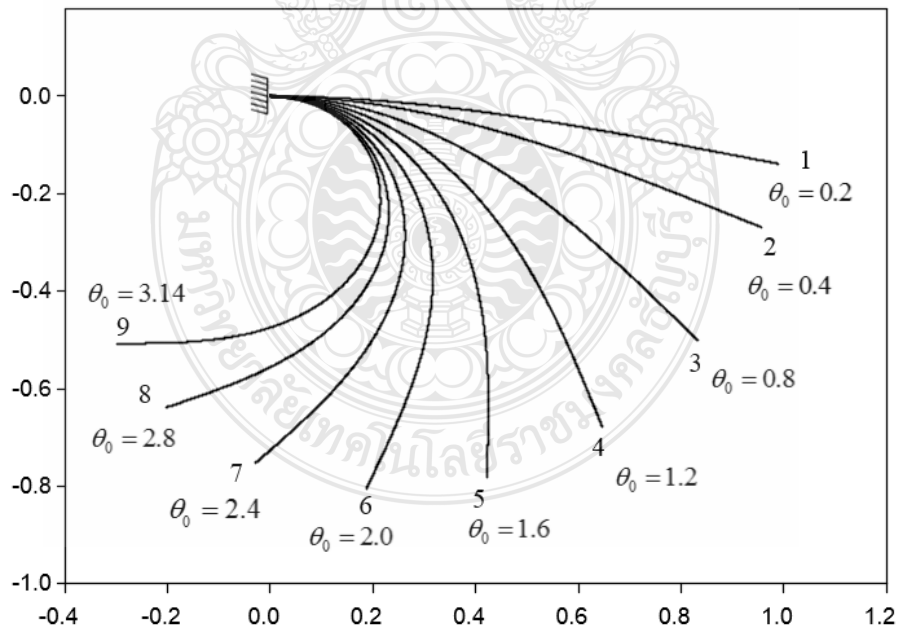


Figure 5.23 Deflection configurations of the nonlinearly cantilever beam subjected to follower distributed load $n = 0.50$

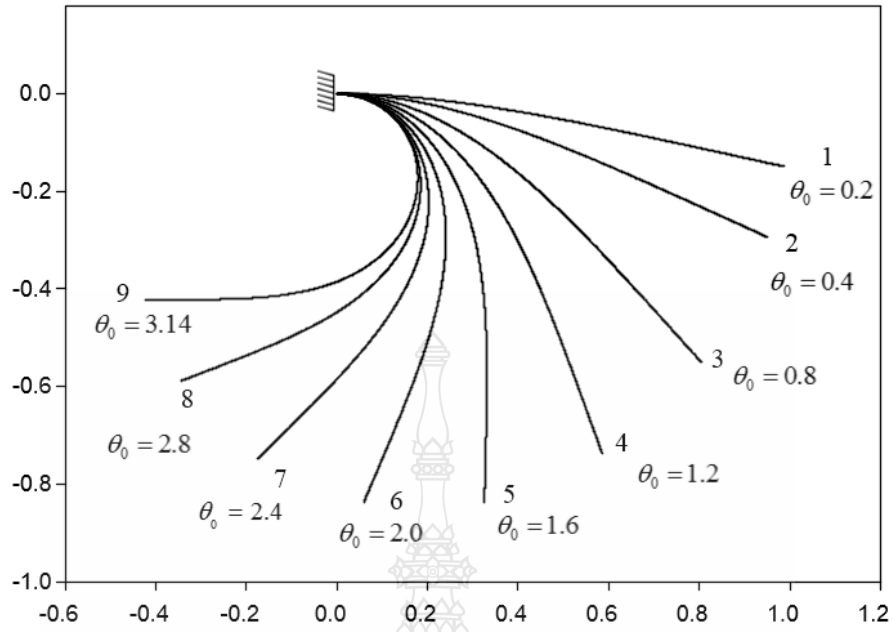


Figure 5.24 Deflection configurations of the nonlinearly cantilever beam subjected to follower distributed load $n = 1.00$

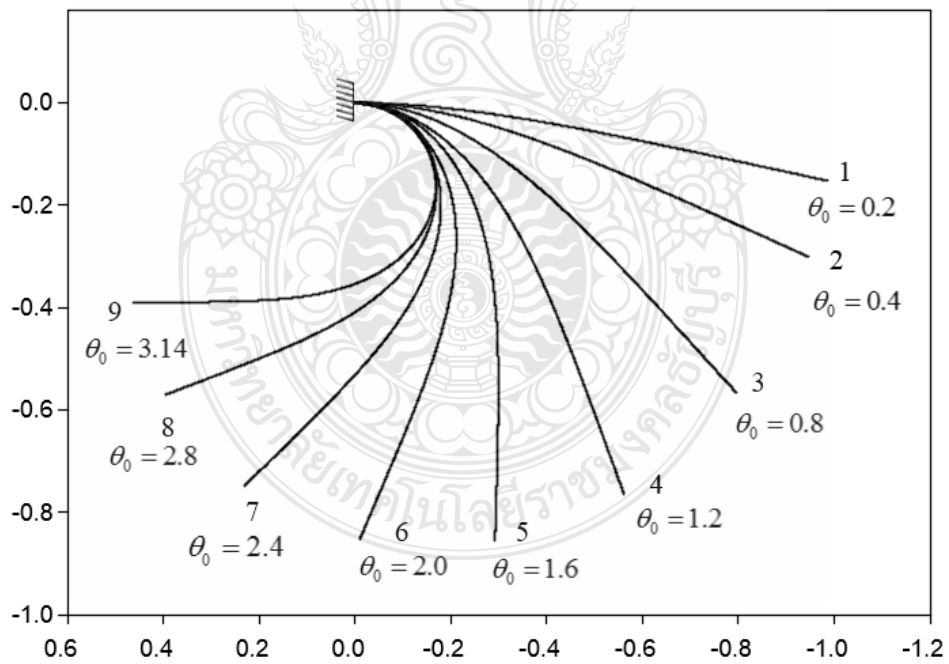


Figure 5.25 Deflection configurations of the nonlinearly cantilever beam subjected to follower distributed load $n = 1.30$

Table 5.19 Numerical results for cantilever beam made of the generalized Ludwick material for $n = 0.50$

Configuration	$n = 0.50$ and $\varepsilon_0 = 0.005$	
	θ_0 (rad)	\bar{w}
1	0.2	0.038297
2	0.4	0.126113
3	0.8	0.453184
4	1.2	0.998375
5	1.6	1.794927
6	2.0	2.897210
7	2.4	4.391156
8	2.8	6.415627
9	3.14	8.725589

Table 5.20 Numerical results for cantilever beam made of the generalized Ludwick material for $n = 1.00$

Configuration	$n = 1.00$ and $\varepsilon_0 = 0.005$	
	θ_0 (rad)	\bar{w}
1	0.2	1.201348
2	0.4	2.410405
3	0.8	4.884284
4	1.2	7.492988
5	1.6	10.325675
6	2.0	13.505593
7	2.4	17.220624
8	2.8	21.790003
9	3.14	26.627199

Table 5.21 Numerical results for cantilever beam made of the generalized Ludwick material for $n = 1.30$

Configuration	$n = 1.30$ and $\varepsilon_0 = 0.005$	
	θ_0 (rad)	\bar{w}
1	0.2	2.424564
2	0.4	4.377278
3	0.8	7.851029
4	1.2	10.849223
5	1.6	14.486503
6	2.0	17.836980
7	2.4	21.967941
8	2.8	27.187173
9	3.14	32.739442



Example 6

As the sixth example, all the parameters are kept the same as in the first example except $\varepsilon_0 = 0.006$. The results listed in Table 5.22 as shown below.

Table 5.22 Numerical results for cantilever beam made of the generalized Ludwick nonlinear elastic material: $\varepsilon_0 = 0.006$ and n varying from 0.50,0.75..2.00

θ_0 (rad)	\bar{w} $\varepsilon_0 = 0.006$					
	$n = 0.50$	$n = 0.75$	$n = 1.00$	$n = 1.50$	$n = 1.75$	$n = 2.00$
0.0	0.000000	0.000000	0.000000	0.000000	0.000000	0.000000
0.2	0.040976	0.409901	1.201348	3.148763	3.995441	4.167546
0.4	0.131737	0.956846	2.410405	5.468486	6.426896	7.612709
0.6	0.272511	1.597078	3.635229	7.491667	8.691016	9.954955
0.8	0.465028	2.317391	4.884284	9.323829	10.896245	12.019552
1.0	0.711944	3.113681	6.166776	10.925664	12.669351	13.817577
1.2	1.016866	3.986680	7.492988	12.875108	14.551091	15.697037
1.4	1.384479	4.940534	8.874687	14.603503	16.309814	17.441472
1.6	1.820748	5.982459	10.325675	16.352287	18.071387	19.114094
1.8	2.333177	7.122768	11.862520	18.150111	19.868270	20.834232
2.0	2.931194	8.375358	13.505593	20.027788	21.734288	22.754923
2.2	3.626664	9.758568	15.280556	22.021389	23.708175	24.675507
2.4	4.434615	11.296562	17.220624	24.176180	25.838259	26.746757
2.6	5.374279	13.021481	19.370067	26.552400	28.189005	28.914848
2.8	6.470615	14.976876	21.790003	29.235776	29.496491	31.169994
3.0	7.756618	17.223375	24.568443	32.356454	33.950562	33.825173
3.14	8.792960	19.014456	26.795508	34.921646	36.182802	36.345580

The relationship of the load-displacement curve ($\varepsilon_0 = 0.006$) for the nonlinearly cantilever beam between the follower distributed load \bar{w} and the rotation angle θ_0 are demonstrated with the figure below.

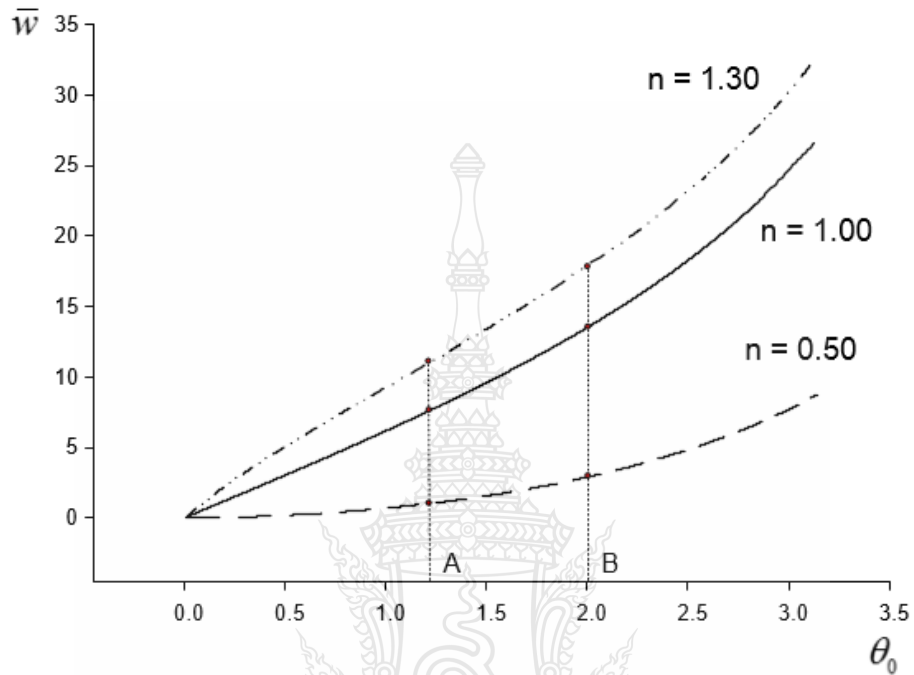


Figure 5.26 Load-displacement curve for the nonlinearly cantilever beam subjected to follower distributed load $\varepsilon_0 = 0.006$

The equilibrium configurations ($\varepsilon_0 = 0.006$) for $\theta_0 = 1.2$ and $\theta_0 = 2.0$ are selected to indicate in the Fig. 5.27.

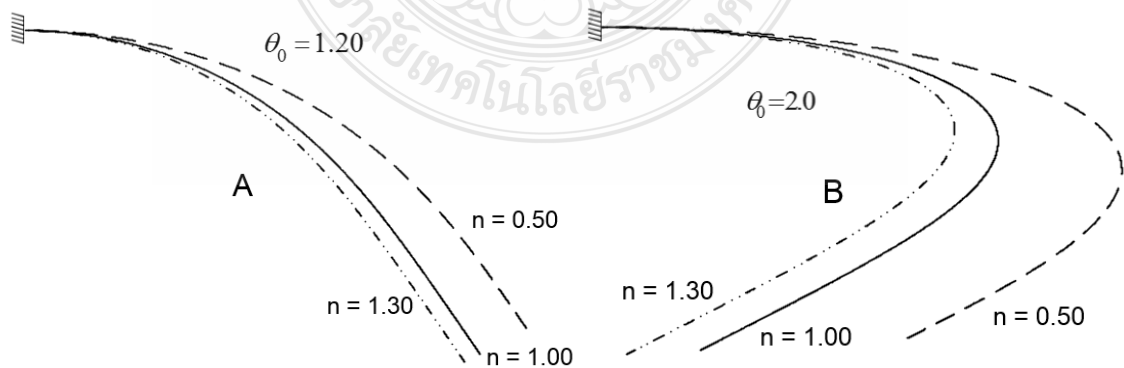


Figure 5.27 Equilibrium configurations for $\theta_0 = 1.2$ and $\theta_0 = 2.0$

Furthermore, the nonlinearity material parameter $n = 0.50$, $n = 1.00$, and $n = 1.30$ are selected to show the deflection configuration in the Fig. 5.28, 5.29 and 5.30, respectively.

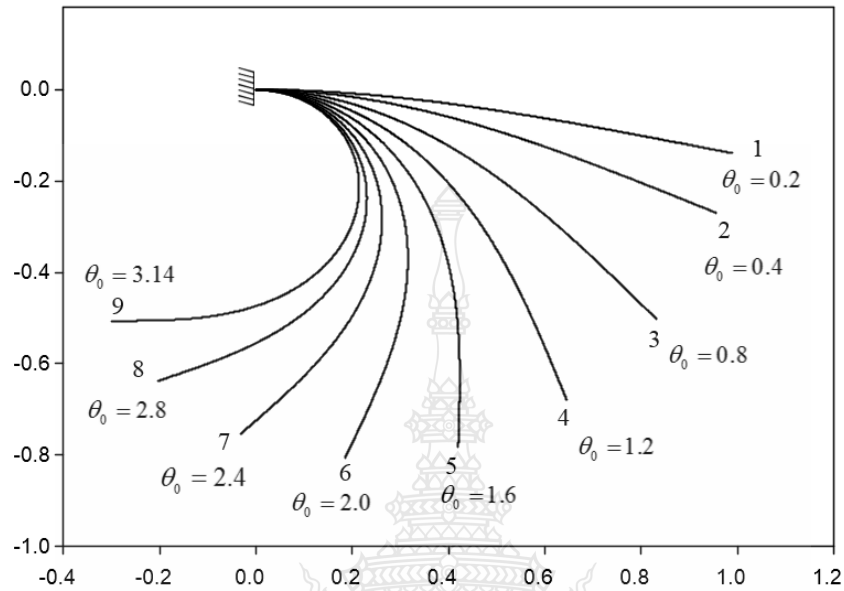


Figure 5.28 Deflection configurations of the nonlinearly cantilever beam subjected to follower distributed load $n = 0.50$

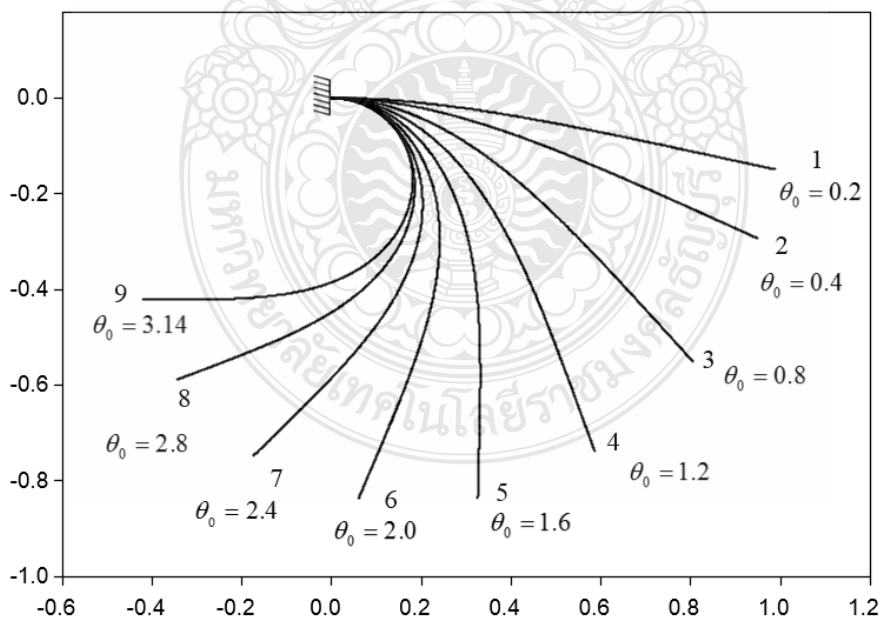


Figure 5.29 Deflection configurations of the nonlinearly cantilever beam subjected to follower distributed load $n = 1.00$

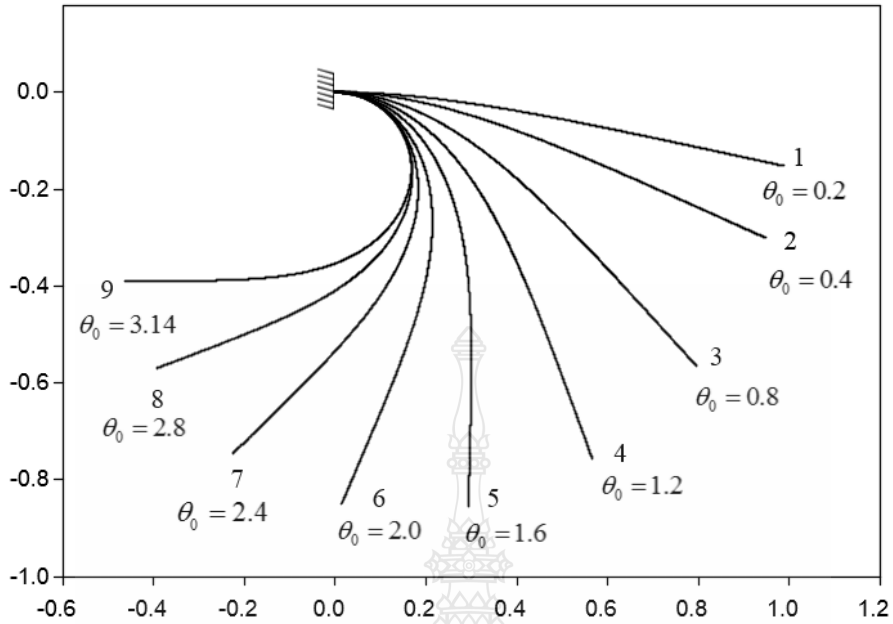


Figure 5.30 Deflection configurations of the nonlinearly cantilever beam subjected to follower distributed load $n = 1.30$

Table 5.23 Numerical results for cantilever beam made of the generalized Ludwick material for $n = 0.50$

Configuration	$n = 0.50$ and $\varepsilon_0 = 0.006$	
	θ_0 (rad)	\bar{w}
1	0.2	0.040976
2	0.4	0.131737
3	0.8	0.465028
4	1.2	1.016866
5	1.6	1.820748
6	2.0	2.931194
7	2.4	4.434615
8	2.8	6.470615
9	3.14	8.792960

Table 5.24 Numerical results for cantilever beam made of the generalized Ludwick material for $n = 1.00$

Configuration	$n = 1.00$ and $\varepsilon_0 = 0.006$	
	θ_0 (rad)	\bar{w}
1	0.2	1.201348
2	0.4	2.410405
3	0.8	4.884284
4	1.2	7.492988
5	1.6	10.325675
6	2.0	13.505593
7	2.4	17.220624
8	2.8	21.790003
9	3.14	26.795508

Table 5.25 Numerical results for cantilever beam made of the generalized Ludwick material for $n = 1.30$

Configuration	$n = 1.30$ and $\varepsilon_0 = 0.006$	
	θ_0 (rad)	\bar{w}
1	0.2	2.382651
2	0.4	4.322404
3	0.8	7.782682
4	1.2	11.064441
5	1.6	14.402936
6	2.0	17.900352
7	2.4	22.087475
8	2.8	27.079972
9	3.14	32.619123

Example 7

As the seventh example, all the parameters are kept the same as in the first example except $\varepsilon_0 = 0.007$. The results listed in Table 5.26 as shown below.

Table 5.26 Numerical results for cantilever beam made of the generalized Ludwick nonlinear elastic material: $\varepsilon_0 = 0.007$ and n varying from 0.50, 0.75..2.00

θ_0 (rad)	\bar{w} $\varepsilon_0 = 0.007$					
	$n = 0.50$	$n = 0.75$	$n = 1.00$	$n = 1.50$	$n = 1.75$	$n = 2.00$
0.0	0.000000	0.000000	0.000000	0.000000	0.000000	0.000000
0.2	0.043625	0.418980	1.201348	3.076992	3.726706	4.363295
0.4	0.137302	0.971522	2.410405	5.115417	6.375783	7.279405
0.6	0.281119	1.616190	3.635229	7.324731	8.630961	9.743064
0.8	0.476788	2.340321	4.884284	9.209134	10.435752	11.486439
1.0	0.726965	3.140056	6.166776	10.843886	12.578253	13.587470
1.2	1.035273	4.016267	7.492988	12.574744	14.182070	15.440389
1.4	1.406424	4.973211	8.874687	14.473858	15.993959	17.102494
1.6	1.846408	6.018167	10.325675	16.041853	17.870449	18.916985
1.8	2.362769	7.161514	11.862520	17.913712	19.661736	20.671316
2.0	2.964982	8.417214	13.505593	19.884386	21.522013	22.483568
2.2	3.664972	9.803677	15.280556	21.873091	23.489730	24.397263
2.4	4.477843	11.345151	17.220624	23.921537	25.612855	26.460621
2.6	5.422928	13.073886	19.370067	26.266941	27.955323	28.560333
2.8	6.525323	15.033581	21.790003	29.067836	29.338203	31.148469
3.0	7.818212	17.285080	24.568444	32.178056	33.353210	33.450571
3.14	8.860008	19.080261	26.615320	33.605084	36.087674	35.082146

The relationship of the load-displacement curve ($\varepsilon_0 = 0.007$) for the nonlinearly cantilever beam between the follower distributed load \bar{w} and the rotation angle θ_0 are demonstrated with the figure below.

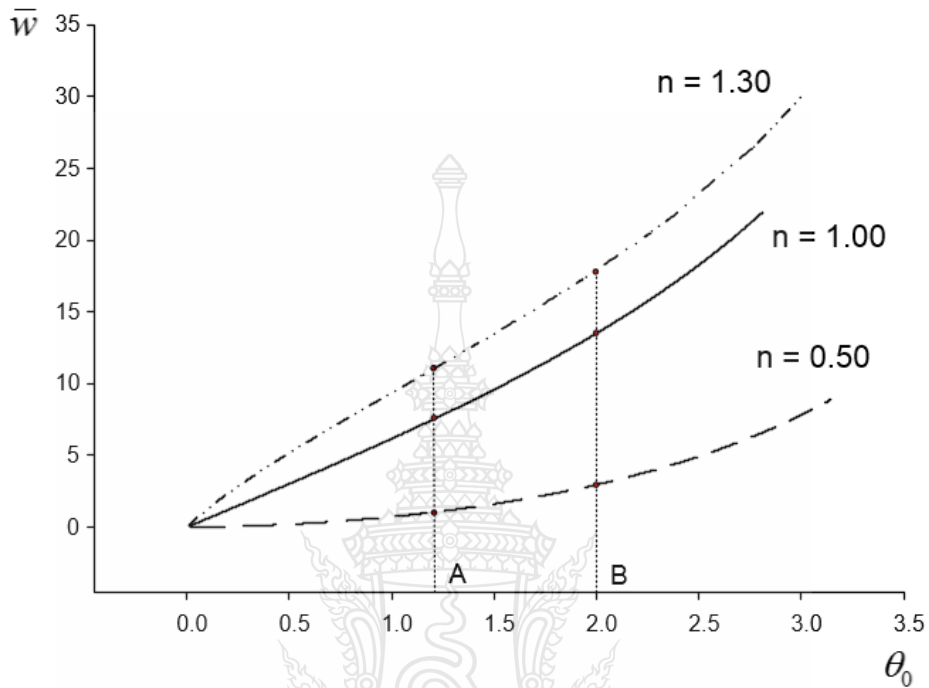


Figure 5.31 Load-displacement curve for the nonlinearly cantilever beam subjected to follower distributed load $\varepsilon_0 = 0.007$

The equilibrium configurations ($\varepsilon_0 = 0.007$) for $\theta_0 = 1.2$ and $\theta_0 = 2.0$ are selected to indicate in the Fig. 5.32.

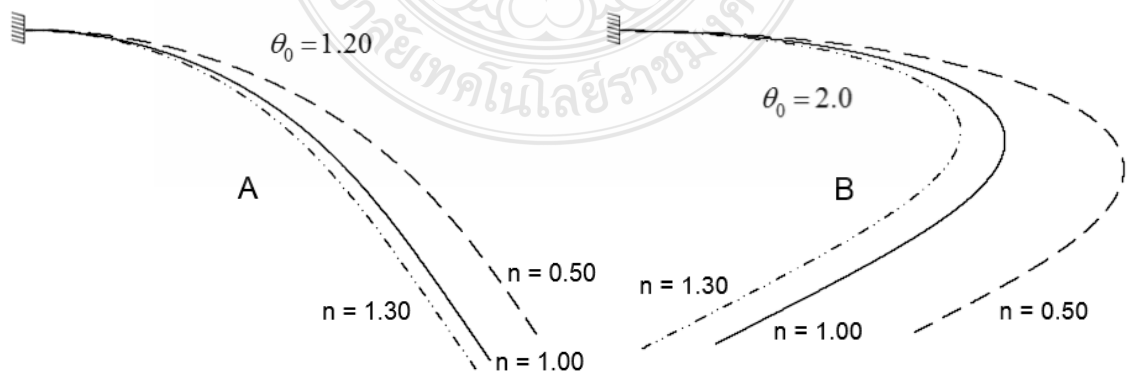


Figure 5.32 Equilibrium configurations for $\theta_0 = 1.2$ and $\theta_0 = 2.0$

Furthermore, the nonlinearity material parameter $n = 0.50$, $n = 1.00$, and $n = 1.30$ are selected to show the deflection configuration in the Fig. 5.33, 5.34 and 5.35, respectively.

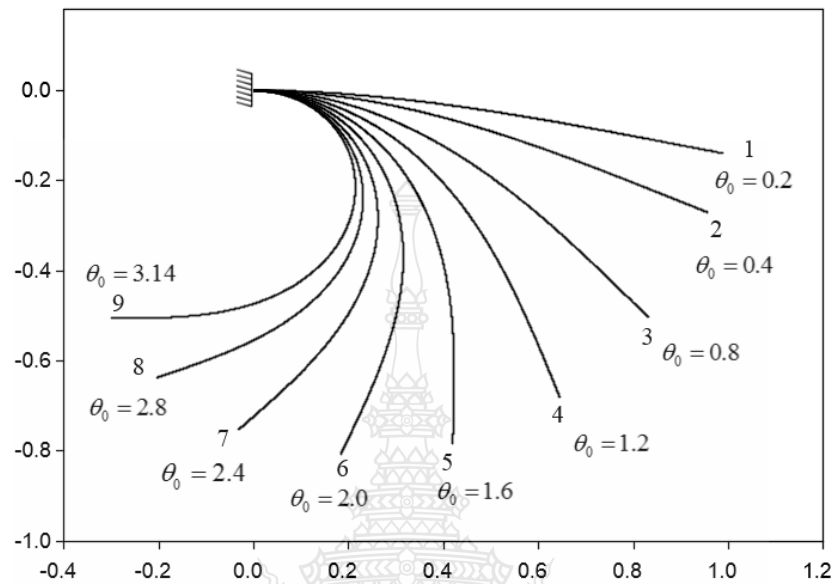


Figure 5.33 Deflection configurations of the nonlinearly cantilever beam subjected to follower distributed load $n = 0.50$

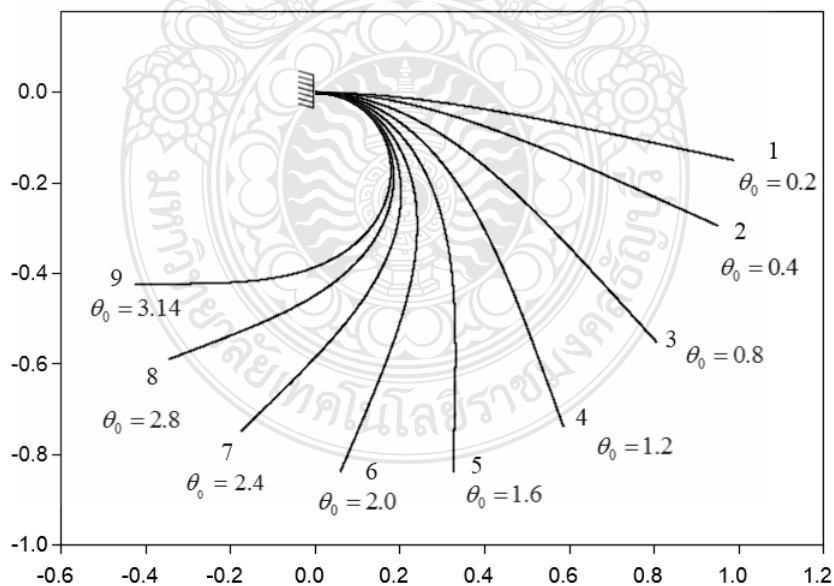


Figure 5.34 Deflection configurations of the nonlinearly cantilever beam subjected to follower distributed load $n = 1.00$

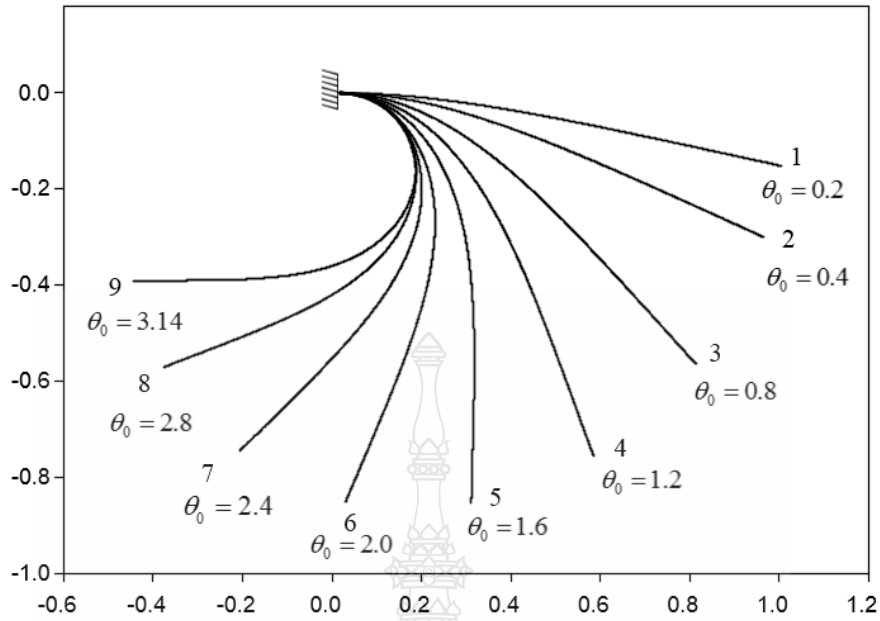


Figure 5.35 Deflection configurations of the nonlinearly cantilever beam subjected to follower distributed load $n = 1.30$

Table 5.27 Numerical results for cantilever beam made of the generalized Ludwick material for $n = 0.50$

Configuration	$n = 0.50$ and $\varepsilon_0 = 0.007$	
	θ_0 (rad)	\bar{w}
1	0.2	0.043625
2	0.4	0.137302
3	0.8	0.476788
4	1.2	1.035273
5	1.6	1.846408
6	2.0	2.964982
7	2.4	4.477843
8	2.8	6.525323
9	3.14	8.860008

Table 5.28 Numerical results for cantilever beam made of the generalized Ludwick material for $n = 1.00$

Configuration	$n = 1.00$ and $\varepsilon_0 = 0.007$	
	θ_0 (rad)	\bar{w}
1	0.2	1.201348
2	0.4	2.410405
3	0.8	4.884284
4	1.2	7.492988
5	1.6	10.325675
6	2.0	13.505593
7	2.4	17.220624
8	2.8	21.790003
9	3.14	26.615320

Table 5.29 Numerical results for cantilever beam made of the generalized Ludwick material for $n = 1.30$

Configuration	$n = 1.30$ and $\varepsilon_0 = 0.007$	
	θ_0 (rad)	\bar{w}
1	0.2	2.345222
2	0.4	4.272630
3	0.8	7.719904
4	1.2	10.993487
5	1.6	14.301371
6	2.0	17.688044
7	2.4	21.996624
8	2.8	26.979744
9	3.14	32.506505

Example 8

As the eighth example, all the parameters are kept the same as in the first example except $\varepsilon_0 = 0.008$. The results listed in Table 5.30 as shown below.

Table 5.30 Numerical results for cantilever beam made of the generalized Ludwick nonlinear elastic material: $\varepsilon_0 = 0.008$ and n varying from 0.50, 0.75..2.00

θ_0 (rad)	\bar{w} $\varepsilon_0 = 0.008$					
	$n = 0.50$	$n = 0.75$	$n = 1.00$	$n = 1.50$	$n = 1.75$	$n = 2.00$
0.0	0.000000	0.000000	0.000000	0.000000	0.000000	0.000000
0.2	0.042283	0.427561	1.201348	3.012606	3.472735	4.275976
0.4	0.142812	0.985517	2.410405	5.292216	6.133971	6.667443
0.6	0.289650	1.634510	3.635229	7.195807	8.385512	9.412610
0.8	0.488449	2.362377	4.884284	8.963237	10.398294	11.355869
1.0	0.741869	3.165492	6.166776	10.215635	11.670345	12.756520
1.2	1.053548	4.044861	7.492988	12.378904	14.188537	15.087512
1.4	1.428218	5.004843	8.874687	14.267386	15.861205	16.957755
1.6	1.871902	6.052780	10.325675	16.093254	17.685191	18.679792
1.8	2.392180	7.199116	11.862520	17.791077	19.471028	20.401969
2.0	2.998574	8.457876	13.505593	19.747971	21.325774	22.141897
2.2	3.703067	9.847541	15.280556	21.529422	23.286668	24.141347
2.4	4.520841	11.392437	17.220624	23.763703	25.351900	24.141347
2.6	5.471327	13.124921	19.370067	26.242613	27.738601	28.459253
2.8	6.579756	15.088837	21.735301	28.910720	29.613800	30.155835
3.0	7.879495	17.345244	24.224703	31.843347	32.976371	32.429332
3.14	8.926707	19.144442	26.792420	33.885535	35.864798	32.429330

The relationship of the load-displacement curve ($\varepsilon_0 = 0.008$) for the nonlinearly cantilever beam between the follower distributed load \bar{w} and the rotation angle θ_0 are demonstrated with the figure below.

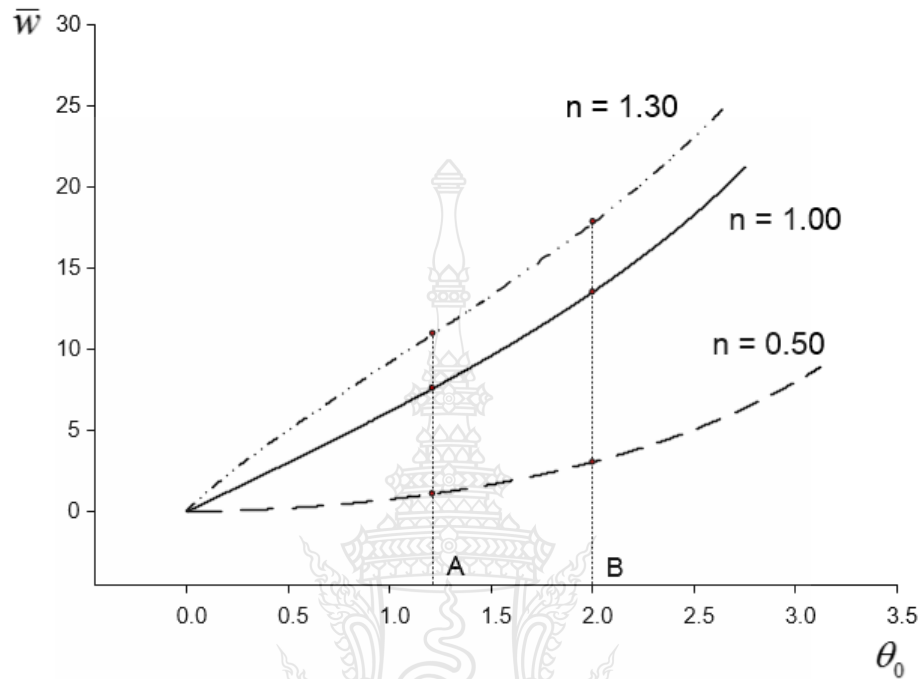


Figure 5.36 Load-displacement curve for the nonlinearly cantilever beam subjected to follower distributed load $\varepsilon_0 = 0.008$

The equilibrium configurations ($\varepsilon_0 = 0.008$) for $\theta_0 = 1.2$ and $\theta_0 = 2.0$ are selected to display in the Fig. 5.37.

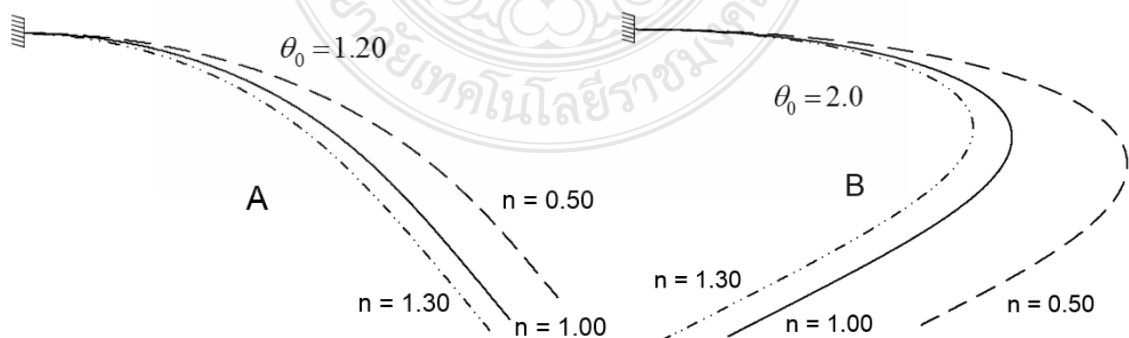


Figure 5.37 Equilibrium configurations for $\theta_0 = 1.2$ and $\theta_0 = 2.0$

Furthermore, the nonlinearity material parameters $n = 0.50$, $n = 1.00$, and $n = 1.30$ are selected to show the deflection configuration in the Fig. 5.38, 5.39 and 5.40, respectively.

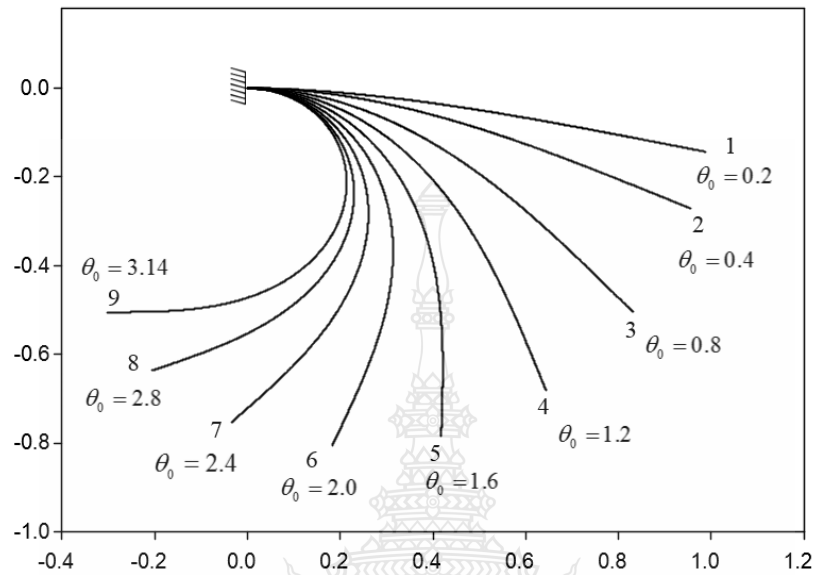


Figure 5.38 Deflection configurations of the nonlinearly cantilever beam subjected to follower distributed load $n = 0.50$

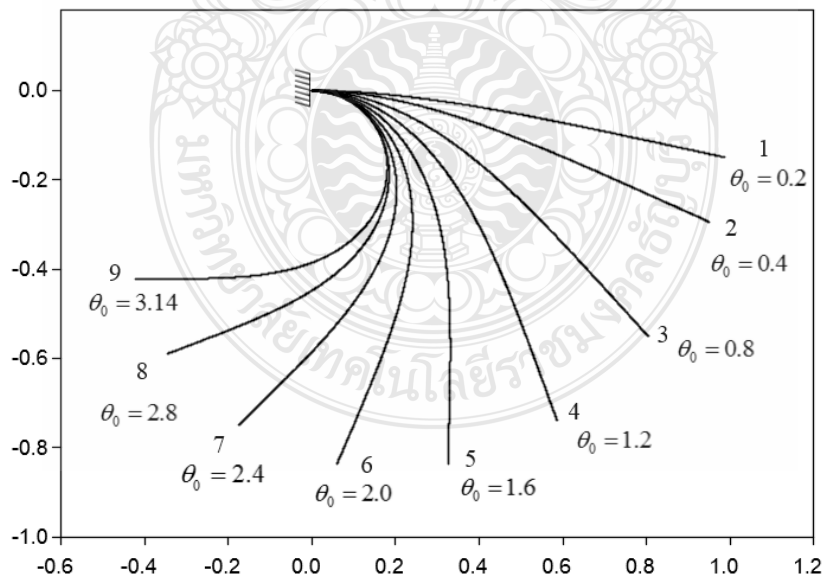


Figure 5.39 Deflection configurations of the nonlinearly cantilever beam subjected to follower distributed load $n = 1.00$

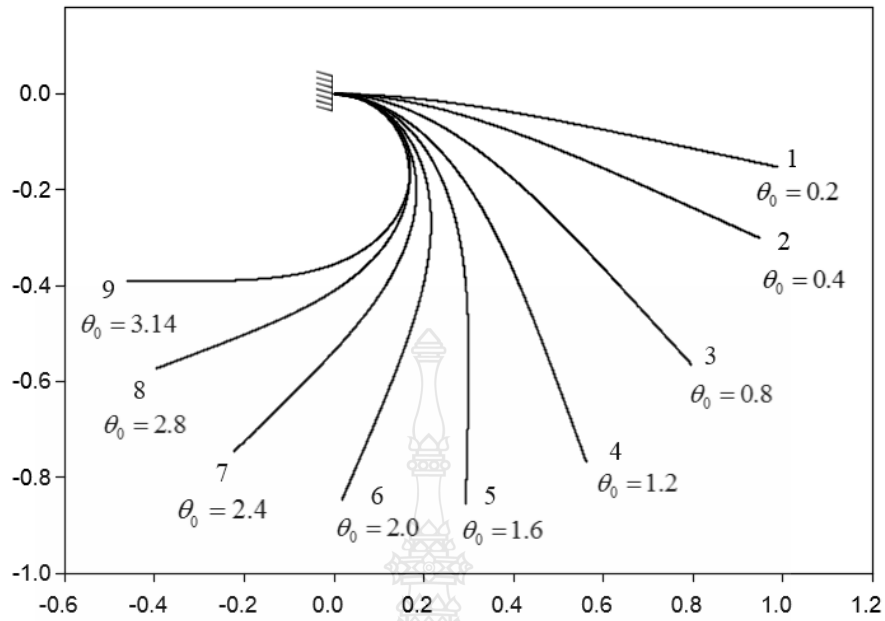


Figure 5.40 Deflection configurations of the nonlinearly cantilever beam subjected to follower distributed load $n = 1.30$

Table 5.31 Numerical results for cantilever beam made of the generalized Ludwick material for $n = 0.50$

Configuration	$n = 0.50$ and $\varepsilon_0 = 0.008$	
	θ_0 (rad)	\bar{w}
1	0.2	0.042283
2	0.4	0.142812
3	0.8	0.488449
4	1.2	1.053548
5	1.6	1.871902
6	2.0	2.998574
7	2.4	4.520841
8	2.8	6.579756
9	3.14	8.926707

Table 5.32 Numerical results for cantilever beam made of the generalized Ludwick material for $n = 1.00$

Configuration	$n = 1.00$ and $\varepsilon_0 = 0.008$	
	θ_0 (rad)	\bar{w}
1	0.2	1.201348
2	0.4	2.410405
3	0.8	4.884284
4	1.2	7.492988
5	1.6	10.325675
6	2.0	13.505593
7	2.4	17.220624
8	2.8	21.735301
9	3.14	26.792420

Table 5.33 Numerical results for cantilever beam made of the generalized Ludwick material for $n = 1.30$

Configuration	$n = 1.30$ and $\varepsilon_0 = 0.008$	
	θ_0 (rad)	\bar{w}
1	0.2	2.311362
2	0.4	4.226970
3	0.8	7.661656
4	1.2	10.512203
5	1.6	14.160443
6	2.0	17.784572
7	2.4	21.910731
8	2.8	26.701534
9	3.14	32.400208

Example 9

As the ninth example, all the parameters are kept the same as in the first example except $\varepsilon_0 = 0.009$. The results listed in Table 5.34 as shown below.

Table 5.34 Numerical results for cantilever beam made of the generalized Ludwick nonlinear elastic material: $\varepsilon_0 = 0.009$ and n varying from 0.50,0.75..2.00

θ_0 (rad)	\bar{w} $\varepsilon_0 = 0.009$					
	$n = 0.50$	$n = 0.75$	$n = 1.00$	$n = 1.50$	$n = 1.75$	$n = 2.00$
0.0	0.000000	0.000000	0.000000	0.000000	0.000000	0.000000
0.2	0.048857	0.435717	1.201348	2.829611	3.682674	4.279377
0.4	0.148279	0.998924	2.410405	5.150877	5.669855	7.069134
0.6	0.298116	1.652138	3.635229	7.012241	8.170487	9.362910
0.8	0.500026	2.383666	4.884284	9.045394	10.035450	11.385183
1.0	0.756671	3.190101	6.166776	10.719117	11.863989	13.157925
1.2	1.071704	4.072578	7.492988	12.441180	13.957979	14.929130
1.4	1.449881	5.035549	8.874687	14.241098	15.767341	16.637077
1.6	1.897250	6.086421	10.325675	15.973252	17.515763	18.455046
1.8	2.421430	7.235702	11.862520	17.761904	19.292924	20.122557
2.0	3.031989	8.497479	13.505593	19.627280	21.142739	21.910108
2.2	3.740970	9.890297	15.280556	21.416982	23.022681	23.718358
2.4	4.563630	11.438563	17.220624	23.743539	25.098780	25.812961
2.6	5.519505	13.174737	19.370067	25.978212	27.525141	28.058526
2.8	6.633972	15.142806	21.782721	28.762620	29.561947	30.730084
3.0	7.940806	17.404035	24.441044	31.624124	32.823993	33.449554
3.14	8.993232	19.207177	26.794311	33.914010	34.640489	36.255189

The relationship of the load-displacement curve ($\varepsilon_0 = 0.009$) for the nonlinearly cantilever beam between the follower distributed load \bar{w} and the rotation angle θ_0 are demonstrated with the figure below.

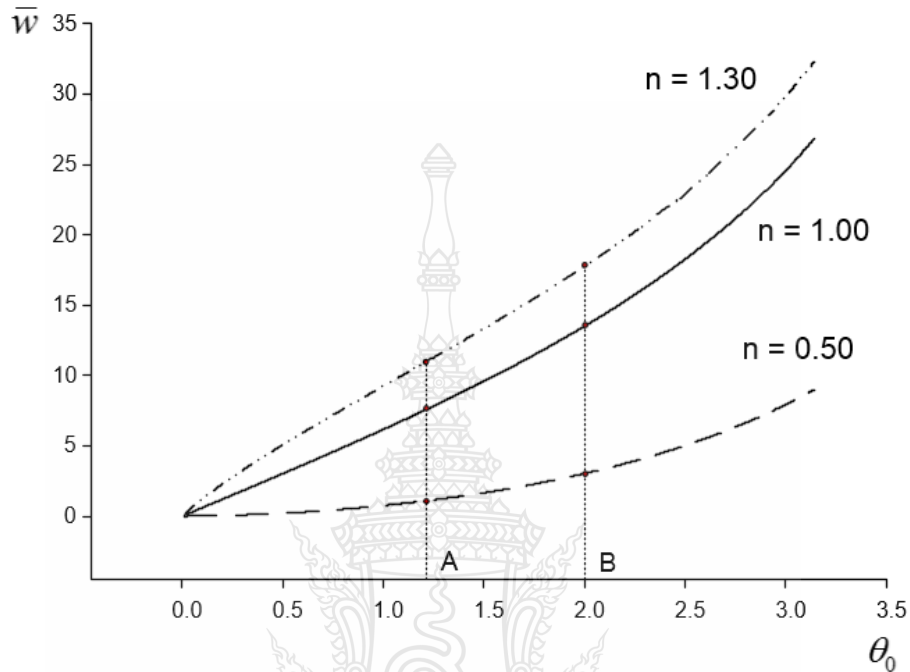


Figure 5.41 Load-displacement curve for the nonlinearly cantilever beam subjected to follower distributed load $\varepsilon_0 = 0.009$

The equilibrium configurations ($\varepsilon_0 = 0.009$) for $\theta_0 = 1.2$ and $\theta_0 = 2.0$ are chosen to indicate in the Fig. 5.42.

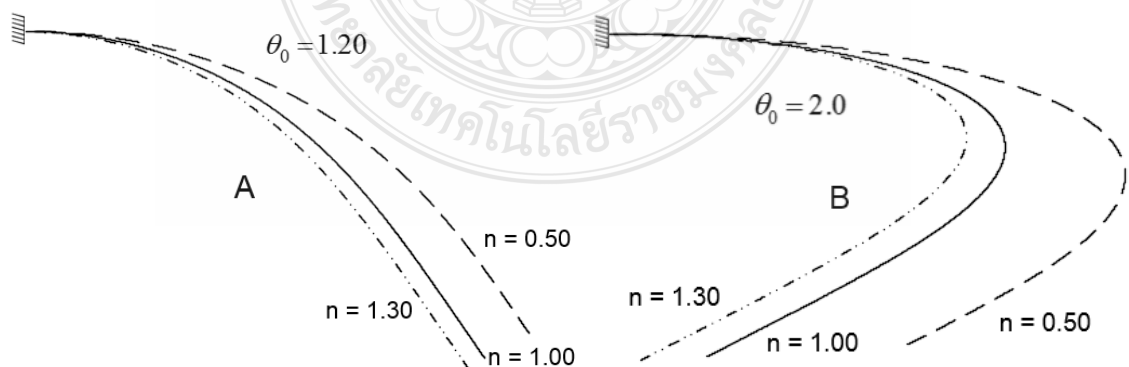


Fig 5.42 Equilibrium configurations for $\theta_0 = 1.2$ and $\theta_0 = 2.0$

Furthermore, the nonlinearity material parameters $n = 0.50$, $n = 1.00$, and $n = 1.30$ are selected to show the deflection configuration in the Fig. 5.43, 5.44 and 5.45, respectively.

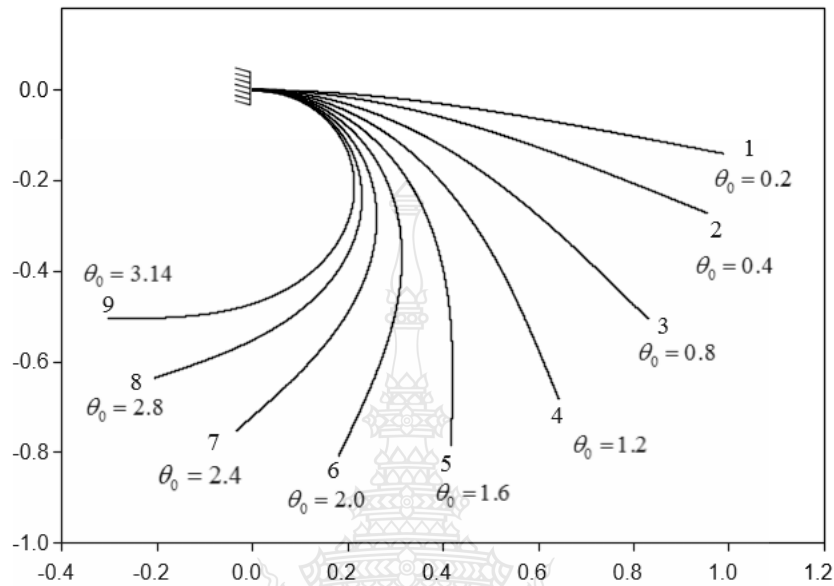


Figure 5.43 Deflection configurations of the nonlinearly cantilever beam subjected to follower distributed load $n = 0.50$

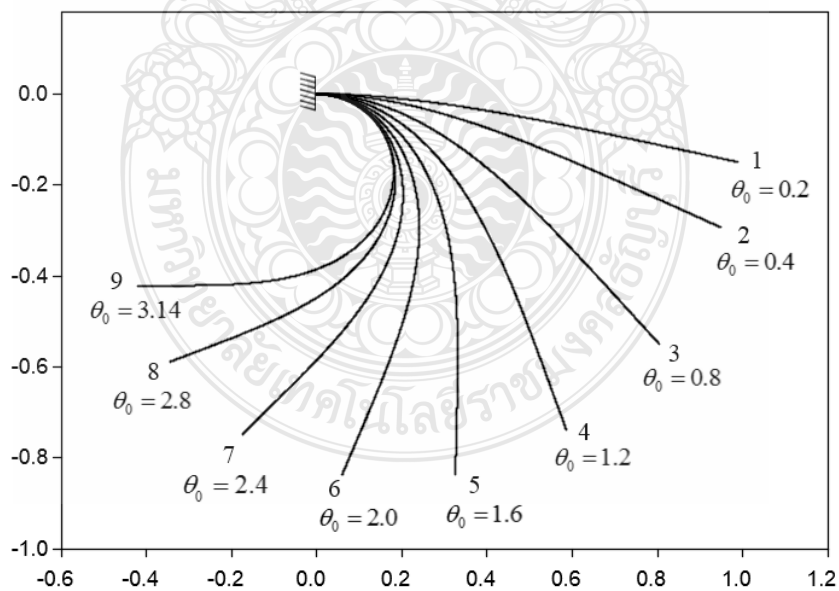


Figure 5.44 Deflection configurations of the nonlinearly cantilever beam subjected to follower distributed load $n = 1.00$

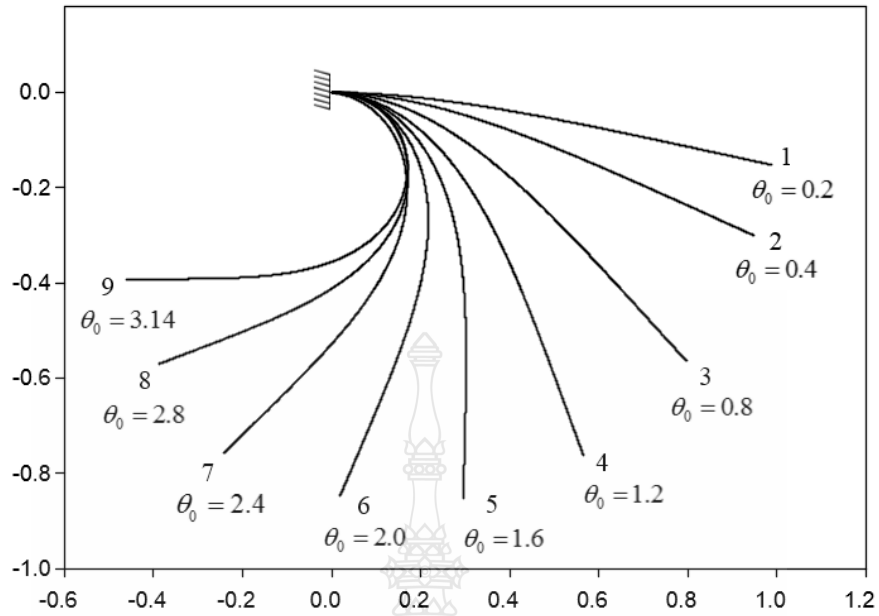


Figure 5.45 Deflection configurations of the nonlinearly cantilever beam subjected to follower distributed load $n = 1.30$

Table 5.35 Numerical results for cantilever beam made of the generalized Ludwick material for $n = 0.50$

Configuration	$n = 0.50$ and $\varepsilon_0 = 0.009$	
	θ_0 (rad)	\bar{w}
1	0.2	0.048857
2	0.4	0.148279
3	0.8	0.500026
4	1.2	1.071704
5	1.6	1.897250
6	2.0	3.031989
7	2.4	4.563630
8	2.8	6.633972
9	3.14	8.993232

Table 5.36 Numerical results for cantilever beam made of the generalized Ludwick material for $n = 1.00$

Configuration	$n = 1.00$ and $\varepsilon_0 = 0.009$	
	θ_0 (rad)	\bar{w}
1	0.2	1.201348
2	0.4	2.410405
3	0.8	4.884284
4	1.2	7.492988
5	1.6	10.325675
6	2.0	13.505593
7	2.4	17.220624
8	2.8	21.782721
9	3.14	26.794311

Table 5.37 Numerical results for cantilever beam made of the generalized Ludwick material for $n = 1.30$

Configuration	$n = 1.30$ and $\varepsilon_0 = 0.009$	
	θ_0 (rad)	\bar{w}
1	0.2	2.280423
2	0.4	4.184718
3	0.8	7.607192
4	1.2	10.646678
5	1.6	14.184550
6	2.0	17.756516
7	2.4	20.816045
8	2.8	26.951947
9	3.14	32.299234

Example 10

As the tenth example, all the parameters are kept the same as in the first example except $\varepsilon_0 = 0.01$. The results listed in Table 5.38 as shown below.

Table 5.38 Numerical results for cantilever beam made of the generalized Ludwick nonlinear elastic material: $\varepsilon_0 = 0.01$ and n varying from 0.50, 0.75..2.00

θ_0 (rad)	\bar{w} $\varepsilon_0 = 0.01$					
	$n = 0.50$	$n = 0.75$	$n = 1.00$	$n = 1.50$	$n = 1.75$	$n = 2.00$
0.0	0.000000	0.000000	0.000000	0.000000	0.000000	0.000000
0.2	0.051445	0.443503	1.201348	2.901503	3.593247	3.983886
0.4	0.153704	1.011815	2.410405	5.143261	5.921480	6.921757
0.6	0.306518	1.669155	3.635229	7.120768	7.907919	8.805891
0.8	0.511521	2.404274	4.884284	8.957290	10.280682	10.993522
1.0	0.771376	3.213972	6.166776	10.278962	12.045345	13.028472
1.2	1.089749	4.099510	7.492988	12.425871	13.559527	14.490595
1.4	1.471416	5.065425	8.874687	13.724187	15.531799	16.546260
1.6	1.922456	6.119190	10.325675	15.735595	17.316238	18.255472
1.8	2.450523	7.271376	11.862520	17.646945	18.973345	19.815532
2.0	3.065234	8.536127	13.505593	19.444520	20.876250	21.781018
2.2	3.778688	9.932056	15.280556	21.563133	22.796860	23.652007
2.4	4.606218	11.483645	17.220624	23.738057	24.659520	25.700992
2.6	5.567467	13.223455	19.370067	25.361291	27.216084	27.884587
2.8	6.688031	15.195612	21.790003	28.498975	29.063963	30.012854
3.0	8.001651	17.461587	24.290324	30.195000	32.586661	31.322268
3.14	9.059432	19.268608	26.459706	32.977805	35.095894	32.315460

The relationship of the load-displacement curve ($\varepsilon_0 = 0.01$) for the nonlinearly cantilever beam between the follower distributed load \bar{w} and the rotation angle θ_0 are demonstrated with the figure below.

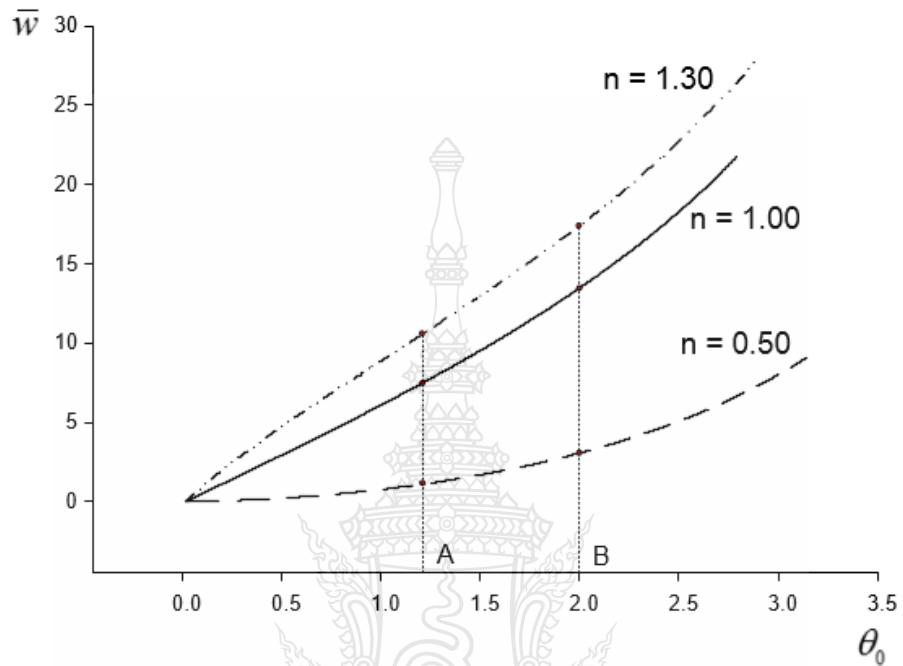


Figure 5.46 Load-displacement curve for the nonlinearly cantilever beam subjected to follower distributed load $\varepsilon_0 = 0.01$

The equilibrium configurations ($\varepsilon_0 = 0.01$) for $\theta_0 = 1.2$ and $\theta_0 = 2.0$ are chosen to indicate in the Fig. 5.47.

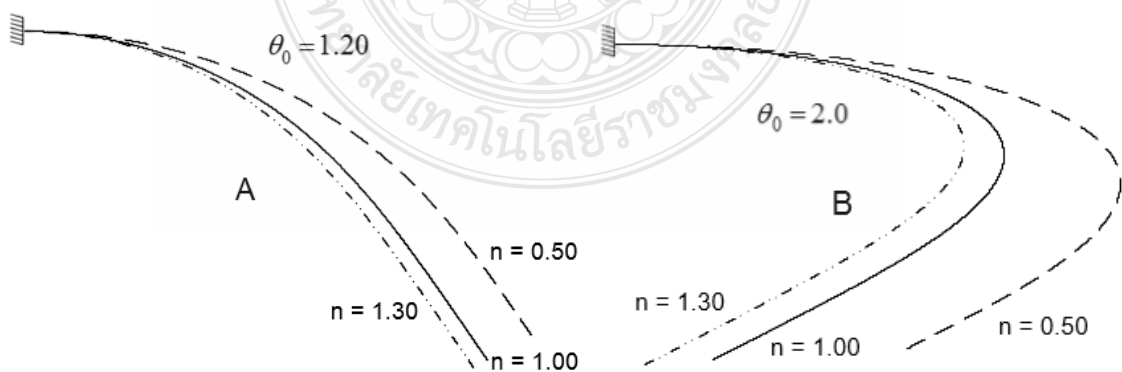


Figure 5.47 Equilibrium configurations for $\theta_0 = 1.2$ and $\theta_0 = 2.0$

Furthermore, the nonlinearity material parameters $n = 0.50$, $n = 1.00$, and $n = 1.30$ are selected to show the deflection configuration in the Fig. 5.48, 5.49 and 5.50, respectively.

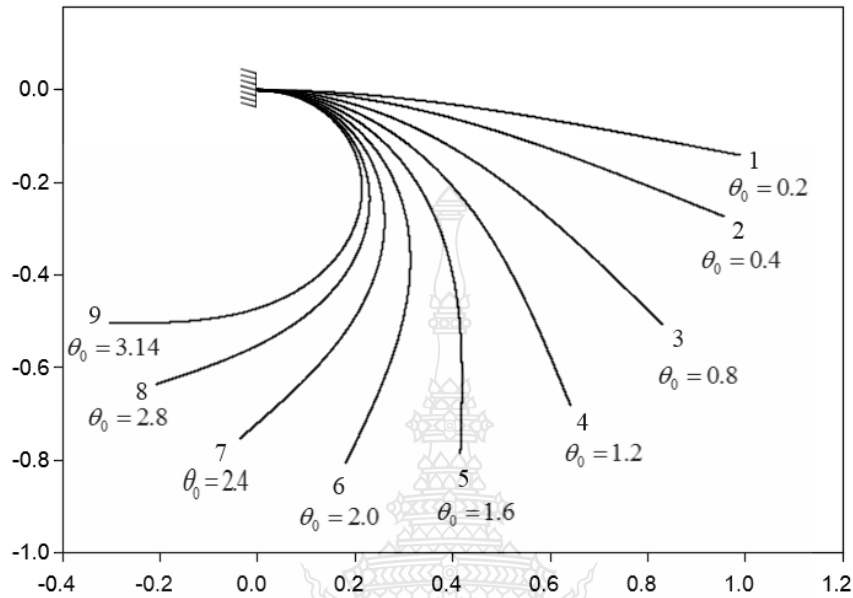


Figure 5.48 Deflection configurations of the nonlinearly cantilever beam subjected to follower distributed load $n = 0.50$

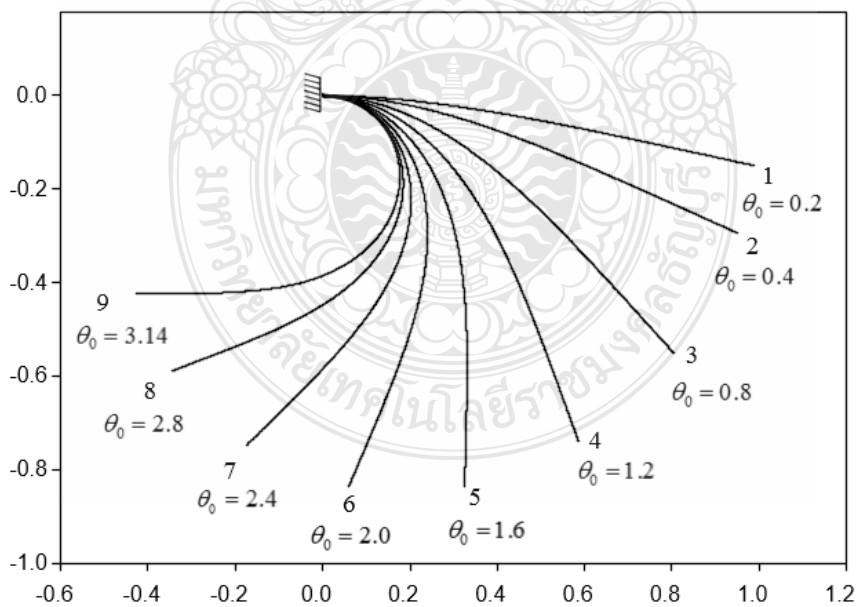


Figure 5.49 Deflection configurations of the nonlinearly cantilever beam subjected to follower distributed load $n = 1.00$

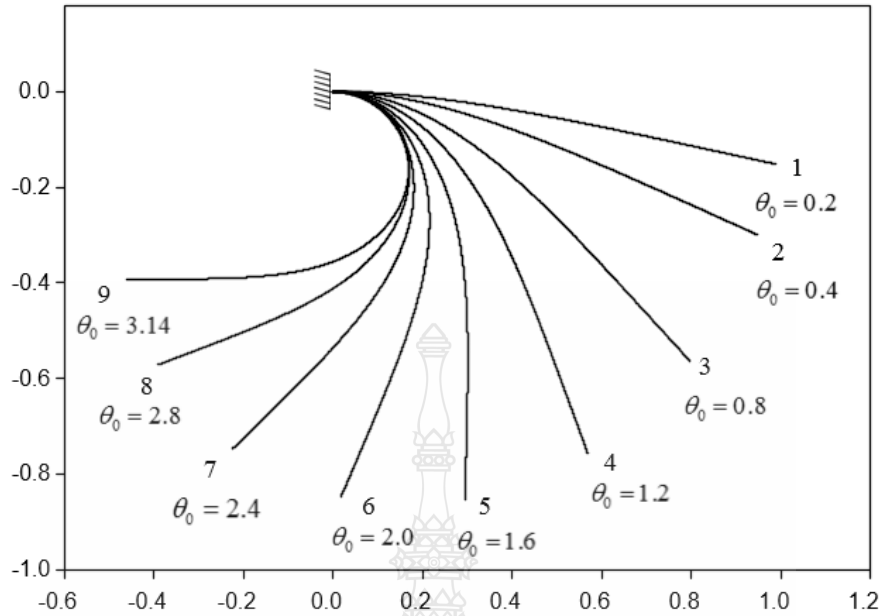


Figure 5.50 Deflection configurations of the nonlinearly cantilever beam subjected to follower distributed load $n = 1.30$

Table 5.39 Numerical results for cantilever beam made of the generalized Ludwick material for $n = 0.50$

Configuration	$n = 0.50$ and $\varepsilon_0 = 0.01$	
	θ_0 (rad)	\bar{w}
1	0.2	0.051444
2	0.4	0.153704
3	0.8	0.511521
4	1.2	1.089748
5	1.6	1.922455
6	2.0	3.065234
7	2.4	4.606218
8	2.8	6.688030
9	3.14	9.059432

Table 5.40 Numerical results for cantilever beam made of the generalized Ludwick material for $n = 1.00$

Configuration	$n = 1.00$ and $\varepsilon_0 = 0.01$	
	θ_0 (rad)	\bar{w}
1	0.2	1.201347
2	0.4	2.410405
3	0.8	4.884283
4	1.2	7.492987
5	1.6	10.325674
6	2.0	13.505593
7	2.4	17.220623
8	2.8	21.790002
9	3.14	26.459706

Table 5.41 Numerical results for cantilever beam made of the generalized Ludwick material for $n = 1.30$

Configuration	$n = 1.30$ and $\varepsilon_0 = 0.01$	
	θ_0 (rad)	\bar{w}
1	0.2	2.251925
2	0.4	4.145347
3	0.8	7.555952
4	1.2	10.806230
5	1.6	14.033920
6	2.0	17.593188
7	2.4	21.541696
8	2.8	26.700222
9	3.14	32.202834

As described above, most of them only mentioned the relationship of the load-displacement curves (ε_0). In the figure below, the relationship of the load-displacement curve ($n = 0.5$) for the nonlinearly cantilever beam between the follower distributed load \bar{w} and the rotation angle θ_0 are demonstrated.

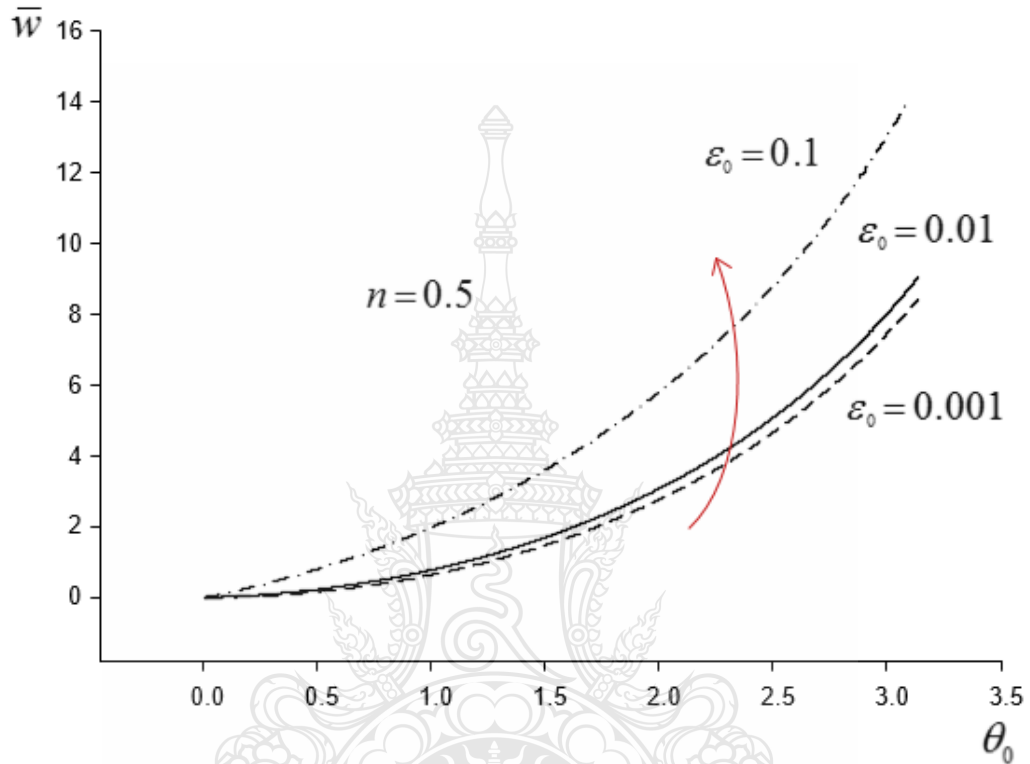


Figure 5.51 Load-displacement curve for the nonlinearly cantilever beam subjected to follower distributed load $n = 0.5$

The load–displacement curves of the cantilever beam with various elastic material parameters ε_0 are plotted in Fig. 5.51. Displayed in this figure is the load–displacement curves to play a major role in detailing the behavior of the cantilever beam for all three possible cases ($\varepsilon_0 = 0.001, \varepsilon_0 = 0.01$, and $\varepsilon_0 = 0.1$) with $n = 0.5$.

It is very interesting and remarkable that the three well-known load-displacement curves are monotonic and stable. Furthermore, it is similar to the load-displacement curves (ε_0). As it can be seen from the Fig. 5.51, the follower distributed load \bar{w} increases as the rotation angle θ_0 increases.

Displayed in the figure below is the relationship of the load-displacement curve ($n = 1.30$) for the nonlinearly cantilever beam between the follower distributed load \bar{w} and the rotation angle θ_0 are shown.

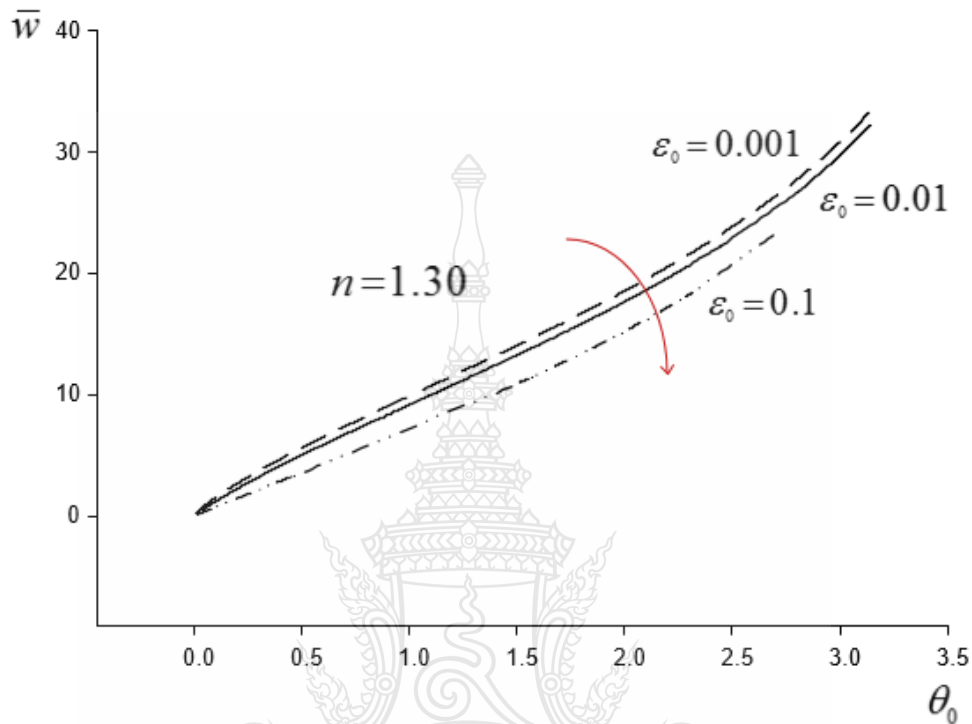


Figure 5.52 Load-displacement curve for the nonlinearly cantilever beam subjected to follower distributed load $n = 1.30$

The load–displacement curves of the cantilever beam with various elastic material parameters ϵ_0 are plotted in Fig. 5.52. The behaviors of the cantilever beam for all three possible cases ($\epsilon_0 = 0.1$, $\epsilon_0 = 0.01$, and $\epsilon_0 = 0.001$) with $n = 1.30$ are described.

It is very interesting that the follower distributed loads \bar{w} for elastic material parameters $\epsilon_0 = 0.001$ with $n = 1.30$ increase rapidly whereas the elastic material parameters $\epsilon_0 = 0.001$ with $n = 0.50$ grow gradually. However, it is remarkable from the Fig. 5.52 that the follower distributed load \bar{w} increases as the rotation angle θ_0 increases.

5.1.2 Case 2: n and ε_0 are related to each other

However, such mentioned expression of the constitutive relationship has one shortcoming—the stress gradient goes to infinity when the strain value reaches zero [38]. In our computation, we assume that the set of material parameters (i.e., ε_0 and n) can be related to each other. Technically, the initial slopes of the stress-strain curves are utilized to obtain the relationship. Hence the initial slopes of the stress–strain curve can be achieved by differentiating Eq. (3.2) [$\sigma = E \{ (|\varepsilon| + \varepsilon_0)^{1/n} - \varepsilon_0^{1/n} \}$]. After differentiating, it can be written as

$$\frac{d\sigma}{d\varepsilon} = \frac{1}{n} E_2 (\varepsilon + \varepsilon_0)^{\frac{1-n}{n}}, \quad (5.1)$$

By setting $\varepsilon = 0$, Eq. (5.1)

$$\frac{d\sigma}{d\varepsilon} = \frac{E_2}{n} (\varepsilon_0)^{\frac{1-n}{n}}, \quad (5.2)$$

$$\frac{1}{E_2} \frac{d\sigma}{d\varepsilon} = \frac{(\varepsilon_0)^{\frac{1-n}{n}}}{n}, \quad (5.3)$$

$$\frac{1}{E_1} \frac{d\sigma}{d\varepsilon} = 1, \quad (5.4)$$

Dividing Eq. (5.3) by Eq. (5.4), it can be obtained

$$\frac{E_1}{E_2} = \frac{(\varepsilon_0)^{\frac{1-n}{n}}}{n}, \quad (5.5)$$

Let $E_2 = \alpha E_1$

$$\frac{1}{\alpha} = \frac{(\varepsilon_0)^{\frac{1-n}{n}}}{n}, \quad (5.6)$$

$$\frac{n}{\alpha} = (\varepsilon_0)^{\frac{1-n}{n}}, \quad (5.7)$$

Finally, the result gives

$$\varepsilon_0 = \left(\frac{n}{\alpha} \right)^{\frac{n}{1-n}}. \quad \text{for } n \neq 1 \quad (5.8)$$

Where the initial slope of the stress-strain curve in generalized Ludwick model is defined as αE . For the example, if the initial slopes are given by $0.5E$, E , and $2E$, and the relationship between $\varepsilon_0 = (2n)^{\frac{n}{1-n}}$, $\varepsilon_0 = (n)^{\frac{n}{1-n}}$, and $\varepsilon_0 = (n/2)^{\frac{n}{1-n}}$, respectively. It should be noted that Eq. (5.8) does not valid for $n = 1$. If $n = 1$, ε_0 would set to be zero automatically. In our numerical experiments, the initial slopes are chosen to be $0.5E$ and $2E$, to show the difference between linear and nonlinear constitutive relationships.

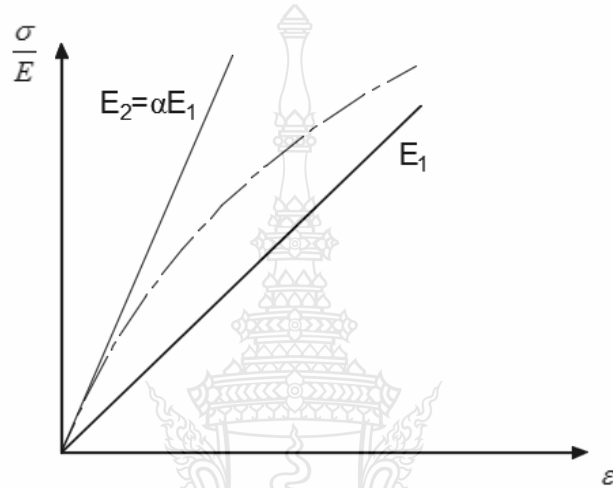


Figure 5.53 Comparison of stress–strain curve between linear and nonlinear generalized Ludwick material

To point out the nonlinear constitutive relationships clearly and simply we have chosen the two following numerical examples, the rectangular cross-section of cantilever beam is subjected to several different follower distributed loads with the degree of material nonlinearity n .

The first case of the cantilever beam with non-dimensional geometric parameters $\bar{b} = 0.2\text{m}$ and $\bar{h} = 0.2\text{m}$. The nonlinearity material parameters to determine are $n > 1$ and $\varepsilon_0 = (2n)^{\frac{n}{1-n}}$.

The second case of the cantilever beam with non-dimensional geometric parameters $\bar{b} = 0.2\text{m}$ and $\bar{h} = 0.2\text{m}$. The nonlinearity material parameters to determine are $n < 1$ and $\varepsilon_0 = (n/2)^{\frac{n}{1-n}}$.

The first two tables below are illustrated the numerical results in sequence.

The result listed in Table 5.42 can be interpreted that when using $n > 1$, the rotation angle θ_0 and the follower distributed load \bar{w} are both increase their values. In contrast, Table 5.43 demonstrated that when applying $n < 1$, the rotation angle θ_0 successively increases with the follower distributed load \bar{w} .

Table 5.42 Numerical results for cantilever beam made of the generalized Ludwick

nonlinear elastic material $n > 1$, $\bar{b} = 0.2\text{m}$ and $\bar{h} = 0.2\text{m}$

θ_0 (rad)	\bar{w}				
	$n = 1.10$	$n = 1.20$	$n = 1.30$	$n = 1.45$	$n = 1.50$
0.0	0.00000	0.00000	0.00000	0.00000	0.00000
0.2	1.68619	2.00236	2.11785	2.17475	2.18264
0.4	3.18441	3.72440	3.95424	4.07691	4.09360
0.6	4.63272	5.34237	5.66153	5.83345	5.85515
0.8	6.06606	6.91150	7.30042	7.50542	7.52825
1.0	7.50603	8.46367	8.82720	9.13123	9.15278
1.2	8.97021	10.02265	10.42959	10.71907	10.67532
1.4	10.47533	11.60927	12.12867	12.27408	12.28291
1.6	12.03887	13.24407	13.70155	13.82244	13.77604
1.8	13.68047	14.94909	15.51492	15.91570	15.43175
2.0	15.42334	16.74968	17.06725	17.21551	17.38962
2.2	17.29611	18.67661	18.58015	19.37626	19.16765
2.4	19.33549	20.76904	21.35352	21.12029	21.36808
2.6	21.59041	23.07919	22.39006	23.37350	23.52711
2.8	24.12888	25.68023	26.01780	24.79714	26.00898
3.0	27.05016	28.51741	29.26955	25.78840	27.68192
3.14	29.40196	31.10185	31.46138	31.33843	29.32568

Table 5.43 Numerical results for cantilever beam made of the generalized Ludwick nonlinear elastic material $n < 1$, $\bar{b} = 0.2\text{ m}$ and $\bar{h} = 0.2\text{ m}$

θ_0 (rad)	\bar{w}				
	$n = 0.55$	$n = 0.65$	$n = 0.75$	$n = 0.85$	$n = 0.95$
0.0	0.00000	0.00000	0.00000	0.00000	0.00000
0.2	0.57700	0.63391	0.64521	0.70084	0.98283
0.4	1.32022	1.33252	1.36696	1.51303	2.04463
0.6	2.06404	2.09450	2.15584	2.39894	3.15034
0.8	2.87544	2.92139	3.00960	3.34930	4.29766
1.0	3.82517	3.81699	3.92982	4.36308	5.49065
1.2	4.52891	4.78707	4.92084	5.44362	6.73660
1.4	5.61243	5.83952	5.98951	6.59744	8.04496
1.6	6.88814	6.98461	7.14524	7.83399	9.42775
1.8	7.61699	8.23546	8.40041	9.16593	10.90002
2.0	9.69558	9.60880	9.77101	10.60975	12.48068
2.2	11.33385	11.12606	11.27775	12.18684	14.19385
2.4	12.90037	12.81505	12.94765	13.92525	16.07088
2.6	14.87062	14.71242	14.81659	15.86234	18.15356
2.8	17.02910	16.86767	16.70870	18.04921	20.49942
3.0	19.89465	19.34963	19.27945	20.55803	23.19071
3.14	19.97827	20.60874	21.33293	22.56080	25.34391

Furthermore, the relationship of the load-displacement curve for the nonlinearly cantilever beam between the follower distributed load \bar{w} and the rotational angle θ_0 are exhibited with the figure below.

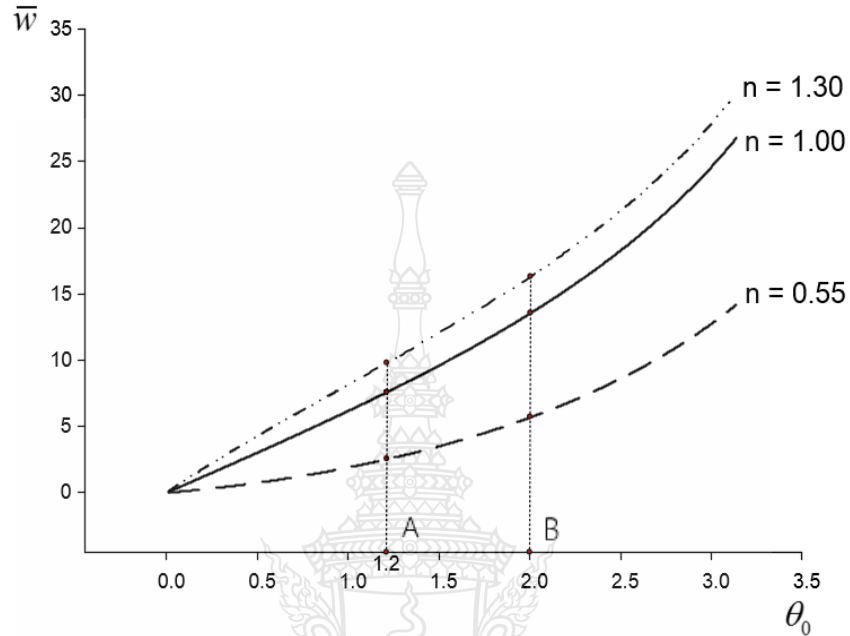


Figure 5.54 Load-displacement curve for the nonlinearly cantilever beam subjected to follower distributed load $n = 0.55$, $n = 1.00$, and $n = 1.30$

Since the Ludwick-type constitutive law has one major shortcoming as mentioned before, the large deflection behavior of a cantilever beam obeying generalized Ludwick's material model subjected to follower distributed load is discussed in this section. The load-displacement curves of the cantilever beam with various material nonlinearity parameters n are plotted in Fig. 5.54.

It is remarkable that a linear case $n = 1$ (Fig. 5.54), the well-known load-displacement curve is monotonic and stable as described in case 1. As it can be seen from the Fig 5.54, the follower distributed load \bar{w} increases as the rotation angle θ_0 increases.

For the case of hardening material, where $n > 1$ and $n < 1$ (Fig. 5.54), the behaviors of the cantilever beam are similar to the linear case $n = 1$.

The equilibrium configurations for $\theta_0 = 1.2$ and $\theta_0 = 2.0$ are selected to indicate in the Fig. 5.55.

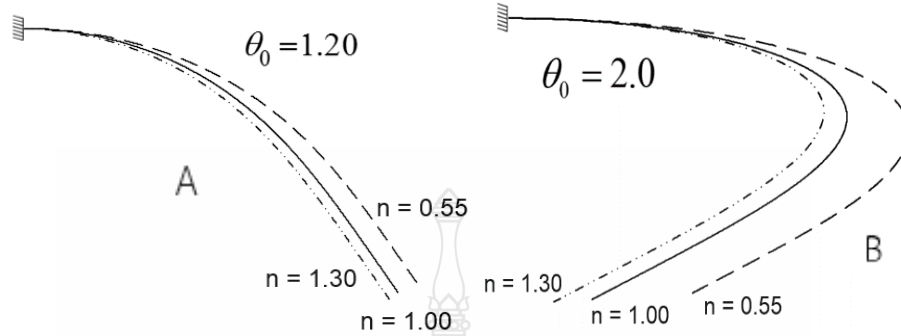


Figure 5.55 Equilibrium configurations for $\theta_0 = 1.2$ and $\theta_0 = 2.0$

In addition, the nonlinearity material parameter $n = 0.55$ is selected to show the deflection configuration.

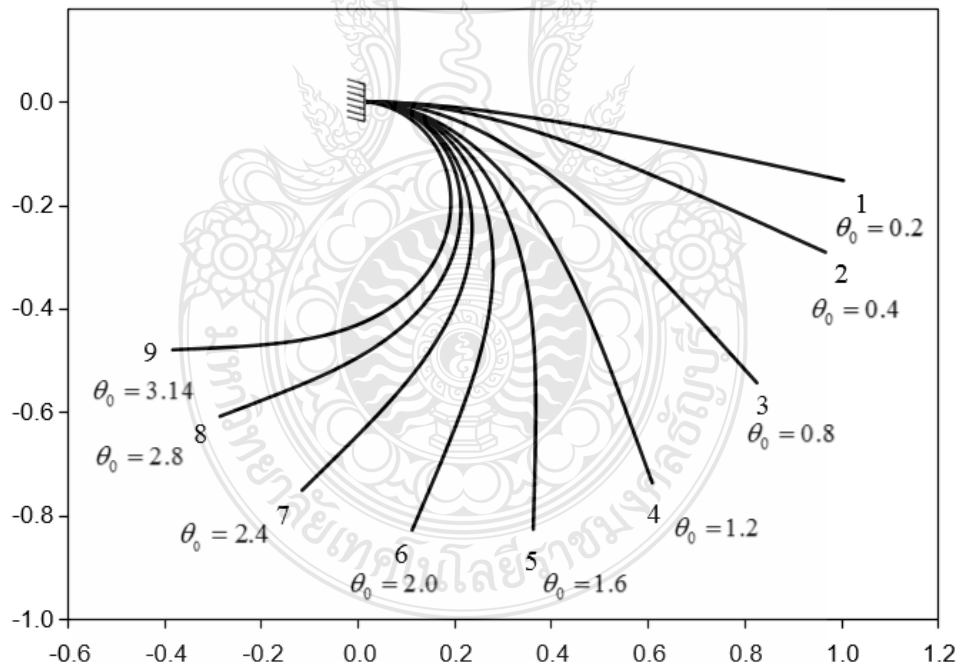


Figure 5.56 Deflection configurations of the nonlinearly cantilever beam subjected to follower distributed load $n = 0.55$ with $\varepsilon_0 = (0.5n)^{\frac{n}{1-n}}$ (Table 5.44)

Otherwise, the nonlinearity material parameter $n = 1.30$ is chosen to demonstrate the deflection configuration.

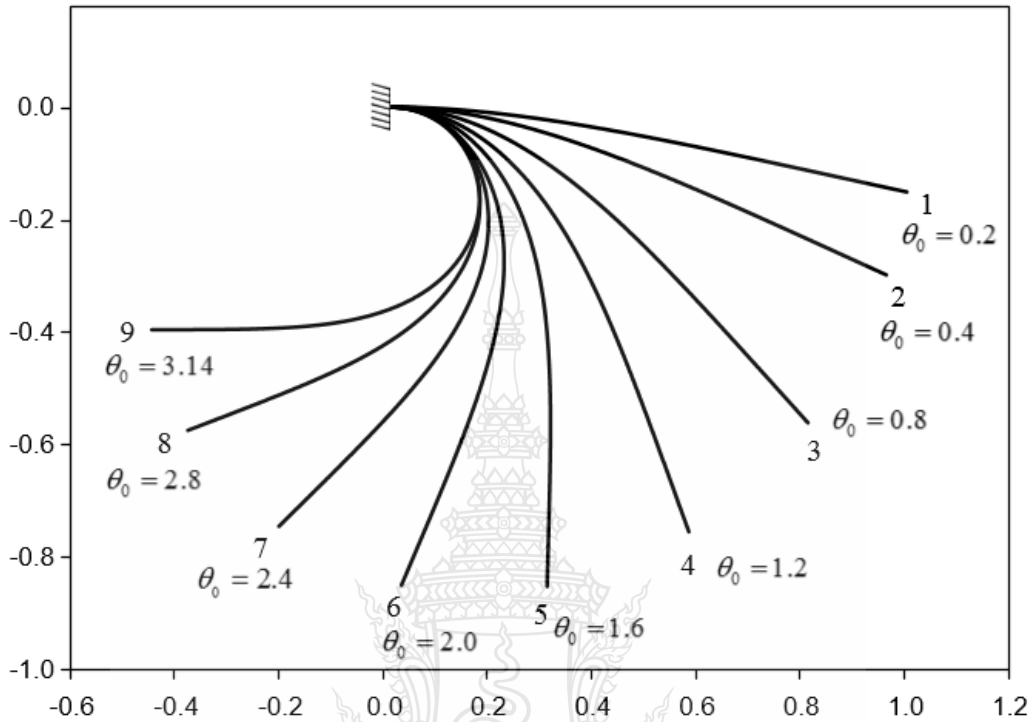


Figure 5.57 Deflection configurations of the nonlinearly cantilever beam subjected to follower distributed load $n = 1.30$ with $\varepsilon_0 = (2n)^{\frac{n}{1-n}}$ (Table 5.45)

As described in case 1, the deflected shapes with the same slope angle in the Fig. 5.56 and 5.57 are indistinguishable whether the nonlinearity material parameters are chosen with different values ($n = 0.55$ and $n = 1.30$). It is remarkable that the follower distributed load \bar{w} increases as the rotation angle θ_0 increases.

Their deflection configuration results are displayed in Table 5.44 and 5.45, respectively.

Table 5.44 Numerical results for cantilever beam made of the generalized Ludwick material for $n = 0.55$

Configuration	$n = 0.55$ and $\varepsilon_0 = (0.5n)^{\frac{n}{1-n}}$	
	θ_0 (rad)	\bar{w}
1	0.2	0.57700
2	0.4	1.32022
3	0.8	2.87544
4	1.2	4.52891
5	1.6	6.88814
6	2.0	9.69558
7	2.4	12.90037
8	2.8	17.02910
9	3.14	19.97827

Table 5.45 Numerical results for cantilever beam made of the generalized Ludwick material for $n = 1.30$

Configuration	$n = 1.30$ and $\varepsilon_0 = (2n)^{\frac{n}{1-n}}$	
	θ_0 (rad)	\bar{w}
1	0.2	2.11785
2	0.4	3.95424
3	0.8	7.30042
4	1.2	10.42959
5	1.6	13.70155
6	2.0	17.06725
7	2.4	21.35352
8	2.8	26.01780
9	3.14	31.46138

Displayed in the figures below are an explanation of stress–strain relationships for generalized Ludwick constitutive law by setting the initial slopes $0.5E$, E , and $2E$, with the three conditions of the supplementary parameter $\varepsilon_0 = (2n)^{\frac{n}{1-n}}$, $\varepsilon_0 = (n)^{\frac{n}{1-n}}$, and $\varepsilon_0 = (n/2)^{\frac{n}{1-n}}$, respectively.

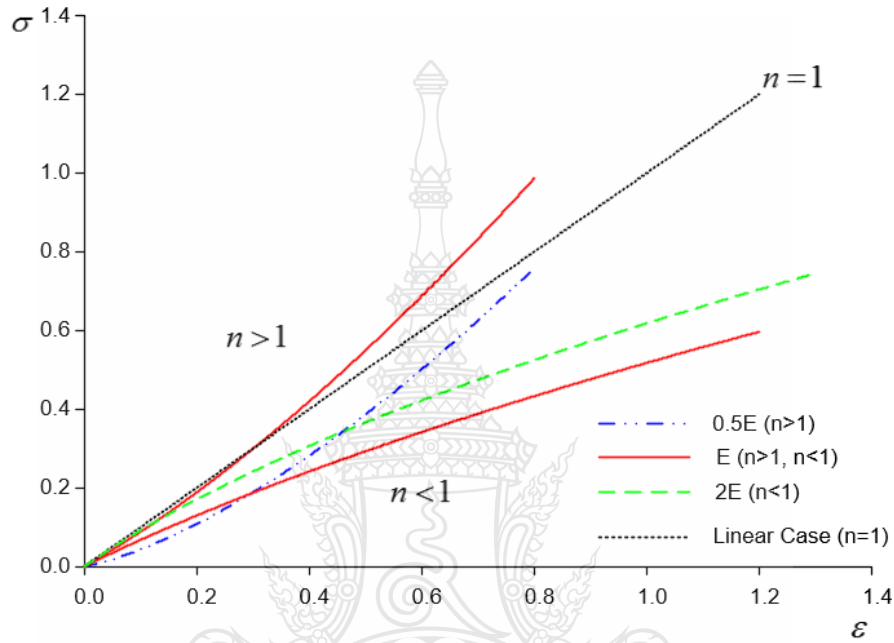


Figure 5.58 Stress–strain relationships in tensile domain for generalized Ludwick

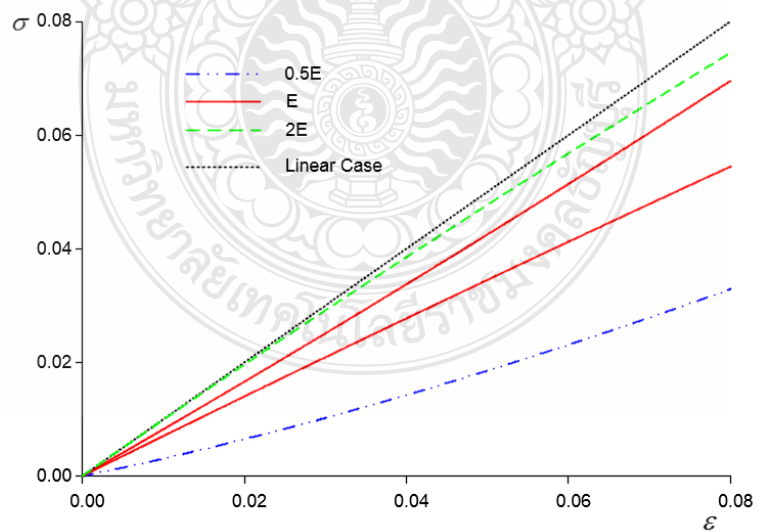


Figure 5.59 Stress–strain relationships (adjusted scale) in tensile domain for generalized Ludwick

5.1.3 Effects of the dimension of the cross-section

Furthermore, the Fig. 5.60 and 5.61 are illustrated the effects of changing the dimensions of the cross-section ($\bar{b} = 0.1-0.2\text{m}$ and $\bar{h} = 0.1-0.2\text{m}$) in the relationships of the load-displacement curves $n=0.5$ with varying $\varepsilon_0 = 0.001$ and $\varepsilon_0 = 0.002$.

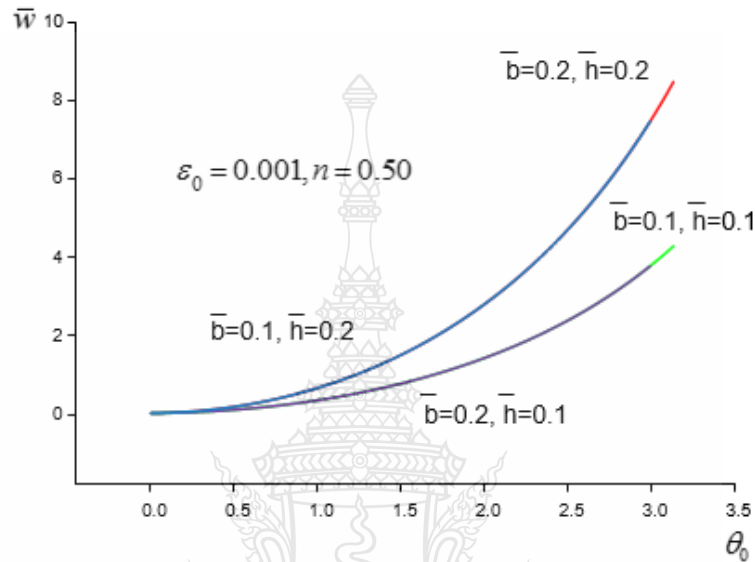


Figure 5.60 Load-displacement for the nonlinearly cantilever beam subjected to follower distributed load $\varepsilon_0 = 0.001$ and $n = 0.50$

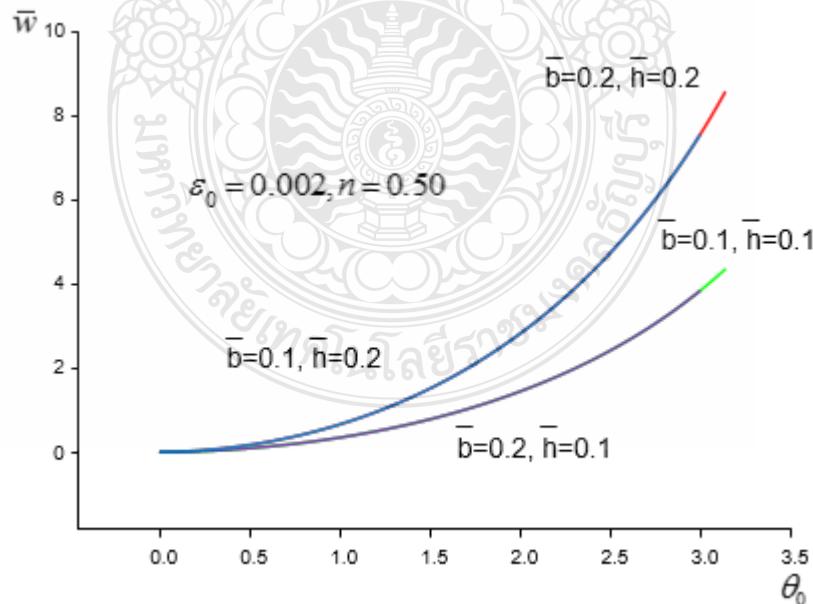


Figure 5.61 Load-displacement for the nonlinearly cantilever beam subjected to follower distributed load $\varepsilon_0 = 0.002$ and $n = 0.50$

Otherwise, the Fig. 5.62 and 5.63 are revealed the effects of changing the dimensions of the cross-section ($\bar{b} = 0.1-0.2\text{m}$ and $\bar{h} = 0.1-0.2\text{m}$) in the relationships of the load-displacement curves $n = 1.30$ with varying $\varepsilon_0 = 0.001$ and $\varepsilon_0 = 0.002$.

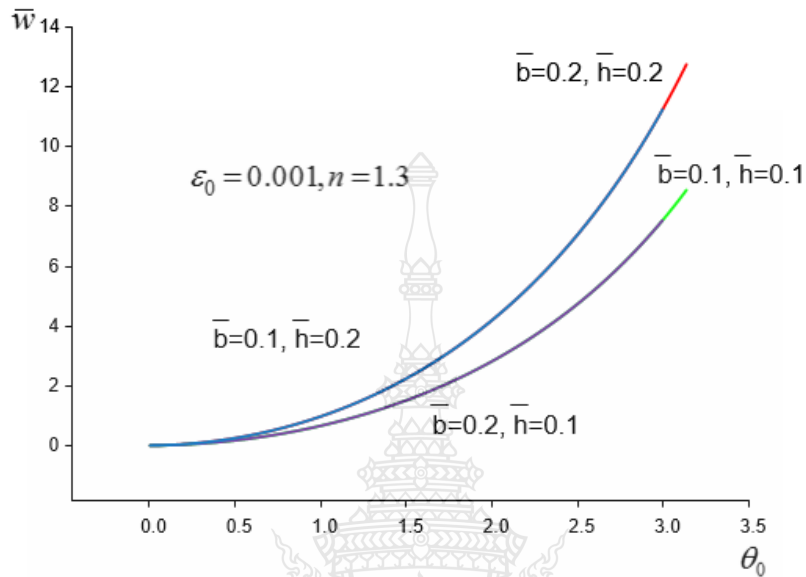


Figure 5.62 Load-displacement for the nonlinearly cantilever beam subjected to follower distributed load $\varepsilon_0 = 0.001$ and $n = 1.30$

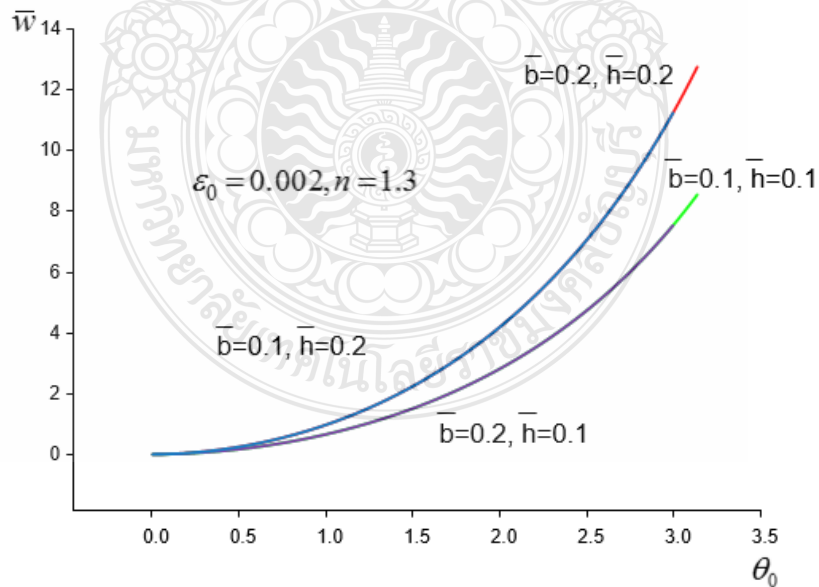


Figure 5.63 Load-displacement for the nonlinearly cantilever beam subjected to follower distributed load $\varepsilon_0 = 0.002$ and $n = 1.30$

As displayed in the Fig. 5.60, 5.61, 5.62, and 5.63, it is worth noting that when varying the width of the cross-section (\bar{b}), there is no effect to the behavior of the beam since the width (\bar{b}) is canceled in Eq. (3.18). However, the height (\bar{h}) influences to the behavior of the beam where the stiffness of the beam increases as the height (\bar{h}) increases.



CHAPTER 6

CONCLUSIONS

6.1 Conclusions

In the presented study the large deflection behavior of the cantilever beam subjected to follower distributed load where material of the cantilever beam obeys the generalized Ludwick's constitutive law is investigated. Both geometrical and material nonlinearities are relevant to this problem since the material of the cantilever beam is assumed to be nonlinearly elastic. This can be surpassed in a three-parametric generalized Ludwick's material model which is described and applied in this study of large deflections of cantilever beam. Since the governing equations were highly nonlinear differential equations, the closed-form solutions are in general impossible. Otherwise, the cantilever beam problem has been solved numerically by the shooting method. We also have generated an exact moment-curvature formula for materials which obey the generalized Ludwick's law.

Several numerical examples were selected to demonstrate the influence of the geometry and configurations of the beam, loading conditions, and constitutive law of the material on the deflection behavior of the discussed cantilever beam. Most of the load-deflection curves revealed in chapter 5 are monotonic and stable.

From a practical standpoint, results obtained in this research study illustrate the effects of the generalized Ludwick's model. It can be concluded as the following.

6.1.1 The effects of nonlinearity materials on the large deflection behavior of a cantilever beam obeying generalized Ludwick's material model subjected to follower distributed load are divided the set of parameters ε_0 and n into two cases. The first case is n and ε_0 are varied independently. Second one is n and ε_0 are related to each other.

6.1.2 In case 1 with cross-sectional area $\bar{b} = 0.2\text{m}$ and $\bar{h} = 0.2\text{m}$, numerical results with material nonlinearity parameters ε_0 ranging from 0.001 to 0.003 and n varying from 0.50, 0.75..2.00 reveal that the follower distributed load increases as the rotational angles goes up. On the other hand, the follower distributed load decreases while employing ε_0 (0.004–0.008) with specifying the value of n at 0.75 and 2.00. However, it is very interesting to take a note that the follower distributed loads and the rotational angles are both rising their values if taking a look at value of n individually.

6.1.3 In case 2 with cross-sectional area $\bar{b} = 0.2\text{m}$ and $\bar{h} = 0.2\text{m}$, specifying the material nonlinearity parameters $n > 1$ and $\varepsilon_0 = (2n)^{\frac{n}{1-n}}$, its numerical results (Table 5.42) demonstrated that the follower distributed loads and the rotational angles both increase in their values from $n = 1.10$ to $n = 1.50$. Interestingly, at the value of the rotational angle $\theta_0 = 3.14$ founded that $n = 1.20$, $n = 1.30$, and $n = 1.45$ obtained close values of follower distributed loads 31.10185, 31.46138, and 31.33843, respectively. Moreover, by further employing the material nonlinearity parameters $n < 1$ and $\varepsilon_0 = (0.5n)^{\frac{n}{1-n}}$, numerical results (Table 5.43) illustrated that the follower distributed loads and the rotational angles both increase for all the values of n .

6.2 Suggestions

This research study is believed that it is the first research that solve the problem of the large deflection behavior of the cantilever beam subjected to follower distributed load where material of the cantilever beam obeys the generalized Ludwick's constitutive law and the effect of nonlinearity materials on large deflection behavior of the beam obeying generalized Ludwick's constitutive law. Thus in this research study can be developed for other applications as below.

6.2.1 According to presented study only dealt with the rectangular cross-section of cantilever beam. For further research study can be handled the variety cross-sectional shapes with varying longitudinal shape subjected to follower distributed load in which more numerical effort is necessary.

6.2.2 The computational program Matlab may be upgraded more program codes to carry out the numerical results more successively. As in case 2 (n and ε_0 are related to each other), the computational process cannot go through while specifying the values of the nonlinearly parameter n greater than 1.80.

6.2.3 The material employing in this research study is a material where stress-strain relationship obeys the generalized Ludwick's constitutive law. One more nonlinearly material can be established for further research on the large deflection behavior of the cantilever beam subjected to follower distributed load is Ramberg-Osgood's Material.

What is more, the recent findings from this study will benefit the analysis and design of the practical problems. This hands out as a benchmark for future experimental investigations as well.

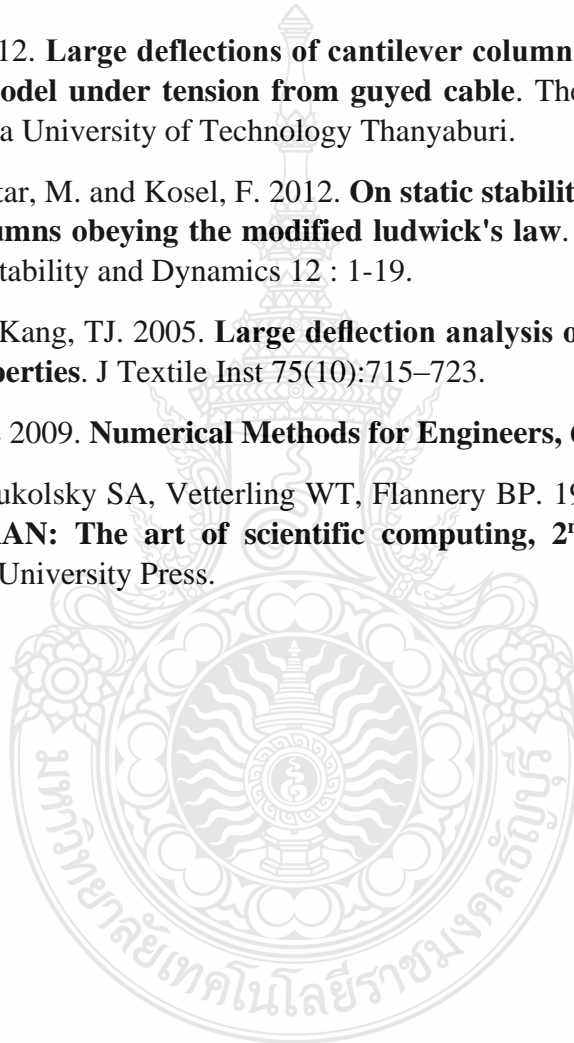
Bibliography

- [1] Brojan, M., Videnic, T. and Kosel, F. 2009. **Large deflections of nonlinearly elastic non-prismatic cantilever beams made from materials obeying the generalized Ludwick constitutive law.** Meccanica 44: 733-739.
- [2] Saetiew, W. and Chucheepsakul, S. 2012. **Post-buckling of linearly tapered column made of nonlinear elastic materials obeying the generalized Ludwick constitutive law.** International Journal of Mechanical Sciences 65 : 83-96.
- [3] Saetiew, W. and Chucheepsakul, S. 2012. **Post-buckling of simply supported column made of nonlinear elastic materials obeying the generalized Ludwick constitutive law.** Zeitschrift für Angewandte Mathematik und Mechanik, Journal of Applied Mathematics and Mechanics 92 : 479-489.
- [4] Brojan, M., Cebron, M. and Kosel, F. 2012. **Large deflections of non-prismatic nonlinearly elastic cantilever beams subjected to non-uniform continuous load and a concentrated load at the free end.** The Chinese Society of Theoretical and Applied Mechanics and Springer-Verlag Berlin Heidelberg : 863-869.
- [5] Hosagrahara, V., Tamminana, K. and Sharma, G. 2010. **Accelerating Finite Element Analysis in MATLAB with Parallel Computing.** Mathworks.
- [6] Kocatürk, T., Akbaş, Ş. D. and Şimşek, M. 2010. **Large deflection static analysis of a cantilever beam subjected to a point load.** International Journal of Engineering and Applied Sciences 4 : 1-13.
- [7] Mutyalarao, M., Bharathi, D. and Rao, B.N. 2010. **Large deflections of a cantilever beam under an inclined end load.** Applied Mathematics and Computation 217 : 3607-3613.
- [8] Brojan, M., Videnic, T. and Kosel, F. 2007. **Non-prismatic non-linearly elastic cantilever beams subjected to an end moment.** Journal of Reinforced Plastics and Composites 26 : 1071-1082.
- [9] Lee, K. 2002. **Large deections of cantilever beams of non-linear elastic material under a combined loading.** International Journal of Non-Linear Mechanics 37 : 439-443.
- [10] Borboni, A. and Santis, D.D. 2014. **Large deflection of a non-linear, elastic, asymmetric Ludwick cantilever beam subjected to horizontal force, vertical force and bending torque at the free end.** Meccanica 49 : 1327-1336.

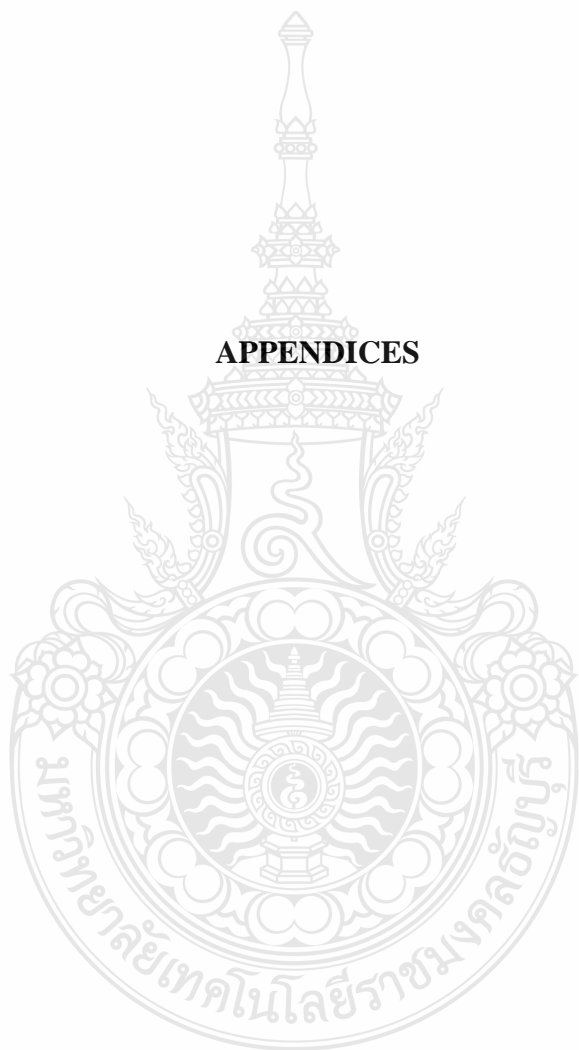
- [11] Solano-Carrillo, E. 2009. **Semi-exact solutions for large deflections of cantilever beams of non-linear elastic behaviour.** International Journal of Non-Linear Mechanics 44 : 253-256.
- [12] Rao, B.N. and Rao, G.V. 1989. **Large deflections of a cantilever beam subjected to a rotational distributed loading.** Forschung im Ingenieurwesen, 55(4) : 116-120.
- [13] Shvartsman, B.S. 2007. **Large deflections of a cantilever beam subjected to a follower force.** Journal of Sound and Vibration 304 : 969-973.
- [14] Shvartsman, B.S. 2009. **Direct method for analysis of flexible cantilever beam subjected to two follower forces.** International Journal of Non-Linear Mechanics 44 : 249-252.
- [15] Phungpaingam, B., Chucheepsakul, S. and Wang, C.M. 2006. **Postbuckling of Beam Subjected to Intermediate Follower Force.** Journal of Engineering Mechanics 132 : 16-25.
- [16] Banerjee, A., Bhattacharya, B. and Mallik, A.K. 2008. **Large deflection of cantilever beams with geometric non-linearity: Analytical and numerical approaches.** International Journal of Non-Linear Mechanics 43 : 366-376.
- [17] Chen, L. 2010. **An integral approach for large deflection cantilever beams.** International Journal of Non-Linear Mechanics 45 : 301-305.
- [18] Nallathambi, A.K., Rao, C.L. and Srinivasan, S.M. 2010. **Large deflection of constant curvature cantilever beam under follower load.** International Journal of Mechanical Sciences 52 : 440-445.
- [19] Kang, Y.A. and Li, X.F. 2009. **Bending of functionally graded cantilever beam with power-law non-linearity subjected to an end force.** International Journal of Non-Linear Mechanics 44 : 696-703.
- [20] Salehi, P., Yaghoobi, H. and Torabi, M. 2012. **Application of the differential transformation method and variational iteration method to large deformation of cantilever beams under point load.** Journal of Mechanical Science and Technology 26 : 2879-2887.
- [21] Li, Q.L. and Li, S.R. 2010. **Nonlinear bending of a cantilever beam subjected to a tip concentrated follower force.** International Conference on Information and Computing (3rd) : 74-77.
- [22] Cai, G.P., Hong, J.Z. and Yang, S.X. 2004. **Model study and active control of a rotating flexible cantilever beam.** International Journal of Mechanical Sciences 46 : 871-889.

- [23] Li, Q.L., Li, S.R. and Xiang, C.S. 2011. **Nonlinear analysis of a cantilever elastic beam under non-conservative distributed load.** International Conference on Information and Computing (4th) : 181-183.
- [24] Kim, J.O., Lee, K.S. and Lee, J.W. 2008. **Beam stability on an elastic foundation subjected to distributed follower force.** Journal of Mechanical Science and Technology 22 : 2386-2392.
- [25] Vazquez-Leal, H., Khan, Y. and May, A.L.H. 2013. **Approximations for large deflection of a cantilever beam under a terminal follower force and nonlinear pendulum.** Journal of Mathematical Problems in Engineering : 1-13.
- [26] Auciello, N.M. 2012. **Effect of subtangential parameter on the stability and dynamic of a cantilever tapered beams subjected to followed forces.** International Virtual Conference of Advanced Research in Scientific Areas : 1721-1726.
- [27] Kang, T.J., Kim, J.G., Kim, J.H., Hwang, K.C., and Lew, B.W. 2008. **Deformation characteristics of electroplated MEMS cantilever beams released by plasma ashing.** Journal of Sensors and Actuators A 148 (2008): 407–415.
- [28] Gong, Y., Zhang, L., Zhao, F., Meng, C., and Liang, L. 2009. **Design Optimization of Cantilever Beam MEMS Switch.** International Conference on Industrial Mechatronics and Automation (2009): 28–31.
- [29] Rogers, B., Manning, L., Sulchek, T., Meng, C., and Adams, J.D. 2004. **Improving tapping mode atomic force microscopy with piezoelectric cantilevers.** Journal of Ultramicroscopy 100 (2004): 267–276.
- [30] Leis, J., Zhao, W., Pinnaduwege, L.A., Shepp, A., and Mahmud, K.K. 2010. **Estimating gas concentration using a microcantilever-based electronic nose.** Journal of Digital Signal Processing 20 (2010): 1229–12371.
- [31] Singh, A., Mukherjee, R., Turner, K., and Shaw, S. 2005. **MEMS implementation of axial and follower end forces.** Journal of Sound and Vibration 286 (2005): 637–644.
- [32] Vettiger, P., Cross, G., Despont, M., Drechsler, U., Dürig, U., Gotsmann, B., Häberle, W., Lantz, M.A., Rothuizen, H.E., Stutz, R., and Binnig, G.K. 2002. **The “Millipede” Nanotechnology Entering Data Storage.** IEEE Transactions on Nanotechnology, Vol. 1, No. 1, March (2002): 39–55.
- [33] Eren, I. 2008. **Determining large deflections in rectangular combined loaded cantilever beams made of non-linear Ludwick type material by means of different arc length assumptions.** Yildiz Technical University, Mechanical Engineering Department, 34349, Besiktas, Istanbul, Turkey : 45-55.

- [34] Athisakul, C., Phungpaingam, B., Juntarakong, G. and Chucheepsakul, S. 2012. **Effect of material nonlinearity on large deflection of variable-arc-length beams subjected to uniform self-weight.** *Mathematical Problems in Engineering* : 1-9.
- [35] Narmluk, M., Poksuk, Y. and Rattanaphan, P. 2548. **Non-prismatic non-linearly elastic cantilever beams subjected to an end moment.** การประชุมวิชาการวิศวกรรมโยธาแห่งชาติครั้งที่ 10 : 53-58.
- [36] Phonok, S. 2012. **Large deflections of cantilever column made from ludwick's material model under tension from guyed cable.** Thesis of master degree at Rajamangala University of Technology Thanyaburi.
- [37] Brojan, M., Sitar, M. and Kosel, F. 2012. **On static stability of nonlinearly elastic euler's columns obeying the modified ludwick's law.** *International Journal of Structural Stability and Dynamics* 12 : 1-19.
- [38] Jung, JH. and Kang, TJ. 2005. **Large deflection analysis of fibers with nonlinear elastic properties.** *J Textile Inst* 75(10):715–723.
- [39] Chapra Canale 2009. **Numerical Methods for Engineers, 6th Edition.**
- [40] Press WH, Teukolsky SA, Vetterling WT, Flannery BP. 1992. **Numerical recipes in FORTRAN: The art of scientific computing, 2nd Edition.** New York: Cambridge University Press.



APPENDICES





APPENDIX A
RUNGE-KUTTA METHODS

Runge–Kutta (RK) methods can be acquired by employing the accuracy of a Taylor series approach without requiring the higher derivatives computation.

$$y_{i+1} = y_i + \phi(x_i, y_i, h)h \quad (\text{A.1})$$

where $\phi(x_i, y_i, h)$ is called an *increment function*, which can be illustrated as a representative slope over the interval. In general, the increment function is given as

$$\phi = a_1k_1 + a_2k_2 + \dots + a_nk_n \quad (\text{A.2})$$

where the a 's are constant and the k 's are

$$k_1 = f(x_i, y_i) \quad (\text{A.2a})$$

$$k_2 = f(x_i + p_1h, y_i + q_{11}k_1h) \quad (\text{A.2b})$$

$$k_3 = f(x_i + p_2h, y_i + q_{21}k_1h + q_{22}k_2h) \quad (\text{A.2c})$$

.

.

.

$$k_n = f(x_i + p_{n-1}h, y_i + q_{n-1,1}k_1h + q_{n-1,2}k_2h + \dots + q_{n-1,n-1}k_{n-1}h) \quad (\text{A.2d})$$

where the p 's and q 's are constants. Notice that the k 's are recurrence relationships. That is, $k_i, i=1,2,3,\dots,n$. The most popular RK methods are fourth order. The most commonly used form, namely the *classical fourth-order RK method* can be summarized as below.

$$y_{i+1} = y_i + \frac{1}{6}(k_1 + 2k_2 + 2k_3 + k_4)h \quad (\text{A.3})$$

where

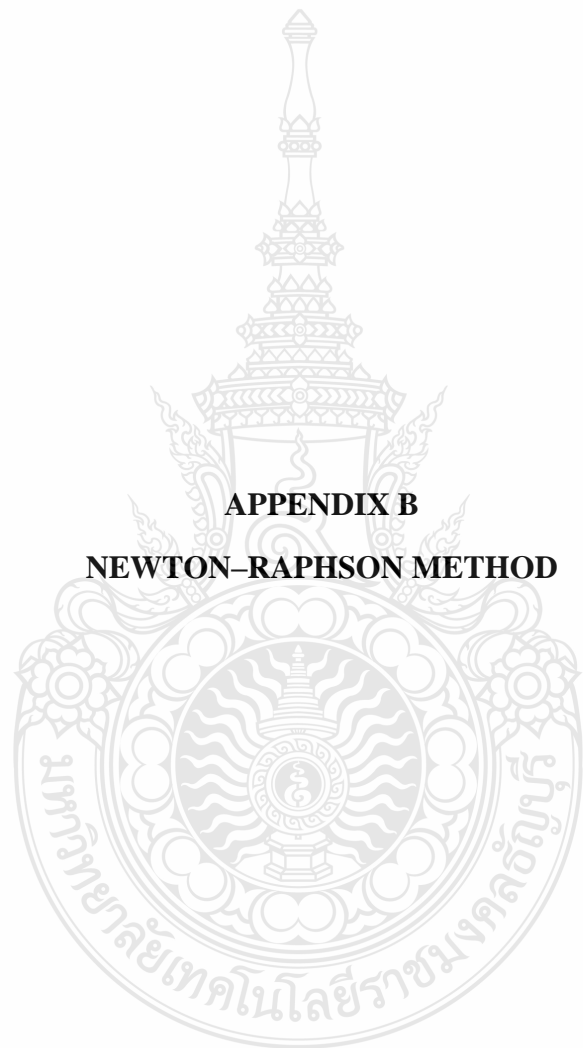
$$k_1 = f(x_i, y_i) \quad (\text{A.3a})$$

$$k_2 = f\left(x_i + \frac{1}{2}h, y_i + \frac{1}{2}k_1h\right) \quad (\text{A.3b})$$

$$k_3 = f\left(x_i + \frac{1}{2}h, y_i + \frac{1}{2}k_2h\right) \quad (\text{A.3c})$$

$$k_4 = f(x_i + h, y_i + k_3h) \quad (\text{A.3d})$$

For more details of this Runge–Kutta methods, be able to learn more from [39]



APPENDIX B

NEWTON-RAPHSON METHOD

The Newton-Raphson equation (Fig B.1) is employed to the usage of root-locating formulas. If the initial guess at the root is x_i , a tangent is supposed to extend from the point $[x_i, f(x_i)]$. The point where the x axis usually reveals an improved estimate of the root.

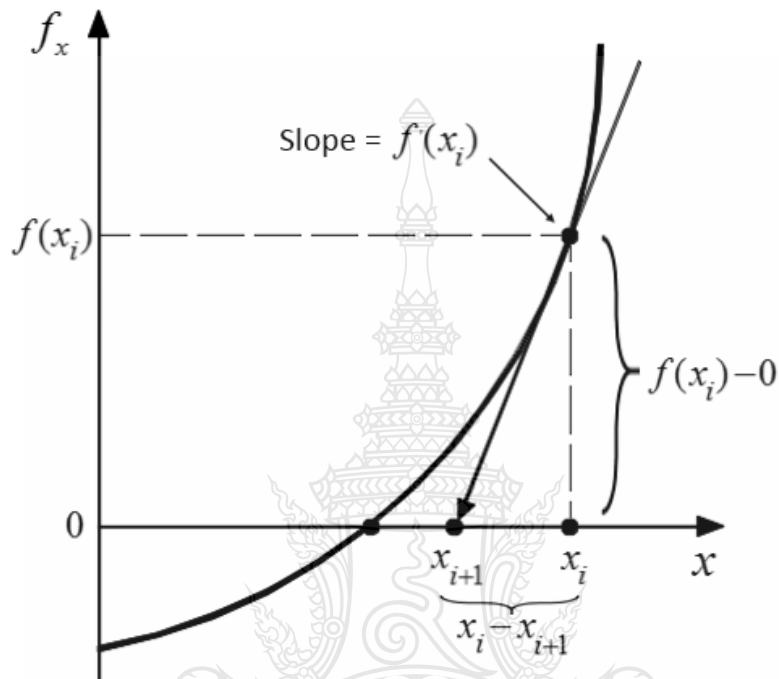


Figure B.1 Graphical depiction of the Newton-Raphson method

(Chapra Canale 2009. **Numerical Methods for Engineers, 6th Edition**)

A method relied on the Taylor series is applied to describe the behavior of the calculation of the Newton-Raphson method. As in Fig B.1, the first derivative at x is equivalent to the slope:

$$f'(x_i) = \frac{f(x_i) - 0}{x_i - x_{i+1}} \quad (\text{B.1})$$

which can be rearranged to yield

$$x_{i+1} = x_i - \frac{f(x_i)}{f'(x_i)} \quad (\text{B.2})$$

which is called the *Newton-Raphson formula*.

Recall from the Taylor series expansion can be represented as

$$f(x_{i+1}) = f(x_i) + f'(x_i)(x_{i+1} - x_i) + \frac{f''(\xi)}{2!}(x_{i+1} - x_i)^2 \quad (\text{B.3})$$

where ξ lies somewhere in the interval from x_i to x_{i+1} . An approximate version is obtainable by truncating the series after the first derivative term:

$$f(x_{i+1}) \cong f(x_i) + f'(x_i)(x_{i+1} - x_i) \quad (\text{B.4})$$

$$0 \cong f(x_i) + f'(x_i)(x_{i+1} - x_i) \quad (\text{B.5})$$

which can be solved for

$$x_{i+1} = x_i - \frac{f(x_i)}{f'(x_i)}$$

which is identical to Eq. (B.2). Apart from the derivation, the Taylor series can also be established to estimate the error of the formula. For this situation $x_{i+1} = x_i$, where x is the true value of the root. Substituting this value along with $f(x_r) = 0$ into Eq. (B.3) yields

$$0 = f(x_i) + f'(x_i)(x_r - x_i) + \frac{f''(\xi)}{2!}(x_r - x_i)^2 \quad (\text{B.6})$$

Equation (B.5) can be subtracted from Eq. (B.6) to give

$$0 = f'(x_i)(x_r - x_{i+1}) + \frac{f''(\xi)}{2!}(x_r - x_i)^2 \quad (\text{B.7})$$

Now, realize that the error is equal to the discrepancy between x_{i+1} and the true value x_r , as in

$$E_{t,i+1} = x_r - x_{i+1}$$

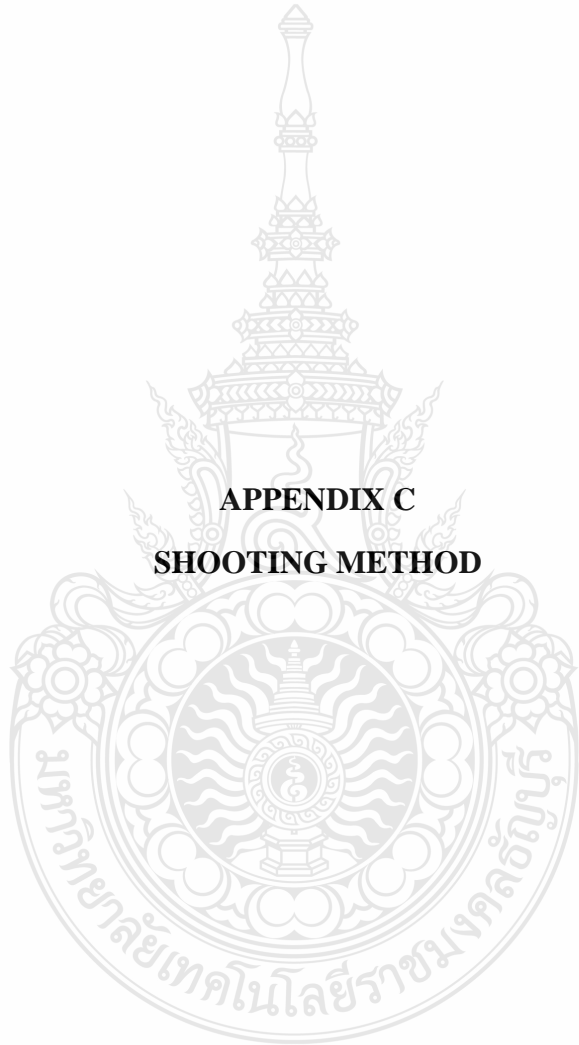
and Eq. (B.7) can be expressed as

$$0 = f'(x_i)E_{t,i+1} + \frac{f''(\xi)}{2!}E_{t,i}^2 \quad (\text{B.8})$$

$$E_{t,i+1} = \frac{-f''(x_r)}{2f'(x_r)}E_{t,i}^2 \quad (\text{B.9})$$

For more details of this Newton-Raphson method, be able to learn more from [39]

APPENDIX C
SHOOTING METHOD



Shooting method is a method dealing with the equations where the integration proceeds from x_1 to x_2 , and we try to match boundary conditions at the end of the integration (Fig C.1). Newton-Raphson method plays important role to carry out this problem.

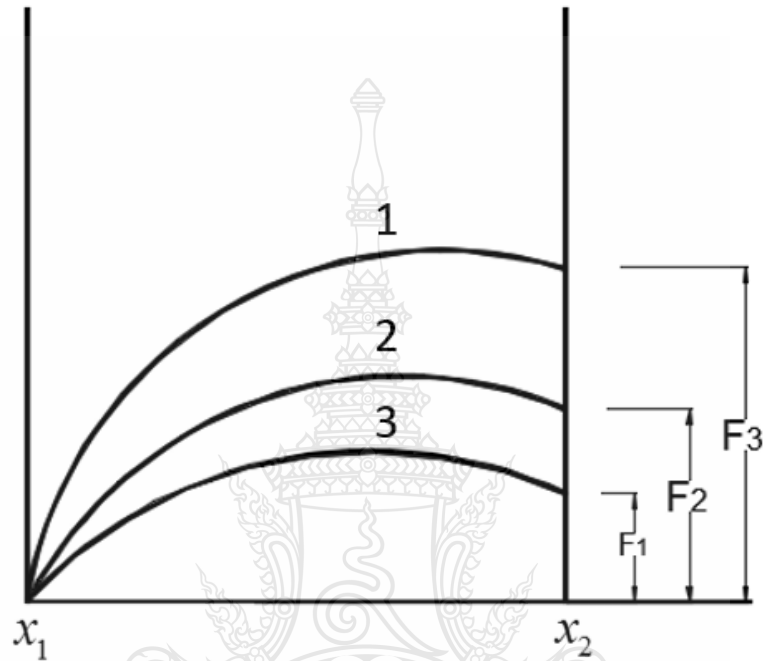


Figure C.1 Shooting method

(Numerical recipes in FORTRAN: The art of scientific computing)

1. At the starting point x_1 there are N starting values y_i to be specified, but subjected to n_1 conditions. Therefore $n_2 = N - n_1$ is the starting values. And a vector V is equaled to $n_2 x_1$. It can be written as below.

$$y_i(x_1) = y_i(x_1; V_1, \dots, V_{n_2}) \quad i = 1, \dots, N \quad (\text{C.1})$$

2. Start integrating the ODEs from x_1 to x_2 at point x_2 and it can find the differences between the integrating values and boundary conditions at x_2 . Now, at x_2 , let us define a discrepancy vector F which equals to $n_2 x_1$ the same as vector V .
3. Newton-Raphson is proposed to solve the problem by finding a vector value of V that zeros the vector value of F .

$$V_{new} = V_{old} + \delta V \quad (C.2)$$

$$J \cdot \delta V = -F \quad (C.3)$$

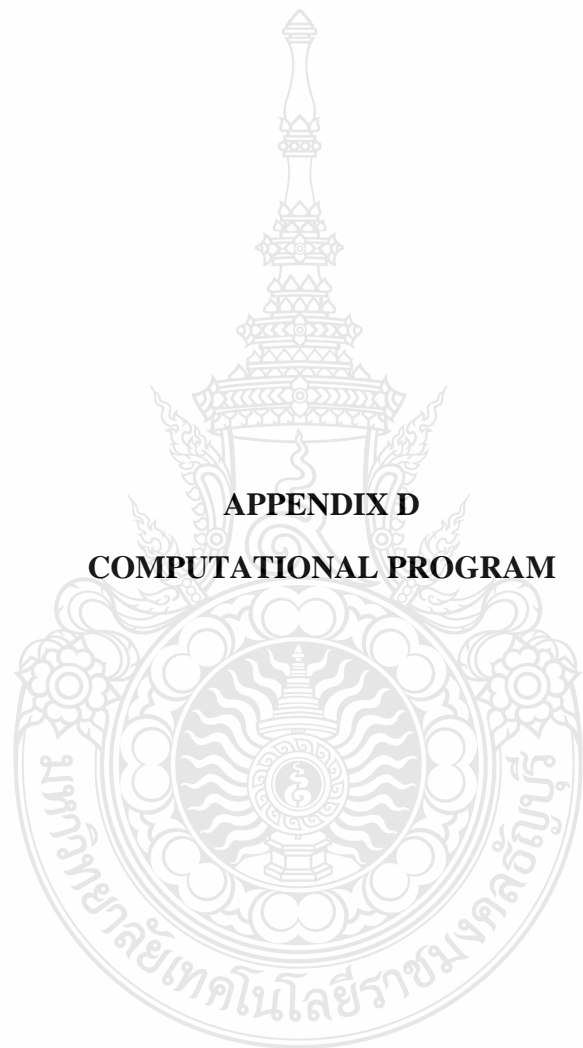
The Jacobian matrix J has components given by

$$J_{ij} = \frac{\partial F_i}{\partial V_j} \quad (C.4)$$

It is not feasible to make a computation these partial derivatives analytically.

For more details of this shooting method, be able to learn more from [40]





APPENDIX D
COMPUTATIONAL PROGRAM

The first case is n and ε_0 are varied independently.

cantilever_self

```
function cantilever_self
% cantilever beam with follower self-weight
clear
global ceta0 pl b h n E0

format long

b=input('Width (b) ');
h=input('Height (h) ');
n=input('Degree of material nonlinearity (n) ');
E0=input('Degree of material nonlinearity (E0) ');
ceta0=input('End rotation ');
v(1)=input('Distributed load (w) ');
pl=input('Plot configuration shapes (yes (1), no (0))= ');
P=v(1);
lim=input('Limitation= ');
inc=input('Increment= ');
fid=fopen('Output_follower_generalized Ludwick.txt','wt');
fprintf(fid,'Output of follower self-weight cantilever beam obeying
generalized Ludwick\n');
fprintf(fid,'ceta0      w \n');
i=0;
dv=0.0001;
while (ceta0<lim)
    v0=[v(1)];

    options=optimset(optimset('fsolve'),'MaxFunEvals',400,'TolFun',1e-
15,'TolX',1.0e-15);

    [v fval]=fsolve('score_cantfollower',v0,options)
    test=max(abs(fval));

while (test>1.0e-8&& i<25)
    i=i+1;
```

```

v(1)=v(1)+dv;

v0=[v(1)];

[v fval]=fsolve('score_canfollower',v0,options)
end

fprintf(fid,'%12.9f                %12.9f
%12.9f\n',ceta0,v(1),test);

ceta0=ceta0+inc

end

fclose(fid)
end

goveqs_follower_self
function dydx=goveqs_follower_self(x,y)
global w b h n E0
dydx=zeros(6,1);

A=((abs(y(3)))^h)/2*(n+1)*(((abs(y(3)))^h)/2+E0)^(1/n)*h;
A1=((abs(y(3)))^2)*((2*n)+1);
B=n*E0*(((abs(y(3)))^h)/2+E0)^(1/n)*h;
B1=((abs(y(3)))^2)*((2*n)+1);
C=n*(((abs(y(3)))^h)/2+E0)^((n+1)/n)*h;
C1=((abs(y(3)))^2)*((2*n)+1);
D=4*(n^2)*E0*(((abs(y(3)))^h)/2+E0)^((n+1)/n);
D1=((abs(y(3)))^3)*((2*n)+1)*(n+1);
E=4*(n^2)*(E0)^((2*n+1)/n);
E1=((abs(y(3)))^3)*((2*n)+1)*(n+1);
Io=(b*(h^3))/12;
Ink=b*((A/A1)-(B/B1)-(C/C1)+(D/D1)-(E/E1));

```

```

dydx(1)=w*sin(y(4));           % Horizontal force (H)
dydx(2)=w*cos(y(4));           % Normal force (V)
dydx(3)=((( -y(2)*cos(y(4)))- (y(1)*sin(y(4))))*Io)/Ink; % Curvature
dydx(4)=y(3);                   % Ceta
dydx(5)=cos(y(4));               % x
dydx(6)=sin(y(4));               % y
end

score_canfollower
function r=score_canfollower(v)
global ceta0 w pl b h n E0

r=zeros(1,1);

w=v(1);

curv=1.0e-5;

odeoptions=odeset('RelTol',1.0e-5,'AbsTol',1.0e-5);

[x y]=ode45('goveqs_follower_self',[0 1],[0 0 curv ceta0 0
0],odeoptions);

lastrow=size(y,1);

if (pl==1)
    figure(1)
    hold on;

    title ('Equilibrium shape');

    plot(y(:,5),y(:,6));

    axis on;

    axis equal;

    grid on;
end

```



```
r(1)=y(lastrow,4);
```

```
end
```

The second case is n and ε_0 are related to each other.

For $n < 1$

cantilever_self

```
function cantilever_self
% cantilever beam with follower self-weight
clear
global ceta0 pl b h n E0

format long

b=input('Width (b) ');
h=input('Height (h) ');
n=input('Degree of material nonlinearity (n) ');
E0=(n/2)^(n/(1-n)); % Good for n<1

ceta0=input('End rotation ');
v(1)=input('Distributed load (w) ');
pl=input('Plot configuration shapes (yes (1), no (0))= ');
P=v(1);

lim=input('Limitation= ');

inc=input('Increment= ');
fid=fopen('Output_follower_generalized Ludwick.txt','wt');

fprintf(fid,'Output of follower self-weight cantilever beam obeying
generalized Ludwick\n');

fprintf(fid,'ceta0          w \n');

i=0;

dv=0.0001;

while (ceta0<lim)
```

```

v0=[v(1)];

options=optimset(optimset('fsolve'),'MaxFunEvals',400,'TolFun',1e-
15,'TolX',1.0e-15);

[v fval]=fsolve('score_canfollower',v0,options)
test=max(abs(fval));

while (test>1.0e-8&& i<25)
    i=i+1;

    v(1)=v(1)+dv;

    v0=[v(1)];

    [v fval]=fsolve('score_canfollower',v0,options)
end

fprintf(fid,'%12.9f          %12.9f
%12.9f\n',ceta0,v(1),test);

ceta0=ceta0+inc

end

fclose(fid)
end

goveqs_follower_self

function dydx=goveqs_follower_self(x,y)
global w b h n E0
dydx=zeros(6,1);

A=((abs(y(3)))*h)/2*(n+1)*((((abs(y(3)))*h)/2)+E0)^(1/n)*h;
A1=((abs(y(3)))^2)*((2*n)+1);
B=n*E0*((((abs(y(3)))*h)/2)+E0)^(1/n)*h;
B1=((abs(y(3)))^2)*((2*n)+1);
C=n*((((abs(y(3)))*h)/2)+E0)^((n+1)/n)*h;
C1=((abs(y(3)))^2)*((2*n)+1);
D=4*(n^2)*E0*((((abs(y(3)))*h)/2)+E0)^((n+1)/n);

```

```

D1=((abs(y(3)))^3)*((2*n)+1)*(n+1);
E=4*(n^2)*(E0^((2*n+1)/n));
E1=((abs(y(3)))^3)*((2*n)+1)*(n+1);
Io=(b*(h^3))/12;
Ink=b*((A/A1)-(B/B1)-(C/C1)+(D/D1)-(E/E1));

dydx(1)=w*sin(y(4));           % Horizontal force (H)
dydx(2)=w*cos(y(4));           % Normal force (V)
dydx(3)=((-y(2)*cos(y(4)))-(y(1)*sin(y(4))))*Io)/Ink; % Curvature
dydx(4)=y(3);                   % Ceta
dydx(5)=cos(y(4));              % x
dydx(6)=sin(y(4));              % y
end

score_canfollower
function r=score_canfollower(v)
global ceta0 w pl b h n E0

r=zeros(1,1);

w=v(1);

curv=1.0e-5;

odeoptions=odeset('RelTol',1.0e-5,'AbsTol',1.0e-5);

[x y]=ode45('goveqs_follower_self',[0 1],[0 0 curv ceta0 0
0],odeoptions);

lastrow=size(y,1);

if (pl==1)
figure(1)
hold on;

title ('Equilibrium shape');

plot(y(:,5),y(:,6));

```

```

axis on;

axis equal;

grid on;

end

r(1)=y(lastrow,4);

end

For n>1
cantilever_self
function cantilever_self
% cantilever beam with follower self-weight
clear
global ceta0 pl b h n E0

format long

b=input('Width (b) ');
h=input('Height (h) ');
n=input('Degree of material nonlinearity (n) ');
E0=(2n)^(n/(1-n)); % Good for n>1
ceta0=input('End rotation ');
v(1)=input('Distributed load (w) ');
pl=input('Plot configuration shapes (yes (1), no (0))= ');
P=v(1);

lim=input('Limitation= ');

inc=input('Increment= ');
fid=fopen('Output_follower_generalized Ludwick.txt','wt');

fprintf(fid,'Output of follower self-weight cantilever beam obeying
generalized Ludwick\n');

```

```

fprintf(fid,'ceta0          w \n');

i=0;

dv=0.0001;

while (ceta0<lim)
    v0=[v(1)];

    options=optimset(optimset('fsolve'),'MaxFunEvals',400,'TolFun',1e-
15,'TolX',1.0e-15);

    [v fval]=fsolve('score_canfollower',v0,options)
    test=max(abs(fval));

while (test>1.0e-8&&i<25)
    i=i+1;

    v(1)=v(1)+dv;

    v0=[v(1)];

    [v fval]=fsolve('score_canfollower',v0,options)
end

fprintf(fid,'%12.9f          %12.9f
%12.9f\n',ceta0,v(1),test);

ceta0=ceta0+inc

end

fclose(fid)
end

goveqs_follower_self

function dydx=goveqs_follower_self(x,y)
global w b h n E0
dydx=zeros(6,1);

A=((abs(y(3)))^h)/2*(n+1)*((((abs(y(3)))^h)/2)+E0)^(1/n)*h;

A1=((abs(y(3)))^2)*((2*n)+1);

B=n*E0*((((abs(y(3)))^h)/2)+E0)^(1/n)*h;

```

```

B1=((abs(y(3)))^2)*((2*n)+1);
C=n*(((abs(y(3))*h)/2)+E0)^((n+1)/n)*h;
C1=((abs(y(3)))^2)*((2*n)+1);
D=4*(n^2)*E0*(((abs(y(3))*h)/2)+E0)^((n+1)/n);
D1=((abs(y(3)))^3)*((2*n)+1)*(n+1);
E=4*(n^2)*(E0^((2*n+1)/n));
E1=((abs(y(3)))^3)*((2*n)+1)*(n+1);
Io=(b*(h^3))/12;
Ink=b*((A/A1)-(B/B1)-(C/C1)+(D/D1)-(E/E1));

dydx(1)=w*sin(y(4)); % Horizontal force (H)
dydx(2)=w*cos(y(4)); % Normal force (V)
dydx(3)=((-y(2)*cos(y(4)))-(y(1)*sin(y(4))))*Io/Ink; % Curvature
dydx(4)=y(3); % Ceta
dydx(5)=cos(y(4)); % x
dydx(6)=sin(y(4)); % y
end

score_canfollower
function r=score_canfollower(v)
global ceta0 w pl b h n E0

r=zeros(1,1);

w=v(1);

curv=1.0e-5;

odeoptions=odeset('RelTol',1.0e-5,'AbsTol',1.0e-5);

[x y]=ode45('goveqs_follower_self',[0 1],[0 0 curv ceta0 0
0],odeoptions);

lastrow=size(y,1);

```

```
if (pl==1)
    figure(1)
    hold on;

    title ('Equilibrium shape');

    plot(y(:,5),y(:,6));

    axis on;

    axis equal;

    grid on;
end

r(1)=y(lastrow,4);

end
```





APPENDIX E

EQUILIBRIUM EQUATIONS OF BEAM SEGMENT

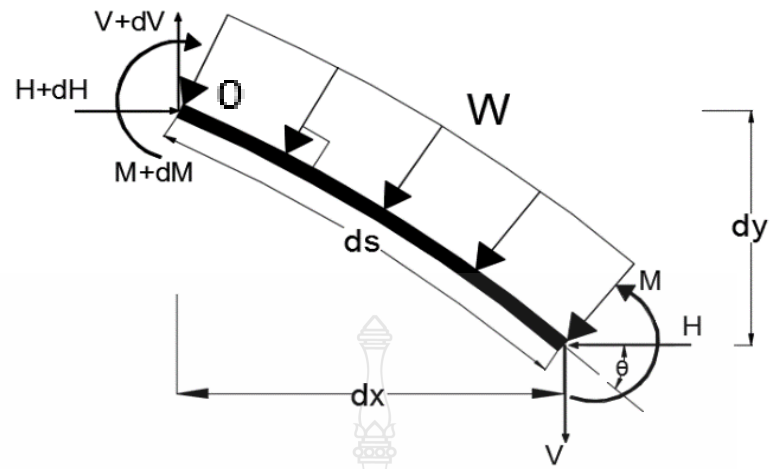


Figure E.1 Free-body diagram of an infinitesimal element of the beam

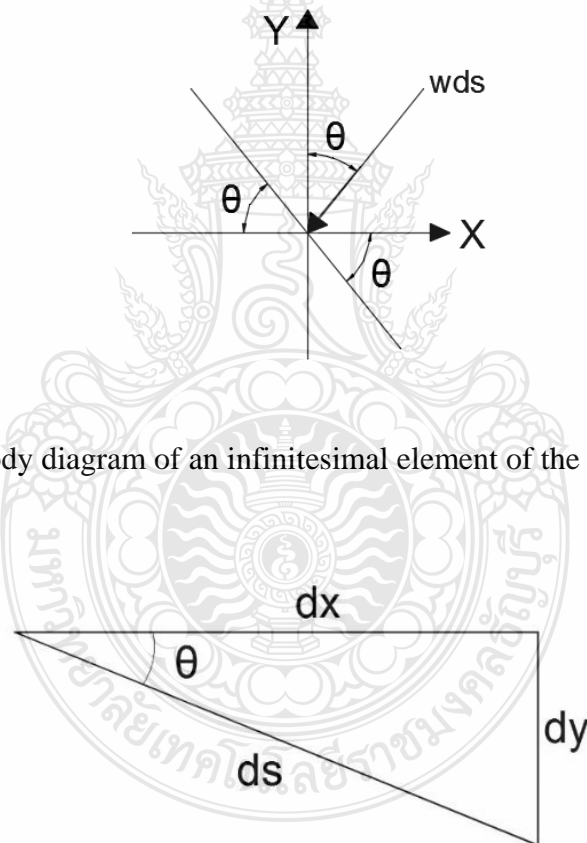


Figure E.2 Geometric relationship of beam element

Summation of forces in Y direction

$$\begin{aligned}\sum F_y &= 0 \quad \uparrow + \\ (V + dV) - V - (wds) \cos \theta &= 0 \\ \frac{dV}{ds} - w \cos \theta &= 0 \\ \frac{dV}{ds} &= w \cos \theta\end{aligned}\tag{E.1}$$

Summation of forces in X direction

$$\begin{aligned}\sum F_x &= 0 \quad \rightarrow + \\ (H + dH) - H - (wds) \sin \theta &= 0 \\ \frac{dH}{ds} - w \sin \theta &= 0 \\ \frac{dH}{ds} &= w \sin \theta\end{aligned}\tag{E.2}$$

Taking moment about point 0

$$\begin{aligned}\sum M_0 &= 0 \quad \curvearrowright + \\ -(M + dM) + M - Vdx - Hdy &= 0 \\ -dM - Vdx - Hdy &= 0 \quad \frac{dy}{ds} = \sin \theta, \quad \frac{dx}{ds} = \cos \theta \\ -\frac{dM}{ds} - V \cos \theta - H \sin \theta &= 0 \\ \frac{dM}{ds} &= -(V \cos \theta + H \sin \theta)\end{aligned}\tag{E.3}$$



APPENDIX F

**THE INNER BENDING MOMENT–CURVATURE RELATIONSHIP
OF GENERALIZED LUDWICK MATERIAL**

As well-known the inner bending moment acting at any cross-section of the beam can be expressed with normal stress σ (Fig 3.6) can be written as

$$M = -\int_A \sigma y dA \quad (\text{F.1})$$

$$\varepsilon = -y\rho^{-1} = -y \frac{1}{\rho} = -\kappa y \quad (\text{F.2})$$

$$\sigma = -E \left[(|\varepsilon| + \varepsilon_0)^{1/n} - \varepsilon_0^{1/n} \right] \quad (\text{F.3})$$

Let $dA = bdy$ be the infinitesimal cross-sectional area of the beam. Furthermore, employing the expression of normal strain-curvature $\varepsilon = -\kappa y$; hence

$$M = \int_A E \left[(|\varepsilon| + \varepsilon_0)^{1/n} - \varepsilon_0^{1/n} \right] y dA \quad (\text{F.4})$$

$$M = 2bE \int_0^{h/2} \left[(|\kappa y| + \varepsilon_0)^{1/n} - \varepsilon_0^{1/n} \right] y dy, \quad dA = bdy \quad (\text{F.5})$$

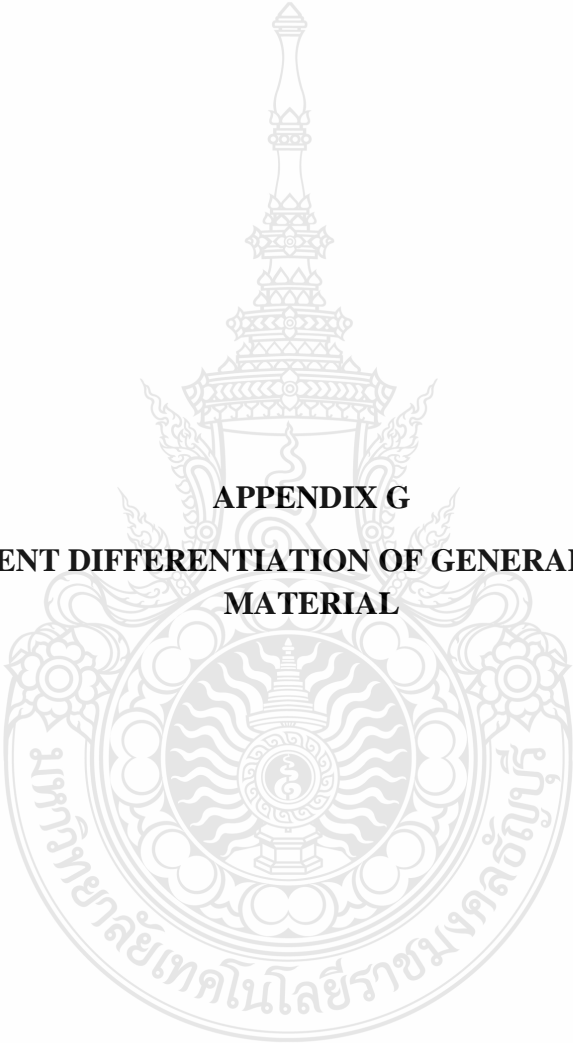
After some works, the inner bending moment for generalized Ludwick's material model can illustrated as below.

$$M = 2bE \left[n\rho^2 \left[\frac{h(n+1) - 2n\varepsilon_0\rho}{2(n+1)(2n+1)\rho} \right] \left(\frac{h}{2\rho} + \varepsilon_0 \right)^{\frac{n+1}{n}} + \frac{n\varepsilon_0^{\frac{2n+1}{n}}}{(n+1)(2n+1)} - \frac{h^2\varepsilon_0^{\frac{1}{n}}}{8n\rho^2} \right] \quad (\text{F.6})$$

where the curvature $\kappa = \frac{1}{\rho}$

Finally, the inner bending moment for generalized Ludwick's material model can be written as,

$$M = Eb \left[\left(\kappa \frac{h}{2} + \varepsilon_0 \right)^{\frac{n+1}{n}} \left[\frac{\kappa hn(n+1) - 2n^2\varepsilon_0}{\kappa^2(2n+1)(n+1)} \right] + \frac{2n^2\varepsilon_0^{\frac{2n+1}{n}}}{\kappa^2(2n+1)(n+1)} - \varepsilon_0^{\frac{1}{n}} \frac{h^2}{4} \right] \quad (\text{F.7})$$



APPENDIX G
MOMENT DIFFERENTIATION OF GENERALIZED LUDWICK
MATERIAL

$$M = Eb \left[\left(\kappa \frac{h}{2} + \varepsilon_0 \right)^{\frac{n+1}{n}} \left[\frac{\kappa hn(n+1) - 2n^2 \varepsilon_0}{\kappa^2 (2n+1)(n+1)} \right] + \frac{2n^2 \varepsilon_0^{\frac{2n+1}{n}}}{\kappa^2 (2n+1)(n+1)} - \varepsilon_0^n \frac{h^2}{4} \right] \quad (G.1)$$

By differentiating the above equation once with respect to the arc length s the result gives:

$$\text{Let } X = \left(\kappa \frac{h}{2} + \varepsilon_0 \right)^{\frac{n+1}{n}} \left[\frac{\kappa hn(n+1) - 2n^2 \varepsilon_0}{\kappa^2 (2n+1)(n+1)} \right], \quad Y = \frac{2n^2 \varepsilon_0^{\frac{2n+1}{n}}}{\kappa^2 (2n+1)(n+1)}, \quad Z = \varepsilon_0^n \frac{h^2}{4}$$

$$\frac{dM}{ds} = \frac{dM}{d\kappa} \frac{d\kappa}{ds}$$

$$\frac{dM}{ds} = Eb \left[\frac{\left(\frac{\kappa h}{2} \right) (n+1) \left(\kappa \frac{h}{2} + \varepsilon_0 \right)^{\frac{1}{n}} h}{\kappa^2 (2n+1)} - \frac{n \varepsilon_0 \left(\kappa \frac{h}{2} + \varepsilon_0 \right)^{\frac{1}{n}} h}{\kappa^2 (2n+1)} - \frac{n \left(\kappa \frac{h}{2} + \varepsilon_0 \right)^{\frac{n+1}{n}} h}{\kappa^2 (2n+1)} \right. \\ \left. + \frac{4n^2 \varepsilon_0 \left(\kappa \frac{h}{2} + \varepsilon_0 \right)^{\frac{n+1}{n}}}{\kappa^3 (2n+1)(n+1)} - \frac{4n^2 \varepsilon_0^{\frac{2n+1}{n}}}{\kappa^3 (2n+1)(n+1)} \right] \frac{d\kappa}{ds} \quad (G.2)$$

Finally, the differentiation of the inner bending moment can be written as below.

$$\frac{dM}{ds} = Eb I_{n\kappa} \frac{d\kappa}{ds} \quad (G.3)$$

where

$$I_{n\kappa} = \left[\frac{\left(\frac{\kappa h}{2} \right) (n+1) \left(\kappa \frac{h}{2} + \varepsilon_0 \right)^{\frac{1}{n}} h}{\kappa^2 (2n+1)} - \frac{n \varepsilon_0 \left(\kappa \frac{h}{2} + \varepsilon_0 \right)^{\frac{1}{n}} h}{\kappa^2 (2n+1)} - \frac{n \left(\kappa \frac{h}{2} + \varepsilon_0 \right)^{\frac{n+1}{n}} h}{\kappa^2 (2n+1)} \right. \\ \left. + \frac{4n^2 \varepsilon_0 \left(\kappa \frac{h}{2} + \varepsilon_0 \right)^{\frac{n+1}{n}}}{\kappa^3 (2n+1)(n+1)} - \frac{4n^2 \varepsilon_0^{\frac{2n+1}{n}}}{\kappa^3 (2n+1)(n+1)} \right] \quad (G.4)$$

APPENDIX H
NUMERICAL RESULTS

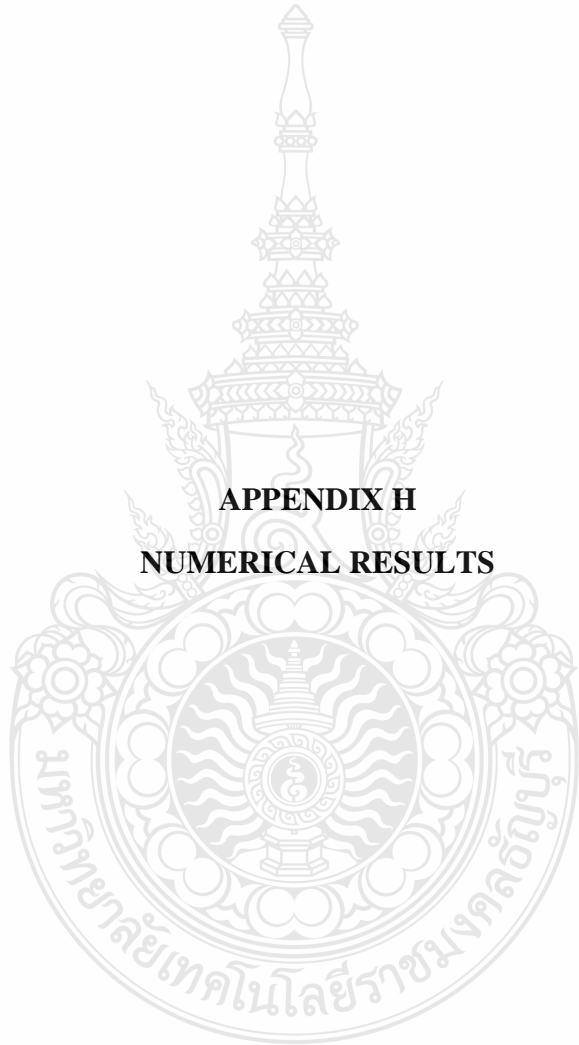


Table H.1 Numerical results for nonlinear elastic material: $\varepsilon_0 = 0.001$ and n varying from 0.50,0.75..2.00 with $\bar{b} = 0.1\text{m}$ and $\bar{h} = 0.1\text{m}$

θ_0 (rad)	\bar{w}					
	$\varepsilon_0 = 0.001$					
	$n = 0.50$	$n = 0.75$	$n = 1.00$	$n = 1.50$	$n = 1.75$	$n = 2.00$
0.0	0.000000	0.000000	0.000000	0.000000	0.000000	0.000000
0.2	0.015000	0.290368	1.201348	4.010447	6.341726	5.790828
0.4	0.054370	0.704797	2.410405	7.542403	9.398551	8.154448
0.6	0.118527	1.197721	3.635229	10.157444	12.348522	10.346395
0.8	0.208369	1.756490	4.884284	12.555389	14.947794	18.833779
1.0	0.325200	2.376914	6.166776	14.833826	18.435452	21.566774
1.2	0.470793	3.059041	7.492988	17.053081	20.975275	24.149175
1.4	0.647440	3.805827	8.874687	19.257990	23.378385	26.657428
1.6	0.858057	4.622715	10.325675	21.487059	25.773683	29.149182
1.8	1.106321	5.517661	11.862520	23.777576	28.235506	31.676120
2.0	1.396849	6.501467	13.505593	26.169533	30.782183	34.290765
2.2	1.735451	7.588447	15.280556	28.709592	33.477402	37.052364
2.4	2.129486	8.797498	17.220624	31.456335	36.388528	40.034934
2.6	2.588367	10.153790	19.370067	34.393770	39.608679	43.334521
2.8	3.124305	11.691354	21.790003	36.973874	43.149206	44.765846
3.0	3.753406	13.457417	24.568444	41.912184	47.564648	51.584895
3.14	4.260574	14.865093	26.648829	44.401270	50.681183	55.351383

Table H.2 Numerical results for nonlinear elastic material: $\varepsilon_0 = 0.002$ and n varying from 0.50,0.75..2.00 with $\bar{b} = 0.1\text{m}$ and $\bar{h} = 0.1\text{m}$

θ_0 (rad)	\bar{w}					
	$\varepsilon_0 = 0.002$					
	$n = 0.50$	$n = 0.75$	$n = 1.00$	$n = 1.50$	$n = 1.75$	$n = 2.00$
0.0	0.000000	0.000000	0.000000	0.000000	0.000000	0.000000
0.2	0.017791	0.309401	1.201348	4.020639	5.669596	7.202317
0.4	0.060207	0.734115	2.410405	7.026639	9.450766	11.437753
0.6	0.127510	1.234914	3.635229	9.624466	12.496705	14.814591
0.8	0.220584	1.800344	4.884284	11.773046	15.216440	17.762188
1.0	0.340752	2.426721	6.166776	14.379966	17.749692	20.479455
1.2	0.489798	3.114370	7.492988	16.583404	20.179189	22.895321
1.4	0.670044	3.866431	8.874687	18.774095	22.596362	25.508308
1.6	0.884437	4.688489	10.325675	20.989692	23.813440	27.281550
1.8	1.136695	5.588611	11.862520	23.266849	27.366717	30.486113
2.0	1.431481	6.577714	13.505593	25.644934	29.902766	33.078881
2.2	1.774669	7.670270	15.280556	28.169941	32.506459	35.814367
2.4	2.173696	8.885290	17.220624	30.899580	35.473010	38.816890
2.6	2.638076	10.248064	19.370067	33.910809	37.666375	42.061798
2.8	3.180153	11.792989	21.790003	37.313179	40.639125	45.755448
3.0	3.816234	13.567821	24.568444	40.707504	46.432039	50.163214
3.14	4.328927	14.982666	26.498360	42.498190	49.672377	53.851176

Table H.3 Numerical results for nonlinear elastic material: $\varepsilon_0 = 0.003$ and n varying from 0.50,0.75..2.00 with $\bar{b} = 0.1\text{m}$ and $\bar{h} = 0.1\text{m}$

θ_0 (rad)	\bar{w}					
	$\varepsilon_0 = 0.003$					
	$n = 0.50$	$n = 0.75$	$n = 1.00$	$n = 1.50$	$n = 1.75$	$n = 2.00$
0.0	0.000000	0.000000	0.000000	0.000000	0.000000	0.000000
0.2	0.020488	0.325339	1.201348	4.022923	3.611590	3.959431
0.4	0.065868	0.759449	2.410405	6.882631	8.974675	10.757654
0.6	0.136255	1.267601	3.635229	9.316591	11.965383	14.078255
0.8	0.232514	1.839312	4.884284	11.785340	14.664244	16.989371
1.0	0.355972	2.471325	6.166776	14.032773	17.174258	19.752742
1.2	0.508432	3.164217	7.492988	15.998408	19.584316	22.199087
1.4	0.692239	3.921296	8.804081	18.129202	21.591380	24.768603
1.6	0.910373	4.748273	10.325672	18.847533	24.213592	27.087118
1.8	1.166588	5.653337	11.388147	22.867709	26.708178	29.454896
2.0	1.465596	6.647517	13.504880	25.233443	29.252293	32.180448
2.2	1.813331	7.745371	14.913749	27.745234	31.769349	34.613222
2.4	2.217306	8.966077	17.220860	30.460081	34.428948	37.673361
2.6	2.687138	10.335144	19.132572	33.453904	37.814943	40.242660
2.8	3.235307	11.887141	21.406614	36.421550	41.300311	43.874641
3.0	3.878308	13.670188	24.348142	39.660934	44.788456	49.081673
3.14	4.396479	15.091769	26.795345	43.594273	46.092712	52.726481

Table H.4 Numerical results for nonlinear elastic material: $\varepsilon_0 = 0.004$ and n varying from 0.50, 0.75..2.00 with $\bar{b} = 0.1\text{m}$ and $\bar{h} = 0.1\text{m}$

θ_0 (rad)	\bar{w}					
	$\varepsilon_0 = 0.004$					
	$n = 0.50$	$n = 0.75$	$n = 1.00$	$n = 1.50$	$n = 1.75$	$n = 2.00$
0.0	0.000000	0.000000	0.000000	0.000000	0.000000	0.000000
0.2	0.023125	0.339355	1.201348	3.324448	0.062500	5.949265
0.4	0.068399	0.782206	2.410405	6.235538	0.062509	9.065929
0.6	0.144825	1.297311	3.635229	7.604717	0.062495	12.401670
0.8	0.244224	1.875019	4.884284	11.517886	3.062505	14.544262
1.0	0.370934	2.512451	6.166776	13.634229	16.572473	19.049177
1.2	0.526774	3.210407	7.492988	15.916156	17.649450	21.327546
1.4	0.714109	3.972343	8.804099	17.310845	20.603599	23.515944
1.6	0.935951	4.804089	10.325621	19.165196	20.603721	26.293839
1.8	1.196090	5.713935	11.234824	22.516161	21.603729	28.581260
2.0	1.499287	6.713012	13.238082	23.391670	24.096985	31.415408
2.2	1.851533	7.815989	15.130891	24.828234	28.928718	34.140064
2.4	2.260420	9.042174	16.861645	30.160362	31.730973	36.644558
2.6	2.735664	10.417245	19.275391	32.075747	33.518426	40.264548
2.8	3.289878	11.976005	21.747189	32.744342	40.773986	43.821888
3.0	3.939748	13.766917	24.120582	34.573231	43.242870	48.338019
3.14	4.463356	15.194941	26.153585	37.136708	45.602538	51.775780

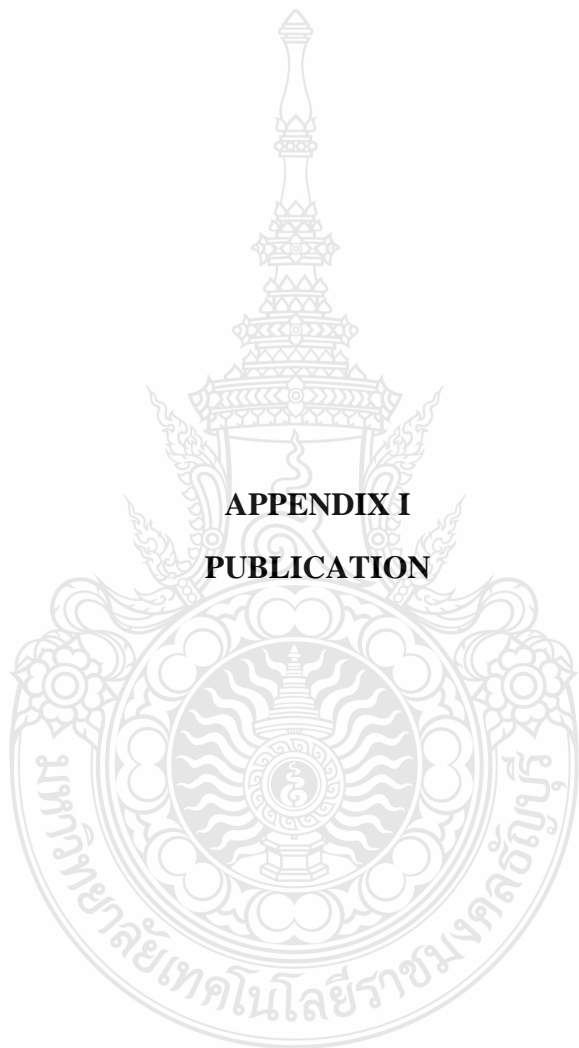
Table H.5 Numerical results for nonlinear elastic material: $\varepsilon_0 = 0.005$ and n varying from 0.50, 0.75..2.00 with $\bar{b} = 0.1\text{m}$ and $\bar{h} = 0.1\text{m}$

θ_0 (rad)	\bar{w}					
	$\varepsilon_0 = 0.005$					
	$n = 0.50$	$n = 0.75$	$n = 1.00$	$n = 1.50$	$n = 1.75$	$n = 2.00$
0.0	0.000000	0.000000	0.000000	0.000000	0.000000	0.000000
0.2	0.025722	0.352008	1.201348	3.658263	4.216660	4.240152
0.4	0.076852	0.803078	2.410405	5.962256	7.323723	9.786189
0.6	0.153259	1.324809	3.635229	8.972874	10.574056	10.904268
0.8	0.255761	1.908274	4.884284	11.170287	13.809668	15.366486
1.0	0.385688	2.550932	6.166776	13.165342	16.319354	18.278525
1.2	0.544874	3.253784	7.492988	15.655592	18.652920	20.352915
1.4	0.735707	4.020427	8.874687	17.576835	20.891037	23.357759
1.6	0.961227	4.856803	10.325675	19.997745	23.174255	25.156561
1.8	1.225261	5.771293	11.862520	22.233420	25.739202	26.847226
2.0	1.532617	6.775127	13.505593	24.574980	27.996658	30.093181
2.2	1.889344	7.883076	15.280556	26.594842	30.813140	33.129506
2.4	2.303109	9.114574	17.220624	29.734910	33.222446	35.976553
2.6	2.783728	10.495462	19.370067	32.663465	36.587291	39.071912
2.8	3.343949	12.060765	21.790003	35.824064	39.358905	43.182714
3.0	4.000641	13.859271	24.290324	39.208893	42.493061	47.439855
3.14	4.529649	15.293505	26.459706	41.820581	43.633979	49.839885

Table H.6 Numerical results for nonlinear elastic material: $\varepsilon_0 = 0.001$ and n varying from 0.50, 0.75..2.00 with $\bar{b} = 0.02\text{m}$ and $\bar{h} = 0.02\text{m}$

θ_0 (rad)	\bar{w}					
	$\varepsilon_0 = 0.001$					
	$n = 0.50$	$n = 0.75$	$n = 1.00$	$n = 1.50$	$n = 1.75$	$n = 2.00$
0.0	0.000000	0.000000	0.000000	0.000000	0.000000	0.000000
0.2	0.005144	0.205856	1.201348	6.251503	0.062520	0.827898
0.4	0.015370	0.469643	2.410405	10.672172	0.062526	12.328170
0.6	0.030652	0.774753	3.635229	15.163382	5.562525	14.328154
0.8	0.051152	1.115965	4.884284	19.019776	6.562518	18.328155
1.0	0.077138	1.491794	6.166776	22.903679	18.986234	21.330686
1.2	0.108975	1.902825	7.492988	26.319076	25.221127	46.895326
1.4	0.147141	2.351162	8.874687	27.328745	28.731695	52.054761
1.6	0.192245	2.840279	10.325675	29.976863	29.115918	57.404022
1.8	0.245052	3.375081	11.862520	31.324495	33.596467	61.498239
2.0	0.306523	3.962137	13.505593	37.343051	38.179301	68.311802
2.2	0.377869	4.610085	15.280556	44.829100	43.179302	72.451607
2.4	0.460622	5.330284	17.220624	50.364028	54.837547	81.344976
2.6	0.556746	6.137793	19.370067	54.879842	73.489961	85.581895
2.8	0.668790	7.053178	21.533413	60.456690	78.647711	89.049600
3.0	0.800128	8.104950	24.426660	62.901893	81.148896	98.532986
3.14	0.905930	8.943696	25.949330	63.930677	92.635957	103.878540

APPENDIX I
PUBLICATION






การประชุมวิชาการ
 วิศวกรรมโยธาแห่งชาติ ครั้งที่ 20
 The 20th National Convention on Civil Engineering



วิศวกรรมโยธากับการก้าวเข้าสู่ประชาคมเศรษฐกิจอาเซียน
 Civil Engineering Moving Towards
 ASEAN Economic Community

วันที่ 8-10 กรกฎาคม 2558 ณ โรงแรมเดอะชาน พัลลาเดียม อ.เขมย์

บริษัท อินทรา วิศวกรรม จำกัด
 อาคารเฉลิมฉลองครบรอบ 100 ปี มหาวิทยาลัยเทคโนโลยีราชมงคลธัญบุรี
 1518 หมู่บ้านพญาไท 1 แขวงบางเขน เขตบางเขน กรุงเทพฯ 10600
 โทร. 0-2555-2000 หรือ 1427
 www.intra.or.th



ผู้ทรงคุณวุฒิพิจารณาบทความการประชุมวิชาการวิศวกรรมโยธาแห่งชาติ ครั้งที่ 20

รายชื่อผู้ทรงคุณวุฒิ

รศ.ดร.บุญไชย สถิตมั่นในธรรม	จุฬาลงกรณ์มหาวิทยาลัย
ผศ.ดร.วิฑิต ปานสุข	จุฬาลงกรณ์มหาวิทยาลัย
ดร.อรอนงค์ ลาภปริสุทธิ	จุฬาลงกรณ์มหาวิทยาลัย
ผศ.ดร.ศรีเลิศ โชติพันธรัตน์	จุฬาลงกรณ์มหาวิทยาลัย
ดร.เบญจพร สุวรรณศิลป์	จุฬาลงกรณ์มหาวิทยาลัย
ศ.ดร.ธีรพงศ์ เสนจันทร์ศิไชย	จุฬาลงกรณ์มหาวิทยาลัย
รศ.ดร.อัศววัชร เล่นวารีย์	จุฬาลงกรณ์มหาวิทยาลัย
รศ.ดร.ธัญวัฒน์ โพธิศิริ	จุฬาลงกรณ์มหาวิทยาลัย
ศ.ดร.ทักษิณ เทพชาตรี	จุฬาลงกรณ์มหาวิทยาลัย
ดร.พิชชา จองวิวัฒน์สกุล	จุฬาลงกรณ์มหาวิทยาลัย
รศ.ดร.วิสุทธิ ช่อวิเชียร	จุฬาลงกรณ์มหาวิทยาลัย
รศ.ดร.วีระศักดิ์ ลิขิตเรืองศิลป์	จุฬาลงกรณ์มหาวิทยาลัย
ศ.ดร.สุเชษฐ ลิขิตเลอสรวง	จุฬาลงกรณ์มหาวิทยาลัย
ผศ.ดร.ธเนศ ศรีศิริโรจนากร	จุฬาลงกรณ์มหาวิทยาลัย
รศ.ดร.จิตติชัย รุจนกนกนาถ	จุฬาลงกรณ์มหาวิทยาลัย
รศ.ดร.เกษม ชูจารุกุล	จุฬาลงกรณ์มหาวิทยาลัย
รศ.ดร.ศักดิ์สิทธิ์ เถลิงพงษ์	จุฬาลงกรณ์มหาวิทยาลัย
ผศ.ดร.นพดล จอกแก้ว	จุฬาลงกรณ์มหาวิทยาลัย
ผศ.ดร.วัชระ เพียรสุภาพ	จุฬาลงกรณ์มหาวิทยาลัย
รศ.ดร.จรูญ รุ่งอมรรัตน์	จุฬาลงกรณ์มหาวิทยาลัย
ผศ.ดร.รัฐวุฒิ ฐู่แทนคุณ	บริษัท ทีม คอนซัลติ้ง เอนจิเนียริ่ง แอนด์ แมเนจเม้นท์ จำกัด
ดร.ธนะ บุญยศิริกุล	บริษัท ผลิตไฟฟ้าราชบุรีโฮลดิ้ง จำกัด (มหาชน)
ผศ.ดร.นันทวัฒน์ ขมหวาน	มหาวิทยาลัยเกษตรศาสตร์ วิทยาเขตกำแพงแสน
ดร.วิญวัฒน์ เต็มสมบัติ	มหาวิทยาลัยเกษตรศาสตร์ วิทยาเขตกำแพงแสน
ดร.จิระกานต์ ศิริวิษณุไมตรี	มหาวิทยาลัยเกษตรศาสตร์ วิทยาเขตกำแพงแสน
ดร.สมชาย คอนเจดีย์	มหาวิทยาลัยเกษตรศาสตร์ วิทยาเขตกำแพงแสน
ดร.ปนัดดา กสิกิจวิวัฒน์	มหาวิทยาลัยเกษตรศาสตร์ วิทยาเขตกำแพงแสน
ผศ.ดร.วัจนวงศ์ กิรพละ	มหาวิทยาลัยเกษตรศาสตร์ วิทยาเขตเฉลิมพระเกียรติ สกลนคร
ผศ.ต่อศักดิ์ ประเสริฐสังข์	มหาวิทยาลัยเกษตรศาสตร์ วิทยาเขตเฉลิมพระเกียรติ สกลนคร
อ.ฐิตาภรณ์ ฟูอนุตรดี	มหาวิทยาลัยเกษตรศาสตร์ วิทยาเขตเฉลิมพระเกียรติ สกลนคร

ผศ.ดร.วันชัย ยอดสุใจ	มหาวิทยาลัยเกษตรศาสตร์ วิทยาเขตบางเขน
ดร.ธิดารัตน์ จิระวัฒนามงคล	มหาวิทยาลัยเกษตรศาสตร์ วิทยาเขตบางเขน
รศ.ดร.คิบุญ เมฆากลุชาติ	มหาวิทยาลัยเกษตรศาสตร์ วิทยาเขตบางเขน
ผศ.ดร.ปิยนุช เวทย์วิวัฒน์	มหาวิทยาลัยเกษตรศาสตร์ วิทยาเขตบางเขน
ผศ.ดร.สุนิรัตน์ กุศลาศัย	มหาวิทยาลัยเกษตรศาสตร์ วิทยาเขตบางเขน
รศ.ดร.ก่อโชค จันทร์วางกูร	มหาวิทยาลัยเกษตรศาสตร์ วิทยาเขตบางเขน
ผศ.ดร.อภินิติ โชติสังกา	มหาวิทยาลัยเกษตรศาสตร์ วิทยาเขตบางเขน
ผศ.ดร.ทวิศักดิ์ ปิติคุณพงศ์สุข	มหาวิทยาลัยเกษตรศาสตร์ วิทยาเขตบางเขน
ดร.สุสิทธิ์ ฉายประกายแก้ว	มหาวิทยาลัยเกษตรศาสตร์ วิทยาเขตบางเขน
ดร.สุรียน เปรมปราวโมทย์	มหาวิทยาลัยเกษตรศาสตร์ วิทยาเขตบางเขน
ผศ.ดร.อติชัย พรพรมินทร์	มหาวิทยาลัยเกษตรศาสตร์ วิทยาเขตบางเขน
ดร.พรธณพิมพ์ พุทธรักษา มะเปี่ยม	มหาวิทยาลัยเกษตรศาสตร์ วิทยาเขตบางเขน
รศ.ดร.สุธาริน สดาศิตานนท์	มหาวิทยาลัยเกษตรศาสตร์ วิทยาเขตบางเขน
ผศ.ดร.วีระเกษม สวนผกา	มหาวิทยาลัยเกษตรศาสตร์ วิทยาเขตบางเขน
ผศ.ดร.เหมือนมาศ วิเชียรสินธุ์	มหาวิทยาลัยเกษตรศาสตร์ วิทยาเขตบางเขน
รศ.ดร.ชวเลข วนิชเวทิน	มหาวิทยาลัยเกษตรศาสตร์ วิทยาเขตบางเขน
รศ.ดร.วัชรินทร์ วิทยกุล	มหาวิทยาลัยเกษตรศาสตร์ วิทยาเขตบางเขน
ศ.ดร.ปริญญา จินดาประเสริฐ	มหาวิทยาลัยขอนแก่น
รศ.ดร.วันชัย สะตะ	มหาวิทยาลัยขอนแก่น
รศ.ดร.วินัย ศรีอำพร	มหาวิทยาลัยขอนแก่น
ผศ.ดร.กิตติเวช ขันดีวิชัย	มหาวิทยาลัยขอนแก่น
ดร.ธนากร เมฆาธรรม	มหาวิทยาลัยขอนแก่น
รศ.ดร.พงศกร พรธรรตน์ศิลป์	มหาวิทยาลัยขอนแก่น
ผศ.ดร.ธเนศ เสถียรนาม	มหาวิทยาลัยขอนแก่น
ผศ.ดร.พนกฤษณ คลังบุญครอง	มหาวิทยาลัยขอนแก่น
ผศ.ดร.วิชุดา เสถียรนาม	มหาวิทยาลัยขอนแก่น
ผศ.ดร.ลัดดา ตันวาณิชกุล	มหาวิทยาลัยขอนแก่น
รศ.ดร.วัชรินทร์ ภาสลัก	มหาวิทยาลัยขอนแก่น
ผศ.ดร.ชลฤดี หอมดี	มหาวิทยาลัยขอนแก่น
ผศ.ดร.พุทธิพล คำรงค์ชัย	มหาวิทยาลัยเชียงใหม่
รศ.ดร.ธนพร สุปรียศิลป์	มหาวิทยาลัยเชียงใหม่
ผศ.ดร.ธวัชชัย ตันชัยสวัสดิ์	มหาวิทยาลัยเชียงใหม่
ดร.เกรียงไกร อนุโณทยานันท์	มหาวิทยาลัยเชียงใหม่

ดร.ปรีดา พิทยาพันธ์	มหาวิทยาลัยเชียงใหม่
ดร.อรรรตวิทย์ อุปโยภิน	มหาวิทยาลัยเชียงใหม่
ผศ.ดร.ปุ่น เทียงบูรณะธรรม	มหาวิทยาลัยเชียงใหม่
รศ.ชูโชค आयหงส์	มหาวิทยาลัยเชียงใหม่
ผศ.ดร.อุมา สีนุญเรือง	มหาวิทยาลัยเทคโนโลยีพระจอมเกล้าเจ้าคุณทหารลาดกระบัง
ผศ.ธีระ ลากิศขยางกุล	มหาวิทยาลัยเทคโนโลยีพระจอมเกล้าธนบุรี
ศ.ดร.ชัย จาตุรพิทักษ์กุล	มหาวิทยาลัยเทคโนโลยีพระจอมเกล้าธนบุรี
ผศ.ดร.วีรชาติ ตั้งจิรภัทร	มหาวิทยาลัยเทคโนโลยีพระจอมเกล้าธนบุรี
รศ.ดร.ทวิช พูลเงิน	มหาวิทยาลัยเทคโนโลยีพระจอมเกล้าธนบุรี
ผศ.ดร.ชูชัย สุจิรวงศ์	มหาวิทยาลัยเทคโนโลยีพระจอมเกล้าธนบุรี
รศ.ดร.วรรษ ก่องกิจกุล	มหาวิทยาลัยเทคโนโลยีพระจอมเกล้าธนบุรี
รศ.ดร.พรเกษม จงประดิษฐ์	มหาวิทยาลัยเทคโนโลยีพระจอมเกล้าธนบุรี
ดร.นงลักษณ์ บุญรัตนกิจ	มหาวิทยาลัยเทคโนโลยีพระจอมเกล้าธนบุรี
ดร.ทรงเกียรติ ภัทรปัทมาวงศ์	มหาวิทยาลัยเทคโนโลยีพระจอมเกล้าธนบุรี
ผศ.ดร.ธิดารัตน์ บุญศรี	มหาวิทยาลัยเทคโนโลยีพระจอมเกล้าธนบุรี
ศ.ดร.ชัยยุทธ ชินณะราศรี	มหาวิทยาลัยเทคโนโลยีพระจอมเกล้าธนบุรี
ผศ.ดร.พิชญ์ สุธีรวรรณา	มหาวิทยาลัยเทคโนโลยีพระจอมเกล้าธนบุรี
ผศ.ดร.สันติ เจริญพรพัฒนา	มหาวิทยาลัยเทคโนโลยีพระจอมเกล้าธนบุรี
รศ.ดร.วิโรจน์ ศรีสุรภานนท์	มหาวิทยาลัยเทคโนโลยีพระจอมเกล้าธนบุรี
ผศ.ดร.มาโนช สรรพกิจทิพากร	มหาวิทยาลัยเทคโนโลยีพระจอมเกล้าพระนครเหนือ
ดร.ณัฐพงศ์ มกรธัช	มหาวิทยาลัยเทคโนโลยีพระจอมเกล้าพระนครเหนือ
ผศ.ดร.กิตติภูมิ รอดสิน	มหาวิทยาลัยเทคโนโลยีพระจอมเกล้าพระนครเหนือ
รศ.ดร.สมิตร ส่งพิริยะกิจ	มหาวิทยาลัยเทคโนโลยีพระจอมเกล้าพระนครเหนือ
รศ.ดร.ขวัญเนตร สมบัติสมภพ	มหาวิทยาลัยเทคโนโลยีพระจอมเกล้าพระนครเหนือ
ผศ.ดร.พิทยา แจ่มสว่าง	มหาวิทยาลัยเทคโนโลยีพระจอมเกล้าพระนครเหนือ
อ.สุรัตน์ ศรีจันทร์	มหาวิทยาลัยเทคโนโลยีพระจอมเกล้าพระนครเหนือ
ดร.ณพล อยู่บรรพต	มหาวิทยาลัยเทคโนโลยีพระจอมเกล้าพระนครเหนือ
รศ.ดร.กীরติกานต์ พิริยะกุล	มหาวิทยาลัยเทคโนโลยีพระจอมเกล้าพระนครเหนือ
ผศ.ดร.ชัยศาสตร์ สกฤกษ์ศักดิ์ศรี	มหาวิทยาลัยเทคโนโลยีพระจอมเกล้าพระนครเหนือ
ผศ.ดร.กวิน ดันดีเสวี	มหาวิทยาลัยเทคโนโลยีพระจอมเกล้าพระนครเหนือ
รศ.ดร.วรรณวิทย์ เต็มทอง	มหาวิทยาลัยเทคโนโลยีพระจอมเกล้าพระนครเหนือ
ผศ.ดร.ศักดิ์ดา กคมาวารักษ์	มหาวิทยาลัยเทคโนโลยีพระจอมเกล้าพระนครเหนือ
ผศ.ดร.ชัยรัตน์ ธีระวัฒนสุข	มหาวิทยาลัยเทคโนโลยีพระจอมเกล้าพระนครเหนือ

รศ.ดร.วีรยา ฉิมอ้อย	มหาวิทยาลัยธรรมศาสตร์
อ.ภัคพงศ์ หอมเนียม	มหาวิทยาลัยนเรศวร
ดร.รัฐภูมิ ปรีชาตปรีชา	มหาวิทยาลัยนเรศวร
ดร.กำพล ทรัพย์สมบูรณ์	มหาวิทยาลัยนเรศวร
ดร.ศิริชัย ตันรัตนวงศ์	มหาวิทยาลัยนเรศวร
ผศ.ดร.ทวีชัย สำราญวานิช	มหาวิทยาลัยบูรพา
ผศ.ดร.ธรรมบุญ รัชมีมาสเมือง	มหาวิทยาลัยบูรพา
ดร.เพชรรัตน์ ลีมีสุปรียรัตน์	มหาวิทยาลัยบูรพา
ดร.วรรณวรางค์ รัตนาณิกม	มหาวิทยาลัยบูรพา
ผศ.ดร.สยาม ยิ้มศิริ	มหาวิทยาลัยบูรพา
ดร.สิทธิภัทร์ เอื้ออภิวัชร	มหาวิทยาลัยบูรพา
ดร.ปิติ โรจน์วรรณสินธุ์	มหาวิทยาลัยบูรพา
ร.อ.ผศ.ดร.สราวุธ ลักยณะ โด	มหาวิทยาลัยบูรพา
ดร.ฐิติมา วงศ์อินดา	มหาวิทยาลัยบูรพา
ดร.พัทธพงษ์ อาสนจินดา	มหาวิทยาลัยบูรพา
ผศ.ดร.ณัฐพงศ์ ดำรงวิริยะนุกาพ	มหาวิทยาลัยพะเยา
ผศ.ดร.สมบูรณ์ เชื้อยงฉิน	มหาวิทยาลัยพะเยา
ผศ.ดร.กริสัน ชัยมูล	มหาวิทยาลัยมหาสารคาม
ผศ.ดร.สมชาย ปฐุมศิริ	มหาวิทยาลัยมหิดล
ดร.วศพร เดชะพีรพานิช	มหาวิทยาลัยมหิดล
ดร.ณัฐวัฒน์ จุฑารัตน์	มหาวิทยาลัยศรีปทุม
ผศ.ดร.ภาสกร ชัยวิริยะวงศ์	มหาวิทยาลัยสงขลานครินทร์
ดร.วิชัยรัตน์ แก้วเจือ	มหาวิทยาลัยสงขลานครินทร์
รศ.ดร.สุชาติ ลีมงคลัญญ	มหาวิทยาลัยสงขลานครินทร์
ดร.ปรเมศวร์ เหลือเทพ	มหาวิทยาลัยสงขลานครินทร์
ดร.ฐกมลพัศ เจนจิวัฒน์กุล	มหาวิทยาลัยสยาม
ผศ.ดร.เกรียงศักดิ์ แก้วกุลชัย	มหาวิทยาลัยอุบลราชธานี
รศ.ดร.สถาพร โภคา	มหาวิทยาลัยอุบลราชธานี
ผศ.ดร.สิทธิา เจนศิริศักดิ์	มหาวิทยาลัยอุบลราชธานี
น.อ.รศ.ดร.ธนากร พิระพันธ์	รร นายเรืออากาศ
ผศ.ดร.ธนาถ คงสมบูรณ์	สถาบันเทคโนโลยีพระจอมเกล้าเจ้าคุณทหารลาดกระบัง
รศ.แหลมทอง เหล่าถาดวงาร	สถาบันเทคโนโลยีพระจอมเกล้าเจ้าคุณทหารลาดกระบัง
รศ.ดร.จักรพงษ์ พงษ์เพ็ง	สถาบันเทคโนโลยีพระจอมเกล้าเจ้าคุณทหารลาดกระบัง

รศ.ดร. โชติชัย เจริญงาม

สถาบันเทคโนโลยีแห่งเอเชีย

ดร.สุเมธ องกิตติกุล

สถาบันวิจัยเพื่อการพัฒนาประเทศไทย

หมายเหตุ: เรียงลำดับตามชื่อสถาบันการศึกษา หน่วยงานราชการ และหน่วยงานเอกชน (ก-ฮ)



17-STR	ANALYSIS OF SPECIAL STRUCTURE OF LARGE CYLINDRICAL WATER TANKS WHICH HAS OPENING WITH FINITE ELEMENT METHOD สรุจฒฒ สีสั่งซ้, สรวฒฒน ถึรเศรษฐ์ และ นัฎพล วัฒนมนันคง
27-STR	LARGE DEFLECTIONS OF CANTILEVER BEAM SUBJECTED TO FOLLOWER DISTRIBUTED LOAD MADE FROM NONLINEARLY MATERIALS OBEYING GENERALIZED LUDWICK'S CONSTITUTIVE LAW S. Touch, B. Phungpaingam and C. Athisakul
36-STR	EVALUATION DAMAGE K-TUBULAR JOINT ON SHIP IMPACT P. Plodpradit , C. Sinsabvarodom , K. D. Kim and B. J. Kim
51-STR	A STUDY BEHAVIOR OF OUTRIGGER AND BELT WALL IN HIGH-RISE BUILDING BASE ON FLEXIBLE FOUNDATION สุวิศล ถือทอง, อำนวน พานิชกุลพงศ์ และ อาทิตย์ เพชรคศิธร
69-STR	TECHNIQUE OF MODELING AND ANALYSIS WELD TENSILE STRENGTH OF ANGLE CONNECTION BY FINITE ELEMENT METHOD โองการ ซัยวณคคูปต์ และ อภินติ อัชกุล
70-STR	INVESTIGATION OF WELD STRENGTH OF ANGLE CONNECTION UNDER TENSILE LOAD BY FINITE ELEMENT METHOD โองการ ซัยวณคคูปต์ และ อภินติ อัชกุล
77-STR	LARGE DEFLECTIONS OF CANTILEVER BEAM MADE OF GENERALIZED LUDWICK MATERIAL SUBJECTED TO TENSION FROM A GUYED CABLE พิรสิทธิ มหาสุวรรณชัย, ซัยนรงค์ อธิสกุล, บุญชัย มั่งไฝงาม และ สมชาย ชูชีพสกุล
35-STR	STRUCTURAL STRENGTH EVALUATION BY NDE AND LOAD TEST OF RC SLAB STRUCTURE CASE STUDY: RC DECK SLAB OF PRIMARY HOSPITAL BUILDING, FACULTY OF MEDICINE, THAMMASAT UNIVERSITY, THAILAND ทรงพล พันธม็เกียรติ และ สหรัฎฐ์ พุทธวรณน
58-STR	EXPERIMENTAL STUDY ON STRESS DISTRIBUTION OF TRUSS MEMBERS SUBJECTED TO OUT-OF-PLANE LOADING ธีรวัฒน์ วงศ์เวิน และ รังสรรค์ วงศ์จิรภัทร
71-STR	EXPERIMENTAL STUDY ON PULTRUDED FIBER REINFORCED PLASTIC BUILT-UP BEAMS WITH DOUBLE CHANNEL SECTIONS UNDER FLEXURE ปรัชญา ก้านบัว, สิทธิชัย แสงอาทิตย์ และ จักษดา อ่ำรงวุฒิ
104-STR	EFFECTS OF CASTING DIRECTIONS ON PUNCHING SHEAR STRENGTH OF ULTRA HIGH PERFORMANCE STEEL FIBER REINFORCED CONCRETE T. N. Thanh and W. Pansuk
127-STR	COMPRESSIVE STRENGTH TESTING OF MASONRY PANELS สมบูรณั ซัยยงฉิน, ประโนย ปวงน้อย, สั้งสรรค์ วงศ์ไชยรัตน และ กิติพงษ์ ทาค้า
166-STR	EFFECT OF CONNECTION TYPES ON SHEAR BEHAVIOR OF REINFORCED CONCRETE BEAMS STRENGTHENED WITH STEEL FIBER REINFORCED CONCRETE PANELS อดิชน คุณาวิศรุต, สิลาภมล พูลทรัพย์ และ พิษชา จอจวิวัฒนสกุล
199-STR	A STUDY ON SEISMIC CAPACITY OF BRICK INFILL WALL IN REINFORCED CONCRETE FRAME อนุชาติ ลือนันตคคัคคิศิริ, ไทบุญย์ ปญญาคะโป, อาณัติ เรืองรัคมี, ณัฐวัฒน์ จุฑารัตน, อภิชาติ วงศ์ติ, V. Terentjvs และ P. S. Theint
224-STR	BONDING STRENGTH AND CREEP BEHAVIOR OF DEFORMED REBAR IN CONCRETE USING CEMENT MORTAR WITH NANOSILICA AS BONDING AGENT จุฑาภรณ์ อัครอริยวงศา และ ทวิษ พูลเงิน
233-STR	STRENGTHENING OF REINFORCED CONCRETE BEAM BY PRESTRESSED NEAR SURFACE MOUNTED WIRE ณัฐพงษ์ อารีมิตร
256-STR	EXPERIMENTAL INVESTIGATION ON BUCKLING RESISTANCE OF FIXED END SUPPORTED PFRP CHANNEL BEAMS UNDER ECCENTRIC LOADING J. Thumrongvut and S. Seangatith
263-STR	SULFATE AND ACID RESISTANCES OF CEMENT MORTARS CONTAINING NANOSILICA สุนิสา ปันติ, ทวิษ พูลเงิน และ วีรชาติ ตั้งจิรภัทร
271-STR	INFLUENCE OF FIBER ORIENTATION ON TENSILE BEHAVIOR OF HIGH PERFORMANCE FIBER REINFORCED MORTAR วิวิท ปานสุข, กฤตชัย เมฆอัมพรพงศ์ และ กาญจนนา สุริยะวงศ์
293-STR	STRENGTHENING OF REINFORCED CONCRETE COLUMNS USING T-SHAPED STEEL HOOPS ครประสิทธิ์ ล้าภา, พชร เกรอิวิทย์ และ อาณัติ เรืองรัคมี
303-STR	STRUCTURAL BEHAVIORS OF HIGH-STRENGTH CONCRETE-FILLED CIRCULAR STEEL TUBE COLUMNS UNDER AXIAL COMPRESSION กมลรัตน์ ถุทธิรักษา และ จักษดา อ่ำรงวุฒิ



Large Deflections of Cantilever Beam Obeying Generalized Ludwick's Material Model Subjected to Follower Distributed Load

Sokheng Touch^{1*}, Boonchai Phungpaingam^{2**} and Chainarong Athisakul³

¹ Graduate student, Department of Civil Engineering, Faculty of Engineering, Rajamangala University of Technology
Thanyaburi, Thailand

² Lecturer, Department of Civil Engineering, Faculty of Engineering, Rajamangala University of Technology Thanyaburi,
Thailand

³ Assistant Professor, Department of Civil Engineering, Faculty of Engineering, King Mongkut's University of Technology
Thonburi, Thailand

Abstract

This paper presents the large deflection behavior of the cantilever beam subjected to follower distributed load where material of the cantilever beam obeys the generalized Ludwick's constitutive law. The cross-section of the prismatic beam is of rectangular. The cantilever beam is subjected to follower distributed load. Moreover, the beam is well deflected so that the large deflection theory of the beam should be taken into account. The stress-strain relationship of such materials is presented by generalized Ludwick's constitutive law. To derive the set of governing differential equations, equilibrium equations, moment-curvature relation obeying the generalized Ludwick's material model and nonlinear geometric relations have been considered. Up to this point, a set of strongly nonlinear simultaneous first-order differential equations with boundary conditions is established and numerically solved by using the shooting method accompanying with the seventh order Runge-Kutta integration technique. Furthermore, some numerical results are carried out and discussed highlighting the significant influences of the material nonlinearity parameters n and ϵ_0 on the equilibrium configurations and the equilibrium paths.

Keywords: large deflection, cantilever beam, follower force, generalized Ludwick's constitutive law, nonlinear elastic

material, shooting method

1. Introduction

In recent years, with the development of technology, increasing demands for optimum or minimum-weight designed structural components makes the slender structures become of importance. To explore this kind of structures, the large deflection theory is necessary. Especially, developments in mechanical engineering, electronic engineering, aerospace engineering, robotics and manufacturing, etc. Furthermore, cantilever beam can be applied to a variety of applications, such as aircraft wings and helicopter blades are just some of the mechanical and structural examples. The follower distributed load acting on the beam can also be viewed as the air pressure on the aircraft wings.

There have been a large number of contributions pertaining to nonlinear analysis of structural elements, of which the majority considers only the geometrical nonlinearities. Contributions that are most relevant to the problem addressed here are briefly discussed below.

Rao and Roa [1] studied large-deflection of a cantilever beam subjected to a rotational distributed loading. The model formulation is formulated by nonlinear differential equation of the second order. Meanwhile, the large deflection problem of a non-uniform spring-hinged cantilever beam under a tip-concentrated follower force and the static analysis of the flexible non-uniform cantilever beams under a tip-

* Corresponding author E-mail address: touchsokheng2013@gmail.com

** E-mail address: boonchai_p@rmutt.ac.th

concentrated and intermediate follower forces, respectively, was considered by Shvartsman [2, 3]. Kocaturk et al. [4] investigated the large deflection static analysis of a cantilever beam subjected to a point load. The method of nonlinear finite element is introduced. Phungpaingam et al. [5] investigated the post-buckling of beam subjected to follower. The elastica theory and the shooting method are applied to carry out the numerical results. Furthermore, the shooting method is set up to solve the problem of the large deflection of a cantilever beam with geometric nonlinearity [6]. While, Chen [7] proposed an integral approach for large deflection cantilever beams. The moment integral treatment are formulated to get the numerical solution. Otherwise, large deflections of a cantilever beam under an inclined end load studied by Mutyalarao et al [8]. Nallathambi et al. [9] described large deflection of constant curvature cantilever beam under follower load. The fourth order Runge–Kutta method and shooting method are proposed to get the numerical solution. Moreover, Xiang et al. [10] researched on nonlinear analysis of a cantilever elastic beam under non-conservative distributed load. The numerical results are solved by using the shooting method. Taking a look at this problem, Kim et al. [11] employed finite element method to deal with beam stability on an elastic foundation subjected to distributed follower force. Vazquez-Leal, et al. [12] examined the approximations for large deflection of a cantilever beam under a terminal follower force and nonlinear pendulum. The homotopy perturbation method and Laplace- Padé post treatment are established to solve the problems. Otherwise, Eren [13] investigated the large deflections in rectangular combined loaded cantilever beams made of non-linear Ludwick type material by means of different arc length assumptions. For mathematical formulation, the materials of geometric nonlinearities are mentioned. The theory of Euler–Bernoulli is established to compute the horizontal and vertical deflections. Moreover, Athisakul et al. [14] applied the shooting method employing with Runge–Kutta method to carry out the numerical results with the problem of the effect of material nonlinearity on large deflection of variable-arc-length beams subjected to uniform self-weight. One more interesting work is that Lee [15] investigated large deflection of cantilever beams of nonlinear elastic material under a combined loading. The shearing force formulation is set up to formulate the governing equation to solve the problem. Butcher’s fifth order Runge–Kutta method is employed to compute the numerical results.

What is more, Brojan et al. [16] dealt with the large deflections of non-linearly elastic non-prismatic cantilever beams made from materials obeying the generalized Ludwick constitutive law. In the model formulation, the moment-curvature formula was set up to get the the governing equations and the boundary conditions in order to solve the problem. The similar problems of generalized Ludwick constitutive law are post-buckling of linearly tapered column and simply supported column made of nonlinear elastic materials obeying the generalized Ludwick constitutive law were studied by Saetiew and Chucheeepsakul [17, 18], respectively. The geometrical material nonlinearities are employed to formulate the governing equations. The shooting method is selected to carry out the numerical results. Last but not least, Brojan et al. [19] illustrated on static stability of nonlinearly elastic Euler’s columns obeying the modified Ludwick’s law. Four system states in static equilibrium are perceived as neutral, unstable, locally stable, and globally stable state.

As described literatures above, it was remarkable that research studies on the behavior of the large deflection problems that are made of material nonlinearities have carry out mostly the cantilever beams and columns. Only the small amount of research studies handled the problem with a slender, follower distributed load cantilever beam. Brojan et al. [20] considered the large deflections of non-prismatic nonlinearly elastic cantilever beams subjected to non-uniform continuous load and a concentrated load at the free end obeying generalized Ludwick’s constitutive law. The cantilever beam encountered the follower loads can be found in Hartono [21] and Rao and Rao [1]. However, in their papers, the material model still employed the Hooke’s law. Hence, in this paper, we aim to tackle the problem of the cantilever beam under uniform follower distributed load in which the material model belongs to the Generalized Ludwick model.

By perceiving the effects of geometrical and material nonlinearities, the governing equations obtained for the large deflection behavior are highly nonlinear. Generally, the closed-form solutions cannot be employed in this situation. The shooting method is then required and played a vital role to obtain numerical solutions. From the results, the load-deflection curves and equilibrium shapes are highlighted.

2. Problem definition and notations

Referring to Fig. 1, OB is the undeformed configuration of a uniform cantilever beam having length L subjected to a

distributed load w . Under loading, the beam undergoes large deflection and the deformed configuration of the beam is presented by OA (Fig. 2). After deformation, the distributed load direction is rotated by θ compared to the original undeformed vertical direction. OX, OY are the rectangular Cartesian co-ordinate system. s and θ are the intrinsic co-ordinate system followed in the present study. It is required to find out the tip angle α , the tip deflections of the cantilever beam X_0, Y_0 and the deformed shape for any given distributed load.

Prior to the mathematical formulation, the basic assumptions have been. They are:

- (1) Material of the beam is made of incompressible, homogeneous, isotropic obeying the generalized Ludwick's constitutive law.
- (2) Bernoulli hypothesis is adapted to this study.
- (3) Shear deformation is negligible because the beam is considered as a slender member.

3. Mathematical formulation and solution

The mathematical formulation derives from considering constitutive relationships, geometric relationships and equilibrium of the beam. Hence a set of highly nonlinear differential equations is obtained to describe the elastica of deformed beam subjected to follower distributed load, as shown in Fig. 2. The solution procedure is also treated in this section.

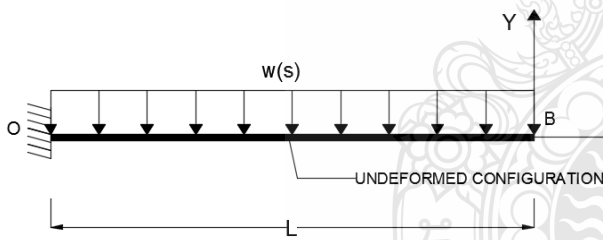


Fig.1. A cantilever beam subjected to the follower distributed load with undeformed configuration

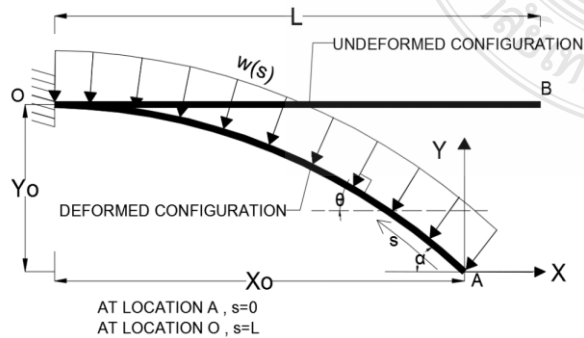


Fig.2. A cantilever beam subjected to the follower distributed load with deformed configuration

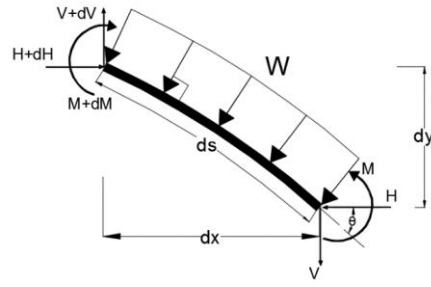


Fig.3. Free-body diagram of an infinitesimal element of the beam

3.1 Constitutive relationships

A well-known Ludwick-type nonlinear elastic constitutive formula is one of the generalizations of the Hooke's law to describe the nonlinear elastic behavior. Its nonlinear stress-strain relationship is a power function as shown below.

$$\sigma = \begin{cases} E|\varepsilon|^{1/n} & ; \varepsilon \geq 0, \\ -E|\varepsilon|^{1/n} & ; \varepsilon < 0. \end{cases} \quad (1)$$

where σ and ε are stress and strain (for tensile $\varepsilon \geq 0$ and compressive $\varepsilon < 0$), respectively; E represents material constant and n is dimensionless parameter indicating the degree of material nonlinearity.

It is important to note that Eq. (1) has one major shortcoming, the stress gradient goes to infinity for $n > 1$, and goes to zero for $n < 1$ when the strain value reaches zero, Fig. 3.

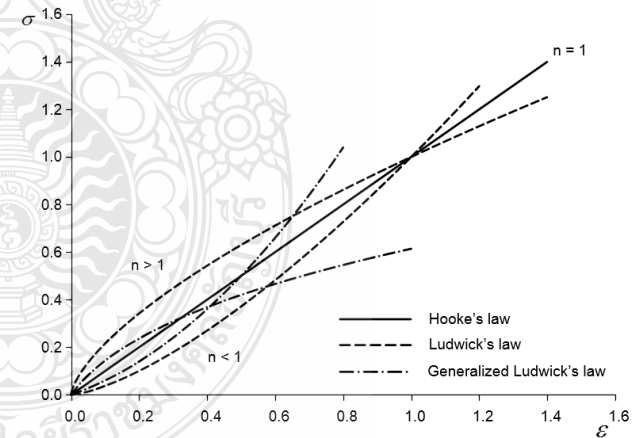


Fig.4. Stress-strain relationships in tensile domain

By eliminating this problem, since it is not possible to represent the actual behavior of material, Jung and Kang [22] suggested a modified (generalized) form of the Ludwick's constitutive law, mathematically described by the following expression,

$$\sigma = \begin{cases} E \left\{ (|\varepsilon| + \varepsilon_0)^{1/n} - \varepsilon_0^{1/n} \right\} & ; \varepsilon \geq 0, \\ -E \left\{ (|\varepsilon| + \varepsilon_0)^{1/n} - \varepsilon_0^{1/n} \right\} & ; \varepsilon < 0. \end{cases} \quad (2)$$

in which an additional parameter ε_0 is supplemented to prevent those shortcomings.

The generalized Ludwick's constitutive law is developed by using three parameters: E , n and ε_0 . These parameters can be used for approximating the stress-strain curves of such materials obtained by experiments. By virtue of Eq. (2), setting $\varepsilon_0 = 0$ leads to Ludwick-type nonlinear elastic constitutive law; consequently, the Hooke's law is obtained by setting $n = 1$.

3.2 Governing equations

The elastica theory is used to obtain the set of governing equations of the aforementioned problem. Applying the equilibrium equations, moment-curvature, and the geometric relations to the infinitesimal element ds of the deformed beam Fig.3, the set of differential equations can be written as:

$$\frac{dx}{ds} = \cos \theta, \quad (3)$$

$$\frac{dy}{ds} = \sin \theta, \quad (4)$$

$$\frac{dV}{ds} = w \cos \theta, \quad (5)$$

$$\frac{dH}{ds} = w \sin \theta, \quad (6)$$

$$\frac{dM}{ds} = -(V \cos \theta + H \sin \theta). \quad (7)$$

As well-known the inner bending moment acting at any cross-section of the beam can be expressed with normal stress σ :

$$M = -\int_A \sigma y dA. \quad (8)$$

where σ is related to the corresponding strain in tension and compression, see (2). Let $dA = bdy$ be the infinitesimal area of the cross-section. Furthermore, using the normal strain-displacement expression $\varepsilon = -\kappa y$; hence

$$M = \int_A E \left[(|\varepsilon| + \varepsilon_0)^{1/n} - \varepsilon_0^{1/n} \right] y dA. \quad (9)$$

By considering the symmetry of the cross-section and after some manipulation, the inner bending moment-curvature relationship of a uniform cross-section rectangular beam made up from nonlinear elastic materials obeying the generalized Ludwick's constitutive law can be written as follows:

$$M = Eb \left[\left(\kappa \frac{h}{2} + \varepsilon_0 \right)^{\frac{n+1}{n}} \left[\frac{\kappa h n (n+1) - 2n^2 \varepsilon_0}{\kappa^2 (2n+1)(n+1)} \right] + \frac{2n^2 \varepsilon_0^{\frac{2n+1}{n}}}{\kappa^2 (2n+1)(n+1)} - \frac{1}{\varepsilon_0^n} \frac{h^2}{4} \right]. \quad (10)$$

As mentioned previously and setting $\varepsilon_0 = 0$ into Eq. (10), the following expression for the inner bending moment-curvature relationship of Ludwick-type nonlinear elastic material can be achieved.

$$M = EI_n (\kappa)^{\frac{1}{n}}, \quad (11a)$$

where

$$I_n = \left(\frac{1}{2} \right)^{\frac{n+1}{n}} \left(\frac{n}{2n+1} \right) b h^{(2n+1)}. \quad (11b)$$

Similarly, by further setting $n = 1$ into Eq. (11), the simple expression for the inner bending moment-curvature relationship of linearly (Hookean) elastic can be obtained.

$$M = EI_0 \kappa, \quad (12)$$

in which $I_0 = \frac{bh^3}{12}$ is the moment of inertia of the rectangular cross-section.

By differentiating Eq. (10) once with respect to the arc length s the result gives:

$$\frac{dM}{ds} = E \left[\frac{b \left(\frac{\kappa h}{2} \right) (n+1) \left(\kappa \frac{h}{2} + \varepsilon_0 \right)^{\frac{1}{n}} h}{\kappa^2 (2n+1)} - \frac{bn \varepsilon_0 \left(\kappa \frac{h}{2} + \varepsilon_0 \right)^{\frac{1}{n}} h}{\kappa^2 (2n+1)} - \frac{bn \left(\kappa \frac{h}{2} + \varepsilon_0 \right)^{\frac{n+1}{n}} h}{\kappa^2 (2n+1)} + \frac{b4n^2 \varepsilon_0 \left(\kappa \frac{h}{2} + \varepsilon_0 \right)^{\frac{n+1}{n}}}{\kappa^3 (2n+1)(n+1)} - \frac{b4n^2 \varepsilon_0^{\frac{2n+1}{n}}}{\kappa^3 (2n+1)(n+1)} \right] \frac{d\kappa}{ds}, \quad (13)$$

$$\frac{dM}{ds} = EI_{n\kappa} \frac{d\kappa}{ds}, \quad (14a)$$

where

$$I_{nk} = b \left[\frac{\left(\frac{\kappa h}{2}\right)(n+1)\left(\kappa\frac{h}{2} + \varepsilon_0\right)^{\frac{1}{n}} h}{\kappa^2(2n+1)} + \frac{4n^2 \varepsilon_0 \left(\bar{\kappa}\frac{\bar{h}}{2} + \varepsilon_0\right)^{\frac{n+1}{n}}}{\bar{\kappa}^3(2n+1)(n+1)} - \frac{4n^2 \varepsilon_0^{\frac{2n+1}{n}}}{\bar{\kappa}^3(2n+1)(n+1)} \right], \quad (19a)$$

$$\bar{I}_0 = \frac{\bar{b} \cdot \bar{h}^3}{12}. \quad (19b)$$

$$\left[\frac{n\varepsilon_0 \left(\kappa\frac{h}{2} + \varepsilon_0\right)^{\frac{1}{n}} h}{\kappa^2(2n+1)} - \frac{n \left(\kappa\frac{h}{2} + \varepsilon_0\right)^{\frac{n+1}{n}} h}{\kappa^2(2n+1)} + \frac{4n^2 \varepsilon_0 \left(\kappa\frac{h}{2} + \varepsilon_0\right)^{\frac{n+1}{n}}}{\kappa^3(2n+1)(n+1)} - \frac{4n^2 \varepsilon_0^{\frac{2n+1}{n}}}{\kappa^3(2n+1)(n+1)} \right]. \quad (14b)$$

By substituting Eq. (7) into Eq. (14), this can be achieved.

$$\frac{d\kappa}{ds} = \frac{-(V \cos \theta + H \sin \theta)}{EI_{nk}}, \quad (15)$$

$$\frac{d\theta}{ds} = \kappa. \quad (16)$$

For the sake of the generality, the non-dimensional terms are introduced as follows.

$$\left. \begin{aligned} \bar{x} &= \frac{x}{L}, \quad \bar{y} = \frac{y}{L}, \quad \bar{s} = \frac{s}{L}, \quad \bar{\kappa} = \kappa L, \\ \bar{w} &= \frac{wL^3}{EI_0}, \quad \bar{V} = \frac{VL^2}{EI_0}, \quad \bar{b} = \frac{b}{L}, \quad \bar{h} = \frac{h}{L}, \\ \bar{I}_0 &= \frac{I_0}{L^4}, \quad \bar{I}_{nk} = \frac{I_{nk}}{L^4}, \quad \bar{M} = \frac{ML}{EI_0}, \quad \bar{H} = \frac{HL^2}{EI_0}. \end{aligned} \right\}, \quad (17a-f)$$

In view of the foregoing non-dimensional terms, Eq. (14) can be rewritten in non-dimensional form as follows:

$$\frac{d\bar{M}}{d\bar{s}} = \frac{\bar{I}_{nk}}{\bar{I}_0} \frac{d\bar{\kappa}}{d\bar{s}}, \quad (18)$$

where

$$\bar{I}_{nk} = \bar{b} \left[\frac{\left(\frac{\bar{\kappa}\bar{h}}{2}\right)(n+1)\left(\bar{\kappa}\frac{\bar{h}}{2} + \varepsilon_0\right)^{\frac{1}{n}} \bar{h}}{\bar{\kappa}^2(2n+1)} + \frac{4n^2 \varepsilon_0 \left(\bar{\kappa}\frac{\bar{h}}{2} + \varepsilon_0\right)^{\frac{n+1}{n}} \bar{h}}{\bar{\kappa}^3(2n+1)(n+1)} - \frac{4n^2 \varepsilon_0^{\frac{2n+1}{n}} \bar{h}}{\bar{\kappa}^3(2n+1)(n+1)} \right]$$

3.3 Method of solution

Since a set of governing equations is a complicated nonlinear differential equation, the numerical solutions are required for describing the deformation behavior of the cantilever beam problem. The geometric relationships in Eqs. (3) and (4) can be expressed in the non-dimensional forms as,

$$\frac{d\bar{x}}{d\bar{s}} = \cos \theta, \quad (20a)$$

$$\frac{d\bar{y}}{d\bar{s}} = \sin \theta, \quad (20b)$$

$$\frac{d\bar{V}}{d\bar{s}} = \bar{w} \cos \theta, \quad (20c)$$

$$\frac{d\bar{H}}{d\bar{s}} = \bar{w} \sin \theta, \quad (20d)$$

$$\frac{d\bar{\kappa}}{d\bar{s}} = -(\bar{V} \cos \theta + \bar{H} \sin \theta) \frac{\bar{I}_0}{\bar{I}_{nk}}, \quad (20e)$$

$$\frac{d\theta}{d\bar{s}} = \bar{\kappa}. \quad (20f)$$

The boundary conditions are as follows:

$$\theta(\bar{s} = 0) = \theta_0 \quad \text{and} \quad \theta(\bar{s} = 1) = 0, \quad (21a)$$

$$\bar{\kappa}(\bar{s} = 0) = 0 \quad \text{and} \quad \bar{\kappa}(\bar{s} = 1) = 0, \quad (21b)$$

$$\bar{x}(\bar{s} = 0) = 0 \quad \text{and} \quad \bar{x}(\bar{s} = 1) = \bar{x}(1), \quad (21c)$$

$$\bar{y}(\bar{s} = 0) = 0 \quad \text{and} \quad \bar{y}(\bar{s} = 1) = \bar{y}(1). \quad (21d)$$

Equation (20a-f) with the boundary conditions in Eqs. (21a-d) forms the nonlinear two-point boundary value problem, which can be solved by the shooting method. For a given value of θ_0 , there is an unknown (\bar{w}) to be evaluated from six of first-order nonlinear differential equations (20a)–(20f) with boundary conditions given in equations (21a)–(21d). The solution steps are summarized below.

In order to find the solution, the shooting method is employed to obtain the numerical solutions. The numerical procedure can be summarized in the following steps.

(1) Specify the non-dimensional cross-section parameters (\bar{b} and \bar{h}), and the material constants (n and ε_0) to the problem.

(2) Assign the value of θ_0 and estimate \bar{w} for the first iteration.

(3) Integrate equations (20a)–(20f) from $\bar{s} = 0$ and $\bar{s} = 1$ by using the seventh-order Runge–Kutta with adaptive step size control.

(4) Minimize the error norm in which the objective function Φ for the minimization process is

$$\text{Minimize } \Phi = |\theta(1)| \quad (22)$$

In the computation, the desired value of Φ is that less than the prescribed tolerance (10^{-7}) for the solution using the Newton-Raphson iterative scheme.

In the equation (19a), it can be seen that the singularity may occur $\bar{\kappa} = 0$. To overcome this problem, the initial curvature at the tip of the beam is set to $\bar{\kappa} = 1 \times 10^{-5}$ instead of zero.

In our computation, we assume that the set of material parameters (i.e., ε_0 and n) can be related to each other. Technically, the initial slopes of the stress-strain curves are utilized to obtain the relationship. Hence the initial slopes of the stress-strain curve can be achieved by differentiating equation (2). The result obtains

$$\varepsilon_0 = \left(\frac{n}{\alpha} \right)^{\frac{n}{1-n}} \quad \text{for } n \neq 1 \quad (23)$$

where the initial slope of the stress-strain curve is defined by αE . For the example, if the initial slopes are given by $0.5E$ and $2E$, and the relationship between ε_0 and n are $\varepsilon_0 = (2n)^{\frac{n}{1-n}}$ and $\varepsilon_0 = (n/2)^{\frac{n}{1-n}}$, respectively. It should be noted that Eq. (23) does not valid for $n = 1$. If $n = 1$, ε_0 would set to be zero automatically. In our numerical experiments, the initial slopes are chosen to be $0.5E$ and $2E$, to show the difference between linear and nonlinear constitutive relationships.

4. Results and discussion

To analyze the numerical computations of the large deflections of cantilever beam obeying generalized Ludwick's material model subjected to follower distributed load, the cross-sectional dimensions and length of the cantilever beam are given by the non-dimensional geometric parameters as follows: $\bar{b} = 0.2\text{m}$, $\bar{h} = 0.2\text{m}$.

To point out the nonlinear constitutive relationships clearly and simply we have chosen the two following numerical examples, the rectangular cross-section of cantilever beam is subjected to several different follower distributed loads with the degree of material nonlinearity n .

The first case of the cantilever beam with non-dimensional geometric parameters $\bar{b} = 0.2\text{m}$, $\bar{h} = 0.2\text{m}$. The nonlinearity material parameters to determine are $n > 1$ and $\varepsilon_0 = (2n)^{\frac{n}{1-n}}$.

The second case of the cantilever beam with non-dimensional geometric parameters $\bar{b} = 0.2\text{m}$, $\bar{h} = 0.2\text{m}$. The

nonlinearity material parameters to determine are $n < 1$ and $\varepsilon_0 = \left(\frac{n}{2} \right)^{\frac{n}{1-n}}$.

The first two tables below are illustrated the numerical results in sequence.

The result listed in Table 1 can be interpreted that when using $n > 1$, the rotation angle θ_0 and the follower distributed load \bar{w} are both increase their values. In contrast, Table 2 demonstrated that when applying $n < 1$, the rotation angle θ_0 successively increases with the follower distributed load \bar{w} .

Table 1 Numerical results for cantilever beam made of the generalized Ludwick-type nonlinear elastic material for case 1.

θ_0 (rad)	\bar{w}				
	$\varepsilon_0 = (2n)^{\frac{n}{1-n}}$				
	$n = 1.10$	$n = 1.20$	$n = 1.30$	$n = 1.45$	$n = 1.50$
0.20	1.68619	2.00236	2.11785	2.17475	2.18264
0.80	6.06606	6.91150	7.30042	7.50542	7.52825
1.40	10.47533	11.60927	12.12867	12.27408	12.28291
2.00	15.42334	16.74968	17.06725	17.21551	17.38962
2.60	21.59041	23.07919	22.39006	23.37350	23.52711
3.14	29.40196	31.10185	31.46138	31.33843	29.32568

Table 2 Numerical results for cantilever beam made of the generalized Ludwick-type nonlinear elastic material for case 2.

θ_0 (rad)	\bar{w}				
	$\varepsilon_0 = (0.5n)^{\frac{n}{1-n}}$				
	$n = 0.55$	$n = 0.65$	$n = 0.75$	$n = 0.85$	$n = 0.95$
0.20	0.57700	0.63391	0.64521	0.70084	0.98283
0.80	2.87544	2.92139	3.00960	3.34930	4.29766
1.40	5.61243	5.83952	5.98951	6.59744	8.04496
2.00	9.69558	9.60880	9.77101	10.60975	12.48068
2.60	14.87062	14.71242	14.81659	15.86234	18.15356
3.14	19.97827	20.60874	21.33293	22.56080	25.34391

In addition, the nonlinearity material parameter $n = 0.55$ and $n = 1.30$ are selected to show the deflection configuration in figure 5 and 6. And their deflection configuration results for $n = 0.55$ and $n = 1.30$ are displayed in Table 3 and 4, respectively.

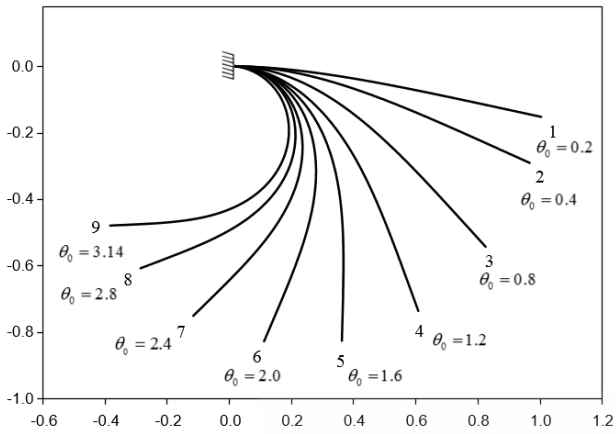


Fig.5. Equilibrium configurations of the nonlinearly cantilever beam subjected to follower distributed load $n = 0.55$.

Otherwise, the nonlinearity material parameter $n = 1.30$ is chosen to demonstrate the deflection configuration.

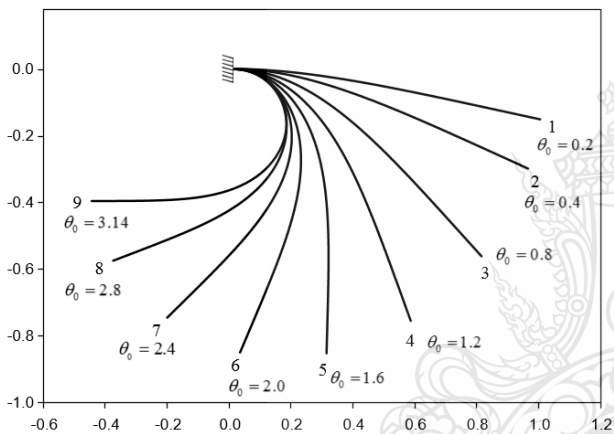


Fig.6. Equilibrium configurations of the nonlinearly cantilever beam subjected to follower distributed load $n = 1.30$.

Table 3 Numerical results for cantilever beam made of the generalized Ludwick-type material for $n = 0.55$.

Configuration	$n = 0.55$ and $\varepsilon_0 = (0.5n)^{\frac{n}{1-n}}$	
	θ_0 (rad)	\bar{w}
1	0.2	0.57700
2	0.4	1.32022
3	0.8	2.87544
4	1.2	4.52891
5	1.6	6.88814
6	2.0	9.69558
7	2.4	12.90037
8	2.8	17.02910
9	3.14	19.97827

Table 4 Numerical results for cantilever beam made of the generalized Ludwick-type material for $n = 1.30$.

Configuration	$n = 1.30$ and $\varepsilon_0 = (2n)^{\frac{n}{1-n}}$	
	θ_0 (rad)	\bar{w}
1	0.2	2.11785
2	0.4	3.95424
3	0.8	7.30042
4	1.2	10.42959
5	1.6	13.70155
6	2.0	17.06725
7	2.4	21.35352
8	2.8	26.01780
9	3.14	31.46138

Furthermore, the relationship of the load-displacement curve for the nonlinearly cantilever beam between the follower distributed load \bar{w} and the rotation angle θ_0 are exhibited with the figure below.

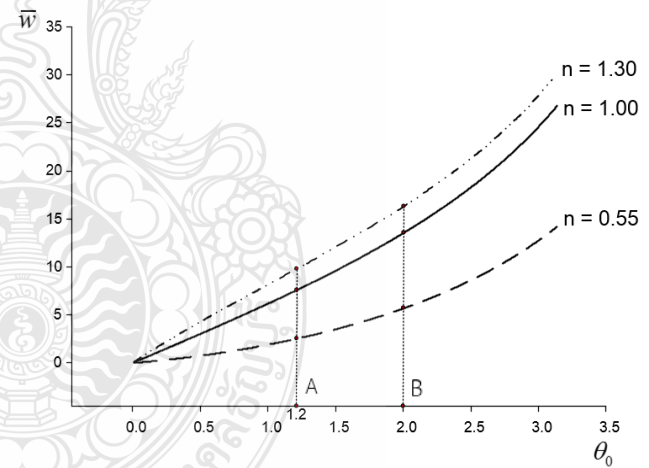


Fig.7. Load-displacement curve for the nonlinearly cantilever beam subjected to follower distributed load.

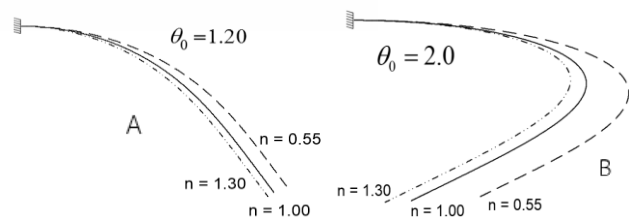


Fig.8. Equilibrium configurations for $\theta_0 = 1.20$ and $\theta_0 = 2.0$

Since the Ludwick-type constitutive law has one major shortcoming as mentioned before, the large deflection behavior of a cantilever beam obeying generalized Ludwick's material model subjected to follower distributed load is discussed in this section. The load-displacement curves of the cantilever beam with various material nonlinearity parameters n are plotted in Fig. 7.

It is remarkable that a linear case $n = 1$ (Fig. 7), the well-known load-displacement curve is monotonic and stable. As it can be seen from the figure, the follower distributed load \bar{w} increases as the rotation angle θ_0 increases.

For the case of hardening material, where $n > 1$ and $n < 1$, the behaviors of the cantilever beam are similar to the linear case $n = 1$.

Having compared the results with Rao and Rao [1], in this research was founded that the values of the rotation angle θ_0 and the follower distributed load \bar{w} are very close to those of Rao and Rao [1] while using $n = 1.0$. It is also shown in Table 5.

Table 5 Comparison results between Rao and Rao [1] and the presented study.

θ_0		\bar{w}	
deg	rad	Rao and Rao [1]	This research
9.54	0.1665	1.0	0.99980
19.04	0.3323	2.0	1.99978
37.75	0.6589	4.0	4.00016
55.83	0.9744	6.0	6.00041
73.02	1.2744	8.0	7.99981
89.15	1.5560	10.0	9.99972
104.12	1.8172	12.0	11.99933
130.43	2.2764	16.0	16.00006
152.09	2.6545	20.0	19.99959
169.68	2.9615	24.0	24.00033
183.86	3.2090	28.0	28.00096
195.27	3.4081	32.0	32.00189

5. Conclusions

In the presented study the large deflection behavior of the cantilever beam subjected to follower distributed load where material of the cantilever beam obeys the generalized Ludwick's constitutive law is investigated. Both geometrical and material nonlinearities are relevant to this problem since the material of the cantilever beam is assumed to be nonlinearly

elastic. This can be surpassed in a three-parametric generalized Ludwick's material model which is described and applied in this study of large deflections of cantilever beam. Since the governing equations were highly nonlinear differential equations, the closed-form solutions are in general impossible. Otherwise, the cantilever beam problem has been solved numerically by the shooting method. Several numerical examples were selected to demonstrate the influence of the geometry and configurations of the beam, loading conditions, and constitutive law of the material on the deflection behavior of the discussed cantilever beam. Load-deflection curves are monotonic and stable.

From a practical standpoint, results obtained in this paper illustrate some benefits of the generalized Ludwick's model. We have generated an exact moment-curvature formula for materials which obey the generalized Ludwick's law.

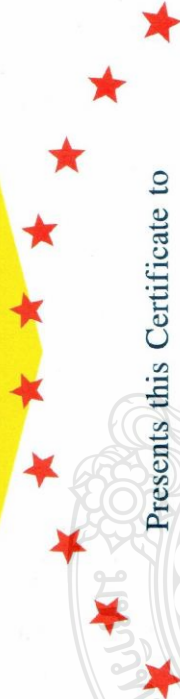
Last but not least, the present method can be developed for a variety of cross-section shapes with varying longitudinal shape subjected to follower distributed load in which more numerical effort is needed. What is more, the recent findings from this study will benefit the analysis and design of the practical problems. This hands out as a benchmark for future experimental investigations as well.

References

- [1] Rao, B.N. and Rao, G.V. "Large deflections of a cantilever beam subjected to a rotational distributed loading". *Forschung im Ingenieurwesen*, 55(4), pp. 116-120, 1989.
- [2] Shvartsman, B.S. "Large deflections of a cantilever beam subjected to a follower force". *Sound and Vibration (JSVI)*, 304, pp. 969-973, 2007.
- [3] Shvartsman, B.S. "Direct method for analysis of flexible cantilever beam subjected to two follower forces". *Int. J., Non-Linear Mechanics*, 44, pp. 249-252, 2009.
- [4] Kocatürk, T., Akbaş, Ş. D. and Şimşek, M. "Large deflection static analysis of a cantilever beam subjected to a point load". *Engineering and Applied Sciences (IJEAS)*, 4, pp. 1-13, 2010.
- [5] Phungpaingam, B., Chucheepsakul, S. and Wang, C.M. "Postbuckling of beam subjected to immediate follower force". *Engineering Mechanics (ASCE)*, 132, pp. 16-25, 2006.
- [6] Banerjee, A., Bhattacharya, B. and Mallik, A.K. "Large deflection of cantilever beams with geometric non-linearity: Analytical and numerical approaches". *Int. J., Non-linear Mechanics*, 43, pp. 366-376, 2008.
- [7] Chen, L. "An integral approach for large deflection cantilever beams". *Int. J., Non-linear Mechanics*, 45, pp. 301-305, 2010.
- [8] Mutyalarao, M., Bharathi, D. and Rao, B.N. "Large deflections of a cantilever beam under an inclined end load". *Applied Mathematics and Computation (amc)*, 217, pp. 3607-3613, 2010.
- [9] Nallathambi, A.K., Rao, C.L. and Srinivasan, S.M. "Large deflection of constant curvature cantilever beam under follower load". *Mechanical Sciences (ijmecsci)*, 52, pp. 440-445, 2010.
- [10] Li, Q.L., Li, S.R. and Xiang, C.S. "Nonlinear analysis of a cantilever elastic beam under non-conservative distributed load". *International Conference on Information and Computing (4th)*, pp. 181-183, 2011.
- [11] Kim, J.O., Lee, K.S. and Lee, J.W. "Beam stability on an elastic foundation subjected to distributed follower force". *Mechanical Science and Technology*, 22, pp. 2386-2392, 2008.
- [12] Vazquez-Leal, H., Khan, Y. and May, A.L.H. "Approximations for large deflection of a cantilever beam under a terminal follower force and nonlinear pendulum". *Mathematical Problems in Engineering (Hindawi Publishing Corporation)*, pp. 1-13, 2013.
- [13] Eren, I. "Determining large deflections in rectangular combined loaded cantilever beams made of non-linear Ludwick type material by means of different arc length assumptions". *Sadhana (India)*, 33(1), pp. 45-55, 2008.
- [14] Athisakul, C., Phungpaingam, B., Juntarakong, G. and Chucheepsakul, S. "Effect of material nonlinearity on large deflection of variable-arc-length beams subjected to uniform self-weight". *Mathematical Problems in Engineering (Hindawi Publishing Corporation)*, pp. 1-9, 2012.
- [15] Lee, K. "Large deflections of cantilever beams of non-linear elastic material under a combined loading". *Int. J., Non-Linear Mechanics*, 37, pp. 439-443, 2002.
- [16] Brojan, M., Videnic, T. and Kosel, F. "Large deflections of nonlinearly elastic non-prismatic cantilever beams made from materials obeying the generalized Ludwick's constitutive law". *Meccanica*, 44, pp. 733-739, 2009.
- [17] Saetiew, W. and Chucheepsakul, S. "Post-buckling of linearly tapered column made of nonlinear elastic materials obeying the generalized Ludwick's constitutive law". *Mechanical Sciences (ijmecsci)*, 65, pp. 83-96, 2012.
- [18] Saetiew, W. and Chucheepsakul, S. "Post-buckling of simply supported column made of nonlinear elastic materials obeying the generalized Ludwick's constitutive law". *Applied Mathematics and Mechanics (ZAMM)*, 92, pp. 479-489, 2012.
- [19] Brojan, M., Sitar, M. and Kosel, F. "On static stability of nonlinearly elastic euler's columns obeying the modified ludwick's law". *Int. J., Structural Stability and Dynamics*, 12, pp. 1-19, 2012.
- [20] Brojan, M., Cebron, M. and Kosel, F. "Large deflections of non-prismatic nonlinearly elastic cantilever beams subjected to non-uniform continuous load and a concentrated load at the free end". *Theoretical and Applied Mechanics (Acta Mech. Sin.)*, pp. 863-869, 2012.
- [21] Hartono, W. "Elastica of cantilever beam under two follower forces". *Advances in Structural Engineering*, Vol 1 (2), pp. 159-165, 1997.
- [22] Jung, J.H. and Kang, T.J. "Large deflection analysis of fibers with nonlinear elastic properties". *J Textile Inst (SAGE)*, 75(10), pp. 715-723, 2005.
- [23] Press WH, Teukolsky SA, Vetterling WT, Flannery BP. "Numerical recipes in FORTRAN: The art of scientific computing, 2nd Edition". New York: Cambridge University Press, 1992.



The Engineering Institute of Thailand Under H.M. The King's Patronage
&
King Mongkut's University of Technology North Bangkok



Presents this Certificate to

Sok Heng Touch

For Participation and Presentation
Entitled

LARGE DEFLECTIONS OF CANTILEVER BEAM SUBJECTED TO FOLLOWER DISTRIBUTED LOAD MADE
FROM NONLINEARLY MATERIALS OBEYING GENERALIZED LUDWICK'S CONSTITUTIVE LAW

Prof. Dr. Suchatvee Suwansawat
President of EIT

Assoc. Prof. Dr. Sunchai Inthapichai
Chairman of the NCCCE 20 Committee



8-10 July 2015
The Zign Hotel, Pattaya, Chonburi

Biography

Name - Surname Mr. Sokheng Touch

Date of Birth September 03, 1989

Address Road N5, Otapong Village, Otapong Commune,
Bakan District, Pursat Province, Cambodia.

Education Bachelor Degree of Civil Engineering at
Norton University, Phnom Penh, Cambodia
(2007-2012),
Master Degree of Civil Engineering at
Rajamangala University of Technology
Thanyaburi, Thailand (2013-2015).

Work Experiences Site engineer at New World Group at Phnom
Penh, Cambodia from (2012 to 2013),
Civil Engineering Trainer at Engineers and
Architects Training Center (EATC) at Phnom
Penh, Cambodia, presently.

Telephone Number (+855) 76 8888 572

Email Address touchsokheng2013@gmail.com